DOE/NASA/0101-1
NASA CR-165463
TRS 107

Design and Evaluation of Low-Cost Laminated Wood Composite Blades for Intermediate-Size Wind Turbines: Blade Design, Fabrication Concept, and Cost Analysis

Seymour Lieblein
Technical Report Services

and

Meade Gaugeon, Georg Thomas,
and Michael Zuteck
Gaugeon Brothers, Inc.

November 1982

Prepared for
NATIONAL AERONAUTICS AND SPACE ADMINISTRATION
Lewis Research Center
Under Contract DEN 3-101

for
U.S. DEPARTMENT OF ENERGY
Conservation and Renewable Energy
Wind Energy Technology Division

DOE/NASA/0101-1
NASA CR-165463
TRS 107

Design and Evaluation of Low-Cost Laminated-Wood-Composite Blades for Intermediate-Size Wind Turbines: Blade Design, Fabrication Concept, and Cost Analysis

DOE/NASA/0101--1

DE83 010077

Seymour Lieblein
Technical Report Services
Rocky River, Ohio 44116

and

Meade Gaugeon, Georg Thomas, and Michael Zuteck
Gaugeon Brothers, Inc.
Bay City, Michigan 48706

November 1982

Prepared for
National Aeronautics and Space Administration
Lewis Research Center
Cleveland, Ohio 44135
Under Contract DEN 3-101

for
U.S. DEPARTMENT OF ENERGY
Conservation and Renewable Energy
Wind Energy Technology Division
Washington, D.C. 20545
Under Interagency Agreement DE-AI01-76ET20320

CONTENTS

1.0 SUMMARY

After a preliminary investigation, a contract (DEN3-101) was awarded to design and fabricate a low-cost wood-composite blade for the 200-kW Mod-0A wind turbine. Several fabrication techniques were considered, and a final blade design and fabrication concept evolved from the first phase of the contract.

The wood composite blade would be built using laminations of Douglas fir veneers for its primary structural spar, and Verticel(R) cored birch plywood panels for its trailing edge section. An epoxy-bonded steel load take-off stud attachment concept at the root is the other key structural feature of this design. Geometric simplifications of blade shape were found to be feasible for reducing mold complexities and simplifying blade fabrication.

Tests were conducted on specimens representing key structural components such as the jointed veneers and the steel load take-off studs. The purpose of these tests was to determine and improve strength and cyclic fatigue performance levels. The primary series of tests on samples of single bonded studs determined both pull-out and cyclic fatigue strength. These tests established the limiting stresses for the epoxy bond of the steel studs as well as the general feasibility of the concept.

Calculations of margins of safety for the emergency shutdown load condition and for normal cyclic operation loads were documented. The hub attachment of the blade design was found to have the lowest margin of safety (about 0.1) because of the estimated low fatigue life of the epoxy bond of the stud. However, the attachment configuration was considered acceptable for this experimental blade because of conservative factors incorporated in the margin of safety determination.

In general, the costs of labor and tooling involved in blade construction are high compared to material costs. Thus, these areas must provide the bulk of cost reductions if significant savings are to occur. Since wood is a low density material, material handling volumes and areas are high, so that only direct manufacturing labor costs could be reduced. A female half-shell mold concept was developed to minimize the labor involved in forming and finishing the blades.

Fabrication cost data were estimated for the Mod-0A wood composite blade. In terms of 1982 dollars, the cost per blade was projected to range (depending on the assumption for inflation) from about $15,000 to $18,700 for a production rate of 100 blades per year. If only a few sets of blades are produced, the cost is expected to be

about $50,000 per blade. The major conclusion of this effort is that the proposed wood composite blade design and manufacturing concept is suitable for blades for Mod-0A size wind turbines at a cost that is very competitive with other methods of manufacture and materials.

2.0 INTRODUCTION

In the quest for the development of alternate energy sources, serious consideration is being given to conversion of solar energy to electric power. Solar energy comes in various forms, one of which is the atmospheric wind which develops because of the sun's heating effect. Historically, wind has played an important role for providing a major power source for travel up until the current century. However, due to the former availability of low-cost fossil fuels, modern development of wind as a major energy source for power generation has been largely ignored.

In 1974, ERDA (subsequently the Department of Energy), was assigned the task of developing the technology for converting wind energy into a more usable form. Preliminary studies indicated that wind driven generators could harness wind energy at reasonable costs. A program was initiated to design, construct and operate large, horizontal-axis, experimental wind turbines for operational experience (ref. 1). These first installations were expensive, and if wind energy was to be a viable alternative, capital costs would have to be reduced.

Programs were subsequently formulated to reduce the major component costs of the system. One of the high cost components is the rotor blade. Rotor blades for the early machines were adopted and developed from aircraft industry technology. Since helicopter and propeller blades and aircraft wing construction are developed technologies, a new approach would be required to significantly reduce system costs. Alternate inexpensive blade materials and fabrication techniques would be essential elements of a low-cost rotor system. Several alternate materials were subsequently chosen to be evaluated for feasibility. Among the materials evaluated were steel-reinforced concrete (ref. 2), urethane foam (ref. 3), fiberglass reinforced plastic (ref. 4), steel (ref. 5), and wood (ref. 6).

NASA/DOE awarded a contract (DEN3-9) to the Gougeon Brothers, Inc., to investigate the feasibility of constructing a rotor blade from wood composite materials. The results of this contract indicated that wood has a good potential to meet Mod-0A blade structural requirements. In a competitive procurement, NASA Lewis Research Center subsequently funded a contract (DEN3-101) to Gougeon Brothers, Inc., to develope a wood composite blade design and fabricate blades for the Mod-0A wind turbine. This wind turbine has a 125-foot rotor diameter and develops 200 kilowatts of electrical power (ref. 7). Figure 1 shows several of the Mod-0A wind turbines currently in operation. The Mod-0A wind turbines were originally designed for, and equipped with, aluminum blades which were up-graded versions of the aluminum blades designed for the 100 kW Mod-0 (ref. 8). At present, three Mod-0A's have wood blades

built by Gougeon Brothers, Inc., and a fourth has tape-wound fiberglass blades manufactured by Structural Composites Industries, Inc. (SCI) under contract DEN3-100 (ref. 9).

The contractor's description of the wood blade design and fabrication concept developed under DEN3-101 was finalized as a NASA technical report by Technical Report Services (Purchase Order C-46981-D). The report includes a description of the blade design concept, the proposed fabrication concept, and the structural design analysis developed by Gougeon Brothers, Inc. Also contained herein are the results of tests of key components, and the blade design contractor's estimate of the cost of Mod-0A-size wood composite blades in quantity production.

3.0 BLADE DESIGN SPECIFICATIONS

Contract DEN3-101 required the design of the wood composite wind turbine blade to be within parameters described in this section. The design parameters included: cost, weight, geometry and aerodynamics, loads, and root end-to-hub interface specifications.

3.1 Fabrication Cost Analysis

A fabrication cost analysis was to be conducted to determine the blade cost for the 62.5 foot Mod-0A application, including amortized cost of tooling for blade procurements of 100 to 1000 blades per year. Costs were to be determined for these quantities of blades for lengths varying from 15 to 200 feet. The rationale for reducing the costs as the production rate is increased was to be described. The blade costs are defined as the cost of the one hundreth and the one thousandth blade manufactured in one year. A low value of blade cost-to-weight was desired. According to contract requirements, the blade cost/weight value must fall within the envelope shown in figure 2. The cost-weight value is defined as 2.5 (dollar/1,000)(lb/1,000).

3.2 Weight and Balance

The specifications for blade weight included restrictions on the center of gravity location and blade-to-blade uniformity. The specification required that the center of gravity be located forward of the 32 percent chordline point, and with a chordwise variation of less than ±1 percent of this location per two-blade set. In addition, for a two blade set, the variation in spanwise center of gravity was required to be within 1 inch, and the tolerance in blade weight was to be within ±2 percent. The maximum root gravity moment was to be less than 50,000 foot pounds, and the blade weight was to be less than 4,000 pounds.

3.3 Geometry and Aerodynamics

The specifications for blade geometry and aerodynamics consisted of blades designed to NACA 230-series airfoil sections (fig. 3) with a linear blade twist of 10° from root to tip. The maximum allowable thickness of the blade section was to be 40 percent of the chord length at the root and 18 percent of the chord length at the tip, with a linear variation between. Uniformity of blade-to-blade thickness and twist was stressed over exact thickness and twist location.

Several blade planforms were acceptable, and are shown in figure 4. The goal of the aerodynamic design was to define a blade which minimized thickness and chord length without an aerodynamic performance penalty. In addition, the specifications permitted a root cutout, provided it was cost effective. Figure 5 was supplied in the specifications so that the root cutout impact could be evaluated on the basis of economic cost versus annual energy developed. All aerodynamic decisions were to be cost justified and consistent with the theme of low-cost wind turbine blade production.

3.4 Loads and Structural Requirements

The specified loads to be considered in the blade design consisted of static hurricane wind and normal cyclic working loads. The "hurricane gust condition" was to be modeled by a static flatwise load of 50 pounds per square foot of planform area. The cyclic load specifications required that there be no edgewise or flatwise fatigue failure resulting from the blade bending moments. Approximate blade bending moments were supplied (from earlier Mod-0 blade designs) as shown in figure 6. The edgewise bending moment could be scaled from the graph in accordance with the ratio of designed blade weight to 2,350 pounds. Definitions and conventions to be used for bending moments are shown in figure 7. No-failure fatigue life under the cyclic loads was specified as four hundred million cycles (for a 30-year life). Also, under these loads the blade must not yield anywhere, and the primary structure must not buckle.

Maximum allowable deflection of the blade tip was 91 inches to provide for adequate tower clearance. The natural static blade frequencies, ω, for both edgewise and flatwise first bending modes were to fall within one of the following ranges:

$$1.50 \text{ Hz} \leq \omega \leq 1.85 \text{ Hz}$$

$$2.15 \text{ Hz} \leq \omega \leq 2.55 \text{ Hz}$$

$$2.75 \text{ Hz} \leq \omega \leq 3.15 \text{ Hz}$$

$$3.45 \text{ Hz} \leq \omega \leq 3.85 \text{ Hz}$$

The design was to also provide a blade which could operate and be maintained under the following environmental conditions:

Temperature (rangė -30° to 120° F)

High humidity and/or salt spray

Sunlight exposure

Fungus attack

Lightning strikes

3.5 Root End-to-Hub Interface

In order for the blades to be utilized on existing Mod-0A machines, the hub flange or root section was to be capable of direct interfacing with the existing hub spindle (fig. 8), or a spool piece could be used to mate the blade root to the hub. Load take-off stud test specimens would be constructed and evaluated to determine the feasibility of bonding studs into wood to provide the blade-to-hub attachment. The design of the stud specimens is shown in figure 9.

4.0 BLADE DESIGN CONCEPT

This section describes the basic blade design concept that was developed for the proposed production of low-cost wood composite Mod-0A blades. Included is a discussion of the reasoning behind the major blade shape and form decisions.

4.1 Blade Geometry

The wood composite blade was designed for a shaft (aerodynamic) power of 300 kW (200 kW electrical power) at 40 rpm and a free-stream wind speed at hub height of 22 mph (15 mph at the rotor disk). The final design (fig. 10) consisted of a linearly tapered blade outboard of Station 150. (Station 150 means 150 inches from the axis of rotation of the rotor when the blade is connected to the hub flange.) The blade inboard of Station 150 is a truncated section formed with no twist down to the root section. The final blade design geometry is given in Table I.

The planform of the blade was selected as a compromise between low blade solidity ratio, as required by the design specifications, and blade angle settings for optimum performance. According to blade design theory, for a given tip speed ratio (blade tip speed/wind speed), there is a fixed optimum radial distribution of the product of chord length and lift coefficient. The planform taper ratio (maximum chord/tip chord) is 2.6.

The specified shape for the blade was the NACA 230-series airfoil (fig. 3), which is non-symmetric about the chord line. The maximum thickness occurs at 30% chord measured from the leading edge. The maximum thickness of the most inboard full airfoil is 19.8 inches (31.7 percent thickness-to-chord ratio) at Station 150 and tapers linearly to 1.8 inches (7.5 percent thickness-to-chord ratio) at the tip. Inboard of Station 150, the blade thickness increases to 22.5 inches. The selected thickness-to-chord ratios are substantially less than the maximums allowed by the design specification.

Although the design specifications called for a 10-degree linear twist schedule from root to tip, the final design twist is only 4.8 degrees and non-linear. The twist distribution resulted from the adoption of linear leading and trailing edges. The blade portions inboard of Station 150 are not twisted since they are not full airfoil sections, and it makes little difference, except for lofting and blade production considerations, to continue twisting this portion of the blade. The external geometry of the blade is shown schematically in figure 10.

The use of a linear geometry for the blades was recognized as a simplification for ease of fabrication. The use of straight lines for taper, bonding edges, lofting and mold building was anticipated to be cost and schedule effective. With a linear taper, the blade can be trimmed in a single smooth plane, which simplifies the half-shell mold concept of blade construction. Furthermore, the smaller twist does provide increased chordwise bending stiffness.

Figure 11 shows the spanwise distribution of twist angle compared to the optimum twist which corresponds to the twist for linear spanwise loading. The twist variation for the wood composite blade design is shown matched to optimum twist for 40, 65, and 100 percent design power levels. For the range of these power levels, the twist of the wood composite blade matches the optimum twist quite well over the outer half of the blade. This is favorable, since most of the power from the rotor is developed over the outer half of the blade. However, the design twist of the wood blade would produce an increased angle of attack near the root end of the blade close to design wind speed. This departure was not considered serious, inasmuch as only a small part of the power is generated in the inner region of the blade. Furthermore, operational experience with full-scale wind turbines has indicated that performance is sustained in the root region of the blades at high angles of attack. This appears to be analogous to turbomachinery experience where the root sections of rotor blades can be loaded quite heavily without producing stall.

The match between design twist and optimum twist improves as wind speed is reduced, with nearly coincident curves at 40 percent design power. Start-up and low speed power generation should, therefore, be favored with this blade design. Thus, there is little deterioration in aerodynamic performance for the improved fabricational and structural situation with a linear blade, since the developed twist closely coincides with the optimum twist over the outer half of the blade. The design twist was, therefore, considered acceptable in view of the estimated substantial savings in blade fabrication cost.

4.2 Comparison with Aluminum Blade

Mod-0A wind turbines at Culebra, Puerto Rico; Block Island, Rhode Island; and Clayton, New Mexico, were originally outfitted with aluminum blades whose design was based on the design developed for the 100-kW Mod-0 wind turbine at Sandusky, Ohio (refs. 10 and 11). Both aluminum and wood composite blades have NACA 230-series airfoil contours and the same coning angle (7 deg). A comparison of the geometric characteristic of chord length, thickness ratio, and twist of these blades is shown in figure 12. As seen in figure 12(a), the chord lengths of the wood composite blade are larger than those of the aluminum blade. (A greater planform area is required to produce the larger design power of the Mod-0A compared to the Mod-0.) The taper ratio of the wood blade is 2.6 compared to 3.0 for the aluminum blade. This decrease results from the larger level of chord length values, since the spanwise variations are essentially parallel.

The maximum thickness ratio of the wood blade design, as shown in figure 12(b), is slightly larger than that of the aluminum blade except near the tip, where it is smaller. However, because of the larger chord length at the tip, the maximum thickness of the tip of the wood blade is not significantly less than that of the aluminum blade (1.8 in. versus 2.16 in.).

Section maximum thickness ratio affects the aerodynamic performance of a wind turbine blade in two principal ways. First, the power generated at given wind and rotor speeds is influenced by the blade lift/drag ratio, which in turn, depends on the blade maximum thickness ratio. The variation of lift/drag ratio with angle of attack for the NACA 230-series airfoils (ref. 12) is shown in figure 13 for a range of maximum thickness ratios. Thus, the wood composite blade would tend to have slightly poorer aerodynamic efficiency over the inner and central portions of the blade, but better performance near the tip. However, since relatively more power is generated near the tip then over the inner sections, the overall difference in power generation between the two blade designs is not expected to be significant.

The second aerodynamic effect relates to the emergency shutdown situation, where the blades are feathered through negative pitch. The bending moment produced on the blade depends on the values of negative stall angle of attack and lift coefficient. These values are determined by the section maximum thickness ratio. The variations of maximum negative lift coefficient and its angle of attack with maximum thickness ratio for the NACA 230-series airfoils are shown in figure 14. The thickness ratio range for the effective length of the aluminum and wood composite blades are also indicated in figure 14. The wood composite blade would tend to generate less negative lift near the tip than aluminum blade, but overall differences should be small.

The most striking difference between the wood composite and aluminum blades is the twist distribution as shown in figure 12(c). The wood composite blade has much less twist in the inner portion of the blade, and will experience greater angle of attack in that region.

However, it is believed that any potential loss in performance in the inner half of the flow for the wood blade compared to the aluminum blade could well be offset by a gain in performance near the tip that would result from the smaller thickness ratios of the wood blade.

4.3 Hub Attachment

The design concept for transferring blade loads to the pitch control hub spindle (fig. 8) involved the use of threaded steel load take-off studs bonded into holes drilled in the thickened blade root. During the design phase, it was necessary to use an 18-inch long steel spool piece between the blade root and the hub spindle to provide the stiffness required to eliminate bending in the studs and in the blade spindle flange. The concept is shown schematically in figure 15.

Twenty-four studs are installed in the blade root at a diameter corresponding to the bolt circle of the spool piece. The threaded studs are bonded into tapered holes in the blade root end by means of an epoxy resin. In this approach, it is necessary to equalize the load along the stud and to keep the resin shear stress as low as possible. This can be facilitated by tapering the stud. A rounded Acme-type thread was machined on the tapered section of the stud to provide a mechanical inter-lock in addition to the epoxy bond. In view of the number of variables involved in the concept (e.g., length, taper, thread design, resin), tests were necessary to evaluate bonded stud performance. These tests would confirm and optimize design theory, provide data on stud fatigue life and failure mode, and qualify a candidate stud design.

A concern with this attachment concept is the need to assure that the stud axes are square with the flange and that the stud bearing shoulders are in the same plane to within less than ± 0.001 inch to each other. If this alignment is not obtained, the installation of the spool piece to the blade may result in bending in the stud shank and/or prestressing of the stud-to-epoxy interface, as shown in figure 16. Proper alignment for both the drilling of the holes and the installation of the studs is critical, and special fixtures and alignment plates are required for the successful construction of the blades.

4.4 Lightning Protection

In the event that lightning were to strike the blades, a possibility exists that local impact, burning, or moisture expansion due to heat could damage the blade. An aluminum screen (window type) will be bonded as a layer in the surface skin of the blade. The screen is then attached to an aluminum grounding strap at the root end of each blade. Flexible straps will then be used to bond the grounding strap to the wind turbine hub. This protective measure should provide a path for the electric current to continue to ground.

The lightning protection concept proposed for the wood composite blade was evaluated in simulated lightning-strike tests (ref. 13). A

full-scale section of the wood composite blade concept was subjected to high voltage and current tests. The 20-foot-long blade section was constructed with a laminated "D"-spar nose section and honeycomb core tail panels. The outer surface of the blade section was covered with a thin layer of epoxy resin-impregnated fiberglass cloth and full coverage aluminum screening. A small aluminum rod was inserted part way inside the leading edge of the spar to simulate internal wiring and other metallic components. Results of the tests (ref. 13) indicated that the proposed protection system effectively maintained the discharge currents on the blade surface and precluded penetration of the structure.

5.0 FABRICATION CONCEPT

Several fabrication concepts were studied before the final fabrication procedure was selected. The concepts studied and the trade-offs investigated during the design phase are herewith reviewed prior to the description of the final fabrication concept. The primary consideration in blade fabrication is the type of mold to be used for fabricating and bonding of the blade components. From the manufacturing standpoint, there are three major elements in the Mod-0A blade design: The "D"-section nose laminate; the tail panels; and the shear web. These elements, although joined together in the completed blade, present dissimilar manufacturing problems requiring different materials, procedures and blade fabrication tooling.

5.1 Mold Concepts

Choices. - During the fabrication development phase a decision was made to utilize female molds. The reasons were:

(1) Exact surface contour reproducibility can be maintained from blade to blade. Surface smoothness and overall blade fairness can be easily maintained once a set of accurate and fair molds are produced.

(2) Blade surface protection can be molded in place, which minimizes labor-intensive exterior finishing costs.

Two basic female molding concepts were evaluated: a three-section mold; and a two-section mold. The first, and early favored concept, was to divide the blade into three molded sections, as shown in figure 17. The sections are the front, load-bearing, D-shaped nose piece (with shear web), and two separate tail panels. This method necessitated three joining points to assemble the molded parts, two about one-third aft of the leading edge, and one at the trailing edge of the airfoil section.

The second molding concept (two-section) was to make the blade in two halves by splitting the NACA 230-series airfoil approximately down the centerline and utilizing two female half-shell molds, as shown in figure 18. The advantage of this concept is that only two external

joining points were necessary, one at the leading edge nose, and one at the trailing edge. The disadvantage of this approach is the problem of accurately machining an entire blade half in one operation.

Initially, it was believed that the female molding of three smaller parts in the three-section concept would be easier than molding two larger parts. In addition, the two-section process was thought to have other complications such as the installation of the shear web and the difficulty of machining six mating surfaces all to fairly close tolerances. Exact dimensions were necessary so that all parts would mate properly during the final bonding operation.

Both of the blade mold concepts produce essentially the same exterior blade shape and interior structural configuration. Both of these molding concepts rely on vacuum bag pressure as the clamping medium during curing of the bonding resin. This is shown schematically in figure 19. A vacuum bag is assembled into the mold over the parts to be bonded and sealed to the edges of the impervious female mold structure.

Selected concept. - The two-part half-shell female blade mold concept was chosen over the three-part concept because of the improved potential for lower manufacturing costs and blade quality. In addition, a solution was found for the problem of accurately machining an entire blade half in one operation. A concept was proposed which utilized a custom built horizontal bandsaw with movable guides that would be capable of accurately trimming an entire half blade in one cutting pass. This bandsaw, as shown schematically in figure 20, is designed to rest on a set of rails positioned at the outer perimeter of each of the half-shell molds so that it can accurately traverse the length of the molds with the saw blade held in the proper cutting plane. It is believed that great accuracy can be achieved with this trimming concept provided that the rails are installed accurately onto the female mold and that the bandsaw is provided with blade guides to insure the proper cutting plane is maintained. A second advantage of the bandsaw trimming concept is that all other interior pieces can be installed in each blade half and trimmed simultaneously while the leading and trailing edges of the blade are trimmed.

It was determined that the trimming point or "cut line" of the bandsaw blade cannot follow the true chord centerline of the airfoil section. The reason is that the chord centerline allows a slight reverse to occur in one of the blade half sections which would cause some unnecessary trouble during female molding. The solution is to establish the cut line from a point at the very leading edge of the airfoil section to a point in the center of the trimmed trailing edge. This departure of the "cut line" from the "chord centerline," while minimal in dimension, simplifed the two-half shell fabrication concept.

Another significant advantage of the two-part half shell mold concept over the three-part concept is the ease of exterior finishing. Blending in the bond joint line between the two half-shell blade parts appeared to be relatively easy at both the leading and trailing edges.

With the three-part molding method, joining lines positioned at 25 to 30 percent aft of the blade leading edge on both the high and low pressure sides were thought to present a potential time-consuming blending problem. Optimization of the female molding concept to produce the best finished surface at the least labor cost is considered highly important in the fabrication procedure. This factor became a major driving force in the evenutal evolution to the two-part female mold concept.

5.2 Nose Piece Laminate

The "D"-section nose piece extends from the leading edge to approximately the point of maximum airfoil thickness (29 percent of chord at Station 150 to 38 percent at Station 750). This section is to be constructed as a curved laminate of bonded strips, as indicated schematically in figures 17 and 18. The material selected for the "D"-section laminate is Douglas fir (in the form of sliced veneers) which accounts for approximately 70 percent of the blade weight. Many species of wood were considered for this application, but the Douglas fir species best fit the following criteria:

(1) Be readily available with a guaranteed long-range supply for large volume production;

(2) Be available at a low cost on a per pound basis;

(3) Have good physical properties for its weight;

(4) Be compatible with the blade manufacturing procedure.

The Douglas fir species has excellent physical properties for its weight with unusually high stiffness and compressive strength factors, as will be shown later. Its specific gravity of 0.5 appears to be ideal to provide a shell thickness that is sufficient to resist buckling loads without adding any unnecessary weight at the 62-foot Mod-0A blade size.

Douglas fir is a tree indigenous to the Northwestern states that is considered a renewable resource because it is being replanted at a rate that exceeds the annual harvest. This species of tree grows in such a manner that a large portion of its bulk can be used to provide the high quality veneer stock necessary for wood composite wind turbine blade construction.

The most economical method of utilizing the Douglas fir wood material with the female mold vacuum bag process had to be determined. Sawn stock, both square and rectangular in shape, was first investigated but soon rejected because of several potential problems that were not readily solveable. First, there was no developed efficient adhesive application method for the sawn stock. Another problem was the likelihood of gaps occurring between the stock edges as it is compressed into the female mold (a male mold would not present a problem in this regard, because the vacuum bag compression would tend to reduce the gaps between the stock). The difficulty of getting the sawn stock to conform to the

tight nose radius was also a factor, especially when the small size to which the stock had to be sawn is considered.

The use of Douglas fir veneer stock then became the first choice because of ready availability from a well-established veneer industry that provides materials for the molded ply and sheet plywood industries. High production equipment already exists for necessary manufacturing steps such as veneer preparation and adhesive application. Finally, initial test runs performed under the contract showed that the use of veneers was compatible with either of the candidate female molding processes.

Veneers are manufactured using two primary methods. The first and most expensive is to slice the veneers from a log that has been sawn into sections. Rotary cutting of veneers is the second and most common veneer cutting method and also the least expensive. A log is positioned in a lathe-type machine and spun against a knife that slowly moves in towards its center, peeling off a given thickness of veneer with each revolution of the log.

The type of cut, sliced or rotary, and the thickness of veneers to be used was determined by testing laminated specimens. Veneers of 1/8-inch thickness, or greater, were examined initially because of fewer adhesive bond lines for a given laminate thickness. Fewer bond lines would produce a lower weight laminate and reduce both material and labor costs. Difficulty was detected in some of the early test laminates in conforming the thicker veneers to some of the sharper curves in the female mold. While most of the blade has gentle curves that are easily negotiated by this thickness of veneer, the leading edge of the airfoil in the outer 40 percent of the blade presents a very tight bend that can only be negotiated by a thinner veneer. Further laminate testing determined that a sliced veneer thickness of 1/16 inch or a rotary veneer thickness of 1/10 inch was the maximum thickness that could be molded into these tight curves with the facuum bag pressure available. The 1/16-inch thick sliced Douglas fir veneer was selected as the laminate material.

The sliced veneer has the advantage of being sliced across the grain thus making it very stable, which is thought to reduce the clamping pressures necessary for bonding. Sliced veneers can be obtained in a length up to 17 feet. The main limitations of the rotary cut veneer is its relatively short length (slightly over 8 ft) and its more wavy make-up due to cutting tangentially with the grain instead of across the grain, as is done with the sliced veneer. The better veneer conformity in the mold and the longer available length (which reduces the number of butt joints) were the principal factors in the choice of the sliced veneer for the blade fabrication effort.

Because sliced veneers inherently have varying widths, depending on the width of the sectioned log, two or more edge trimmed veneers are temporarily bonded edge-to-edge by using a "stiching" machine that lays a resin preimpregnated thread in a zig-zag pattern along both edges of

adjoining veneers. This provides veneers of suitable width for blade fabrication. The stitching remains in place during blade fabrication. The effects of stitching thickness on veneer bond line thickness variations is negligible.

5.3 Tail Panels

To develop the best aeroelastic stability in the Mod-0A blade, it is advantageous to keep the chordwise center of gravity as far forward as possible. While a large percentage of the blade weight is already concentrated in the forward "D"-section laminate, it was still considered worthwhile to develop lightweight tail panels that would help to provide a forward center of gravity. Other design drivers for developing candidate tail panels were as follows:

(1) Structural adequacy

(2) Manufacturing labor costs

(3) Ease of manufacture with the female mold concept

(4) Material cost

(5) Tooling cost

(6) Applicability of the chosen tail panel concept for use with both larger and smaller blades.

Choices. - Nine different tail panel configurations were investigated. All of these tail panels are classified under one of three basic configurations, that is, unsupported, partially-supported, and fully-supported. The unsupported panel concept is the simplest and least expensive option, but also produces the greatest weight for the amount of buckling resistance offered. All of the tail panel configurations examined under this concept required at least a 3/8-inch thickness of solid wood to provide the necessary strength and stiffness to prevent buckling in the tail panel near the root. The combinations that were considered for the unsupported panel were: (1) low-density single sheet Okumme plywood; (2) laminated low-density Western red cedar veneer; and (3) laminated Okumme plywood (two to three plies). Trade-off studies for the competing methods involved balancing the labor and material costs against panel weight.

The trade-off studies showed that a significant amount of weight could be reduced by partially supporting the tail panels to increase buckling resistance. Among the options considered for this type of support were: (1) longitudinal stringers with bulk-heads; and (2) periodic ribs made either with laminated wood or with the use of a honeycomb core. Both material and labor costs were shown to be unacceptable for the partially-supported tail panel concept.

The fully-supported tail panel was explored in detail because this concept offered the best potential for both lightweight and low-cost construction. All of the options considered required the use of a core material (honeycomb) to form a sandwich panel up to 1 inch in thickness. Three different core materials were evaluated: PVC (polyvinylchloride) foams; balsa wood; and resin-impregnated Kraft paper honeycomb. Both plywood and laminated veneer of various species were considered as the inner and outer skin material for the cored laminate. Because coring was to be incorporated, the use of a high density species such as birch for the skins would produce the most structurally efficient panels.

Full coring of the entire inner volume of the blade tail was also considered, but was not thought to be practical because of the large section thicknesses involved and the resulting heavier than necessary weight. However, this option looked promising for the outer blade area toward the tip where sections are thin.

Selected configurations. - The chosen tail panel configuration is a fully-supported cored sandwich section that utilizes a resin-impregnated Kraft paper honeycomb (Verticel brand) as a core material with 1/8-inch thick birch plywood as the inner and outer skin material, as shown schematically in figure 21. This three-piece laminate is bonded together in the female mold using the same resin that is used to construct the rest of the blade. This configuration was chosen when it was determined that it could be assembled with reasonable fabrication and material costs. It produced the most structurally efficient tail panel at the lowest weight of any of the options considered.

Near the tip of the blade, the blade thickness becomes thinner and the inner birch plywood sheets become less effective. Consequently, from Station 600 to the tip (Station 750), a fully cored tail panel, as shown schematically in figure 22, was selected. Adoption of full internal coring in the outer tip area provides both weight savings and extreme shape rigidity in the part of the blade which experiences the highest airloads and produces the most energy. Another significant advantage of full coring the tail panel in the tip area is the improvement of the chordwise center of gravity location. In the tip region the "D"-section assumes a larger percentage of the airfoil section (x/c increases to 0.38), so that the center of gravity tends to move aft. Full coring, with its lighter relative weight, tends to minimize this shift. The cored panels taper linearly between Stations 500 to 600 so that there is a transition between the fully-supported cored panel and fully-cored blade tail.

5.4 Shear Web

The shear web piece, which is made of 1/4-inch thick birch plywood, provides rigidity to the overall structure (e.g., fig. 18). A Douglas fir stringer, made from scarfed and overlapped dimension lumber, is used for the bonded interface between the shear web and tail panels (fig. 21).

Between Station 150 and the blade root, a buildup occurs in the shear web. The purpose of the buildup is to provide a thick section at the root end to provide sufficient structural thickness to support the imbedded load take-off studs. The web buildup consists of blocking and stringer pieces made of Douglas fir stock, as shown schematically in figure 23. The buildup is thickest at the root end and is step tapered to zero t station 150. The open root end is capped with 1/4-inch thick (five-ply) birch plywood. The truncated aft end of the blade is also covered with a bonded 1/4-inch birch plywood tail cap section.

5.5 Fabrication Procedure

Blade fabrication consists of two major activities: a preparation of materials; and assembly, bonding, and finishing of the complete blade.

Material preparation. - Materials preparation is the most time consuming step of the manufacturing procedure. Preparation of the veneers, which make up a significant portion of the blade weight, requires the most labor. The preparation of plywood and sawn wood stock, while not requiring much equipment or labor, will require a significant amount of floor space for efficient handling.

The following is an outline of material preparation procedures:

(1) Veneer preparation
  (a) Select veneer of adequate quality and trim to straighten longitudinal edges
  (b) Stitch veneers together as required to achieve mold width
  (c) Trim butt joint ends
  (d) Assemble veneers on layout table with adequately staggered butt and longitudinal joints
  (e) Final trim one edge of layout pile
  (f) Inspect and assemble veneer layers for run through glue machine

(2) Plywood preparation
  (a) Cut to size 1/8-inch birch plywood for nose laminate
  (b) Cut to size, scarf edges and bond together 1/8-inch birch plywood panel for tail assembly
  (c) Cut to size and scarf 1/4-inch birch plywood for shear web

(3) Wood stock preparation
  (a) Cut to size Douglas fir dimension lumber for root end buildup
  (b) Make joining cleats on shear web
  (c) Cut to size Sitka spruce stock for trailing edge stringer
  (d) Cut to size Douglas fir stock for stringers aft of shear web

(4) Core preparation
  (a) Precut 3/4-inch Verticel core material to fit in tail area
  (b) Precut 3-inch core material for outer solid tail area

(5) Preparation of glass cloth and wire screen
  (a) Precut layers of 10-ounce glass cloth to proper size in preparation for mold insertion
  (b) Precut aluminum lightning protection screen for insertion in mold

Fabrication sequence. - Blade fabrication is to begin with the molds coated to about 4 mils thickness with while pigmented WEST (R) epoxy resin. This resin will be allowed to partially cure before the glass cloth and lightning protection screen are placed. With the outer skin ingredients completed, all of the prepared wood parts will be installed in the mold and vacuum bag pressure applied. The pictorial sequence of figures 24 and 31 is used to schematically detail these operations together with the subsequent operations necessary to complete the blade. Details of the assembly sequence are as follows:

(1) Material loading. Materials are inserted into two separate half-shell molds. The mold is first coated and allowed to partially cure with a white pigmented epoxy. This provides an erosion-resistant and light-resistant outer skin on the blade. Then, as shown in figure 24, the glass cloth and aluminum lightning protection screen are inserted in place (each layer is coated with adhesive), immediately followed by the outer tail panel with shear web and stringer. This assembly must be accurately located and temporarily attached with staples so that it will not move under subsequent molding pressures. The rest of the prepared wood stock is placed in the mold, as shown schematically in figure 25. Included in this operation are the nose veneers and the inner plywood, core, and stringer pieces of the tail panel. All wood pieces are coated on all sides with the epoxy adhesive prior to being placed in the mold.

(2) Vacuum bag pressure. As shown schematically in figure 26, the vacuum bag is applied over the entire assembly and sealed along the edges. Air is evacuated between the bag and the mold to create the proper molding pressure. A vacuum is maintained until the adhesive is fully cured.

(3) Wood buildup for studs. The Douglas fir root end buildup for stud installation is bonded into position, as shown in figure 27. The buildup consists of a stringer piece forward of the shear web, and a blocking piece aft of the shear web. This buildup extends into the blade to Station 150, tapering in a linear manner to a zero addition.

(4) Trimmings. After bonding of the blade elements is completed, a band saw is set on tracks that are positioned on the outer perimeter of the mold, as shown in figure 20. The two blade halves are trimmed to an exact centerline dimension by the saw blade. The blade surfaces are then planned to remove surface irregularities caused by band sawing.

(5) Blade assembly. After the upper and lower blade halves are fabricated and trimmed, a dry fit operation is performed to assure proper blade assembly. Contact areas are then primed and coated with epoxy, and the two halves are bonded together, as shown schematically in figure 28. Afterwards, the truncated open blade end in the root section is covered by bonding the transom piece to the exposed ends of the nose piece (fig. 29).

(6) Root end close-out. The blade is placed in a holding fixture, accurately aligned, and then the root end is machined in preparation for stud hole drillings, as shown in figure 29. A step-tapered drill attached to a guideplate (accurately aligned with the blade axis) is positioned at the blade root end, as shown in figure 30. Holes are drilled separately in the root end by rotating the guide plate to each indexed location. The steel studs with centering nuts are attached to the guideplate, as shown in figure 31. Adhesive is then applied to both the holes and the studs, and they are then inserted in the holes of the blade root. Insertion is made with the hydraulic ram. The guideplate and the centering nuts are removed after the adhesive has cured.

(7) Finish and balance. The outer surfaces of the blade are finished by trimming and sanding, and the complete blade is installed in a fixture so that proper blade-to-blade and center of gravity balance can be checked and achieved.

As indicated in figure 10(a), the blade is to be constructed to an overall length from hub end to tip of 718 inches. However, as indicated previously, it was necessary to insert an 18-inch spool piece between the blade end and the pitch control spindle (fig. 15). The tip of the blade would therefore be shortened by 18 inches in order to maintain the maximum blade radius of 62.5 feet. The cut section of the blade tip would then be capped by a plywood rib.

5.6 Quality Assurance and Inspection

To assure the blades meet all engineering specifications, a quality assurance program will be implemented during material preparation and blade construction. A quality assurance program must typically contain three main categories:

(1) Specification and inspection of materials

(2) Written procedures for critical phases of production

(3) Inspection of blades during production

Before quality blades could be built, material of adequate properties must be specified and obtained. The wood purchased must be sound, of correct species, with acceptable moisture content, and then properly stored while awaiting construction. The adhesive resin and hardener types should be certified chemically correct before acceptance, and be dated so that shelf life is not exceeded. The resin and hardeners should also be color toned so that mixed adhesive can be visually discerned from unmixed

resin, and so that resin and hardener cannot be mistaken for one another. Other ingredients used as fillers and additives in uncured adhesive are to be certified by the original manufacturers that the material complies with all specifications. Containers and invoices should state both material and shelf life dates, if applicable. The metal studs should be manufactured in accordance with drawings which will instruct the supplier as to material, composition, hardness, dimensions, tolerances, finish, and any nondestructive testing required. The vendor shall certify that the studs delivered comply with drawing specifications.

During the blade molding process, there are many opportunities to inspect the quality of the blades being constructed. Tolerances for shape and twist are controlled by the molds. During the molding sequence, quality control of adhesive coating are continuously performed. The blade should be inspected during several key phases of production. After each vacuum process, the exposed joints can be inspected for flaws or gaps. Suspect areas of poor lamination usually reveal themselves at the surface, since the adhesive sags away from the surface leaving bubbles or gaps. Before gaps are filled, investigation of void extent can be performed by using small probes or drilling along the suspect joint. After investigation, the voids along with any probe areas should be filled with an adhesive mixture.

The final quality assurance technique is to ensure that all components and operations have been accomplished and checked before construction progresses. Several tools may aid in the performance of this function. For complex operations such as axis alignment and drilling of root studs, detailed procedures should be developed and followed. In addition, at major steps such as blade half-shell bonding, check lists should be followed to reveal any defects before the process continues to a point where access has been limited.

6.0 MATERIAL PROPERTY DATA

The selected blade design concept involves a number of different materials such as Douglas fir, birch, steel, epoxy resin, and honeycomb core. The physical and mechanical properties of these materials are described below.

6.1 Wood

Basic properties. - The basic building material in the wood composite blade is Douglas fir, which has the following nominal properties at room temperature and in the dry (12 percent moisture content) condition:

Density: 32.5 lb/ft^3 (specific gravity, 0.52)

Compression: 7,500 lb/in^2 (parallel to grain)

Tension: 15,000 lb/in^2 (parallel to grain)

Shear: 1,200 lb/in^2 (parallel to grain)

Elastic modulus: $2x10^6$ lb/in^2

These values were obtained from tables 4-2 and 4-6 in reference 14 with adjustments for the effect of the epoxy in the laminate.

For equivalence with the parallel-to-grain mechanical properties of fir given above, other common structural materials, on a per unit-weight basis, would need to exhibit the following properties (in lb/in^2):

Material	Compression	Tension	Elastic modulus, $x10^6$
Steel	112,500	225,000	30
Aluminum	38,900	77,800	10.4
Fiberglass composite	27,400	54,800	7.3

Those familiar with typical properties of steel, aluminum, or fiberglass will recognize that the strength of Douglas fir in the grain direction is most competitive. However, the cross grain strength of fir is up to 50 times less than the grainwise direction. Thus, for wood structures, care must be taken to align the major forces and material and to insure that cross-grain strength is not exceeded.

Birch plywood is used in areas where a balance of cross grain strength is desired, or where the use of plywood can save installation time with adequate performance. When plywood is used, the strength value must be used according to the proportionate wood grain direction in the plies. The two major structures made of plywood in the wood composite blade are the shear web and tail panel faces. The shear web is balanced ply, while the tail panel faces are unbalanced. (A balanced plywood sheet has equal amounts of grain-oriented wood running in both major directions.) Although the birch used is approximately 20 percent heavier than an equal panel of fir, birch has almost 70 percent greater shear strength than fir. The ability to change strength characteristics by alteration of wood species is one of the major advantages of wood composite blade construction.

Nominal properties of dry (12 percent moisture content) yellow birch at room temperature are:

Density: 38.7 lb/ft^3 (0.62 specific gravity)

Compression strength: 8,200 lb/in^2

Tension strength: 20,000 lb/in^2

Elastic modulus: $2x10^6$ lb/in^2

Values (except tension) were obtained directly from table 4-2 of reference 14. Tensile strength parallel to the grain was estimated from the modulus of rupture (16,600 psi) and the ratio of tensile strength to modulus of rupture for similar woods (~1.2).

The low density of wood means that a relatively large volume of material must be used for structures. As a consequence, wood structures entail large material thicknesses as compared to metal structures. Therefore, buckling stability, which is related to the cube of the material thickness is rarely a problem in a wood structure. For the wood composite blade for wind turbines, the material thickness required for the structural loads is more than adequate for buckling prevention.

Effect of moisture and temperature. - Increased moisture and temperature have an adverse effect on wood static properties. Commercial dried wood normally has a moisture content of about 12 percent, as compared to fiber saturation values of about 24 percent for fir and 27 percent for birch. As indicated previously, nominal strength properties for wood are given for the condition of 12 percent moisture content. The strength properties of wood decrease significantly with increasing moisture content. For example, for birch and Douglas fir, an increase in moisture content from 10 to 15 percent results in about a 25 percent decrease in strength in compression.

Moisture absorption can also change the dimensions of the wood which can have a secondary effect on strength (e.g., stressing of fibers at joint). It is important, therefore, for a design to determine either the probable wood moisture content that would result from the exposure to the environment of the application, or, if the part is coated or laminated, the long-term equilibrium moisture content of the wood.

The key to the successful use of wood in a variable atmospheric environment is the adoption of measures to seal the structure from moisture absorption. As indicated previously, the blade outer surfaces are covered by fiberglass cloth, aluminum screen, a 4-mil thickness of epoxy resin and polyurethane paint. In addition, each surface of the individual wood blade components is to be coated with epoxy resin during the fabrication process. The inner surfaces will have two coats of epoxy resin. This coverage serves as a retardant to significant moisture penetration and minimizes attendant moisture-related problems such as cracking, checking, delamination, and rot.

In general, the mechanical properties of wood decrease when wood is heated and increase when it is cooled. This effect is immediate, and at temperatures below 200° F, it is reversible. Also, below 200° F, the mechanical properties vary linearly with temperature. Furthermore, the strength variation with temperature depends on the moisture content.

Figure 32 shows the temperature effect on strength and modulus of elasticity of wood in general, as given in reference 14. The variations are expressed for two levels of moisture content as percent of value at 68° F (room temperature). The trends illustrated are from studies on three strength properties - modulus of rupture in bending, tensile

strength perpendicular to grain, and compressive strength parallel to grain. The bands in the figure represent the variability in reported results. There was no indication in the reference whether the slope of the variation would continue to steepen with moisture content greater than 12 percent.

Specifically, the temperature effect on design properties of wood will depend on the local temperature at the critically stressed area. For a wind turbine blade stressed in bending, the outer fibers are subjected to the greatest loads. The outer fibers are also those subjected to direct contact with the ambient environment. Thus, it is clear from figure 32 that wood strength degradation can be severe for conditions of high temperature and humidity, as would be the condition in a damp tropical environment. In a desert environment, the dry air would tend to counteract the effect of the elevated temperature. However, if the blade has a protective coating, the temperature effect may also depend somewhat on the moisture content of the wood at the time of application of the coating.

For the Mod-0A blade design, the specifications call for adequate performance up to 120° F. Such temperatures are most likely to occur in desert areas. For such sites, the air is very dry, so that wood moisture content is expected to be lower than 12 percent. A 12-percent moisture content is more likely at a site near a warm-climate coast, such as the Gulf states or Hawaii, where peak temperatures are closer to 100° F. This condition is shown in figure 32. The figure also shows that the strength reductions resulting from the Gulf-coast environment should adequately represent the desert site as well. Thus, the wood design environment for the Mod-0A blade was taken as 100° F and 12 percent moisture content. Accordingly, for static loads such as for a hurricane gust or emergency shutdown, the wood property reduction factor for elevated temperature was taken as 0.8 of the nominal value for strength, and 0.9 of the nominal value for modulus of elasticity (fig. 32).

Fatigue. - Cyclic fatigue is a factor which must be considered when utilizing wood for the design of wind turbine blades. By its very nature as a fibrous material, wood is not subject to the kind of fatigue crack propagation that is common in metals. It cannot be discussed in terms of yield strength, but must be viewed in terms of crushing or tearing of fibers. Also, crack propagation due to stress concentration should not be a significant problem in wood laminates. If some fibers are damaged, the load is generally distributed among adjacent fibers without high stress concentration in the damaged area. Crack propagation is inhibited in laminated structures because of the adhesive bond lines which must be crossed. Also, minor surface flaws or damage, which would cause stress concentrations in a high-density material, can be disregarded in an equivalent-weight wood structure because of its cellular composition.

Fatigue strength for the wood composite blade design was estimated from the data of reference 15. This reference presents fatigue data for several wood species in terms of the ratio of stress at fatigue failure to the ultimate modulus of rupture of 75° F (very close to reference

temperature of 68° F). After correction to ultimate compressive strength (compressive strength is less than modulus of rupture), it was determined that an appropriate design value of ratio of fatigue stress at $4x10^8$ cycles to nominal compressive strength for Douglas fir was 0.3. It was further determined that the knockdown factor for fatigue strength due to the design environment (100° F max. temperature, and 12 percent moisture content) should be 0.9. This adjustment factor represents less of a reduction in strength than for the static loads (factor of 0.8) because of the periodic variations in temperature (from about 20° to 100° F) during the operating life of the blades.

Creep. - Creep in wood is another factor which may significantly affect a wood structure or blade. Wood, like other materials, will continue to deflect or elongate after the initial load has been applied. Creep variations in wood, as obtained from reference 14, are shown in figure 33 for three nominal stress levels. It is seen that the deflection from creep may vary from 0.5 to 1.0 times the initial deflection, with full creep reached from 300 to 400 days.

The creep behavior is approximately the same for all wood species, with creep at low stress levels being similar in bending, tension, or compression parallel to the grain. Ordinary climatic variations in temperature and humidity will cause variations in the creep rate. According to reference 14, an increase of 50° F in temperature can produce a two- to three-fold increase in creep. Creep will, therefore, have to be considered in a blade design if the blade will be subjected to a static working load for a long length of time.

The weight of the blade is also a consideration for the effect of creep on the blade structure. This effect is minimal during normal operation, since the stresses are cyclic and are in a given direction for a very short time. However, creep can be a factor if the wind turbine is shut down for an extended period of time. If the blades are parked horizontally and feathered, one blade would deflect toward the high pressure side, while the opposing blade would deflect toward the low pressure side. This could create an out-of-plane imbalance between blades and increase the centrifugal force component of bending stress when operation is resumed. To avoid this problem, the blades should be parked in a vertical position when not in operation, or they should be allowed to rotate freely while fully feathered so that all orientations are experienced. When in the vertical position, the out-of-plane stresses due to weight will be negligible and creep deflection of either blade will be inconsequential.

Wood is also subject to creep rupture in which a sustained steady load, lower than that corresponding to the static ultimate strength, can produce failure after an extended period of time. A wood member under a continuous bending load for 10 years can carry only about 60 percent of the load required to produce a single cycle-to-failure load in the same specimen loaded in a standard bending strength test (ref. 14). For the assumption of linear variation with time, the fatigue strength at the blade design life of 30 years would be around 55 percent of the static value. Thus, the creep rupture strength may not be as severe a factor as the cyclic fatigue strength.

6.2 Other Materials

Hub attachment studs. - The load take-off studs for attachment to the hub are to be made from heat treated steel alloy SAE 4140. The result is a high strength stud with good toughness characteristics. Strength values for SAE 4140, oil quenched are:

Rockwell hardness: C40-C42

Ultimate strength: 186,000 psi minimum

Yield strength: 160,000 psi minimum

Bonding agent. - The bonding agent used to bond the studs into the blade is the WEST System(R) epoxy system formulated and distributed by the blade design contractor (Gougeon Bros., Inc.). Basic physical properties of this epoxy system are:

Density: 71 lb/ft^3 (1.14 specific gravity)

Tensile strength: 6,500 lb/in^2

Compressive strength: 7,000 lb/in^2

Ultimate elongation: 8 to 9 percent

Hardness (Rockwell M): 73

Elastic modulus: $3x10^5$ lb/in^2

Ultimate shear strength was not specifically measured for the bonding resin. However, a value of 7,000 psi was estimated from consideration of the ultimate tensile and compressive strengths of the resin and the ultimate shear strengths of similar epoxies.

Unlike wood, the bonding resin is stronger in compression than in tension. The resin, therefore, reinforces the wood fibers to increase compressive strength. The bonding resin acts as a moisture barrier and helps protect the wood from high-moisture-content effects as well as from the effects of salt spray, fungus, and sunlight. Furthermore, the epoxy resin coating provides a hard surface which resists local denting when used with a surface skin of glass cloth. This same coating produces an aerodynamically smooth finish for the blade surface.

Two types of hardeners are used with West System epoxy resin to produce the desired pot life of the adhesive. Hardener types 205 and 206 provide short and long resin cure times, respectively. The physical properties of the epoxy resin systems after cure are within 10 percent of each other, with the 105-205 mixture being the stronger of the two. Several types of fillers are also used with the epoxies to modify the physical characteristics by reinforcing the resin. The fillers change the viscosity of the resin formulation which is important in maintaining position of the mix until cure is completed. A matrix of data describing

the effect of various fillers on density and elastic modulus is given in Table II.

Honeycomb core. - The structural honeycomb material proposed for use in blade fabrication is made from a phenolic reinforced Kraft paper. The core material used is manufactured by the Verticel Company and is designated by the number 1/2-60-60-15. The first number (1/2) refers to the cell size in inches. The next two numbers (60-60) refer to paper weight used. The last number (15) represents the phenolic resin content by percent weight. Properties are:

Density: 1.54 lb/ft^3 (0.025 specific gravity)

Longitudinal shear strength: 45.1 lb/in^2

Longitudinal shear modulus: 5,843 lb/in^2

Transverse shear strength: 15.1 lb/in^2

Transverse shear modulus: 1,880 lb/in^2

Compression strength: 32.0 lb/in^2

The Verticel$^{(R)}$ honeycomb core resists compression and deformation, and when bonded between panel skins, it increases panel stiffness by resisting movement of the load-carrying skins.

7.0 KEY COMPONENT TESTS

Two of the key components of the blade design concept, the nose piece laminate and the hub-to-root attachment, were of such significance to the ultimate success of the blade, that tests of their performance were conducted. In addition, several material sample tests were conducted to obtain design property values for the materials that would be used in blade construction, such as the filler and resin combinations for the adhesive described in the previous section on material properties.

7.1 Veneer Joints

Because the 1/16-inch thick Douglas-fir veneers used for the nose piece laminate (main structural beam member) have a maximum length of about 18 feet, lengths of veneer strips are butt joined with adhesive to provide the materials used for blade construction. Although care is taken to stagger these joints so that adjoining plies do not align, it was regarded significant to test samples of multiple butt joints for static strengths. The tests also determined the effect of joint gap width on laminate strength.

According to the values the previous section on material properties, the compressive strength of the bonding resin (7,000 psi) is about the

same as the compressive strength of the fir (7,500 psi). However, the resin tensile strength (6,500 psi) is substantially less than that of the fir (15,000 psi). Tension, therefore, is the critical concern for the butted veneer joints. When heavily loaded in tension, a laminate sample would fail at the location with the least amount of cross-sectional wood fiber.

In order to investigate the tensile strength of butted joint veneers, samples were constructed for the most adverse case of 50 percent aligned joints. This is illustrated in figure 34(a). Two gap widths were used. A small gap refers to the separation when the veneers are tightly butted, while a large gap constitutes a space of 1 to 2 veneer thicknesses. In both cases the gaps were filled with adhesive.

The butt-joint test specimens were approximately 1 in. by 1 in. by 12 in. long, and were tested to failure (modulus of rupture) in simple beam bending with a central load. The test load was applied in the plane of the sample at the center of the edge. A specimen with continuous veneers was also tested to provide the reference value for no butt joints. Three replicates were used for each configuration.

Test results revealed that the 50 percent jointed specimen had approximately 70 percent of the strength of the specimen without joints. For a modulus of rupture type of failure, this result implied that the behavior of the jointed configuration was related to loss in cross-sectional area alone, and that there were no adverse interactions in the region of the joints. Thus, the laminates can be considered to be free of any stress concentration or notch effects. The tests also showed no significant differences between the performance of small and large gap joints, as long as the joints were accurately aligned.

In applying the preceding results to the blade design, the blade was considered as a cantilevered wood beam with joined veneers, as shown in figure 34(b). The bending moments induced by wind, centrifugal, or gravitation forces cause the laminations on one side of the neutral axis to be in tension, while the opposite side is in compression. Since no adverse effects are caused by butt joints under compression, the compressive capability of the lamination is not affected. The tension-side strength is affected, but only in proportion to the reduction in cross-sectional area. During lamination of the veneers, the chance of alignment of more than two neighboring butt joints is statistically remote, and the chance of 50 percent alignment should be effectively zero. Thus, the first failure in the beam would still be the crushing of wood fibers on the compression side of the laminated beam.

These veneer tests did not take into account the long-term effects of fatigue from cyclic loading on the aligned butt joints. The results from this most adverse case of 50 percent aligned joints indicated that stress concentration effects arising from the butt joints should not be a major factor. However, the fatigue strength of the veneered laminate is expected to be lower than that of the corresponding solid material.

7.2 Hub Attachment

The root-to-hub attachment concept of transferring blade loads through studs bonded into the blade root (fig. 15) is a key structural feature in the design, and a better understanding of this concept was required. Therefore, an extensive bonded-stud testing program was performed at an early phase in the blade design process. These stud tests are described and analyzed in reference 16. The stud investigation involved two phases: tests on individual stud samples for both ultimate load-carrying capability (pull-out load) and fatigue strength; and bending tests of a 20-foot-long, full-scale inboard blade section.

Load take-off stud tests. - In the first phase of the stud test program, a number of single-stud test specimens were constructed to define problem areas, explore the many variables involved, and establish a baseline test configuration. These samples were typically constructed of a wood block 4 in. by 4 in. by 24 in. long in which a hole was bored in one end. A threaded steel stud was then inserted in the hole, held in alignment, and bonded in place with WEST System(R) epoxy adhesive. Variables evaluated included the type of wood construction (solid, laminated veneers), the epoxy/filler system used to bond the stud in place, the stud configuration (length, diameter, taper, imbedded thread), and the hole configuration (straight, tapered, step-tapered).

The experimental evaluation of stud configuration was supported by theoretical analysis. The critical strength property for the hub attachment is the shear stress in the epoxy generated by the axial load produced by the blade bending moment at the root. Epoxy shear stress varies along the length of the stud, with peak values at the ends of the stud due to stress concentration effects. A representative value of peak shear stress in the epoxy was calculated from a finite-difference computer program developed by the blade contractor. This analysis treated the steel stud and the epoxy as linear elements with variable elasticity. The peak shear calculation was used to select improved stud/hole geometries through better balancing of wood and stud stress distributions along the length of the stud.

The baseline stud and block configuration that evolved from these early tests and studies is shown in figure 35. Both the stud and the wood hole were tapered, with an imbedded length of 15 inches. The studs were turned from 2¼-inch diameter bar stock to provide a 2-inch diameter threaded section which could be directly adapted into the test machine. The test block was constructed of laminates made from 1/8-inch-thick Douglas-fir veneers trimmed to the 4-in. by 4-in. by 24-in. size. The wood grain was oriented parallel to the load direction. It was also found that a thin cap of birch plywood bonded to the open end of the laminated fir block prevented cracking of the wood longitudinally, and resulted in a substantial improvement in the stud pull-out load. A photograph of several test studs is shown in figure 36.

A second set of stud samples with the baseline configuration of figure 35 was then tested for ultimate load-carrying capability and fatigue. These test specimens included studs with various amounts of taper and

different thread geometries which were designed to lower the stress concentration in the adhesive. The effects of a mold release agent and several epoxy fillers were also evaluated.

The result of this second phase of the investigation was a tapered stud with significantly improved fatigue performance, even when the stud was treated with a mold release agent so that no adhesion action was present. About 3×10^6 cycles were obtained at a maximum load of 35,000 pounds. An endurance load of up to 28,000 pounds was estimated for the blade design life of 4×10^8 cycles. The improved stud configuration also sustained a pull-out load of at least 70,000 pounds. Both the fatigue and pull-out test loads were considered satisfactory for the blade design loads determined at the time of the tests.

Full-scale blade section tests. - The stud attachment concept was also tested in a full-scale, 20-foot long blade section which contained the entire root end with imbedded studs. The studs were untapered with 1-in. diameters and 15-in. lengths in the imbedded portion. The stud shank had 3/4-in. diameter threads on the head portion. Wood thickness in the laminated sections around the studs was 3.0 inches. This blade section was tested at the NASA Lewis Research Center for load capability and deflection in the edgewise, flatwise, and combined modes. Following these tests, the blade was shipped to the U.S. Army Research and Technology Laboratories at Fort, Eustis, Virginia, for fatigue testing. The blade was cantilever mounted with the load applied at the free end. The blade chord was set at 45 degrees to the load in order to approximate the combined application of flatwise and chordwise design loads. A steady-plus-cyclic loading profile was used. These tests are described in reference 16.

After initial problems due to test fixture flexibility, the blade was cycled 1×10^6 times without failure at loads that produced bending moments of 8×10^4, 11×10^4, and 14×10^4 foot-pounds. The respective maximum tensile loads on the studs were 8,590, 11,810, and 15,040 pounds. Failure at a high stress concentration in the steel stud occurred at 0.67×10^6 cycles with an applied moment of 20×10^4 foot-pounds (21,480 lb maximum load on the stud). The conclusion reached from this test with untapered studs, as stated in reference 16, was that adequate stress margin should be available for both the 30-year fatigue and the ultimate load (high wind) capabilities to warrant use of the attachment concept for fabrication of full-scale Mod-0A blades.

Final stud design. - As a result of the above stud attachment tests, as well as further analysis of peak epoxy shear stress, a final stud configuration was developed for the full-scale blade design. This design stud configuration is shown in figure 37. The tapered stud had a maximum diameter of 1.5 inches at the root and 0.75 inches at the tip and penetrated the blade for a depth of 15 inches. The configuration was found to produce a lower value of calculated peak epoxy shear stress than for any of the tapered stud specimens tested.

The root diameter of the stud was maintained at 1.5 inches for approximately 3 inches in length before tapering linearly to the 0.75 inch diameter at the tip. The hole was to be step-taper-drilled approximately 3/8-inch diameter larger than the stud for increased wood bonding area. To reduce stress concentrations in the epoxy, a rounded Acme thread with 0.2-inch pitch and 0.1-inch depth was incorporated on the tapering stud section. The thread was started gradually at the stud root and did not reach full depth until around 3 inches from the root. The purpose of this transition was to avoid stress concentration in the steel at the stud root due to rapid changes in area that are usually associated with the start of a thread.

The bonding agent chosen was a mixture of the slow hardening adhesive with asbestos fiber reinforcing filler. The slow curing adhesive was selected because of the time required to coat the 24 studs and bond them into place. The design studs were grit blasted prior to application of the adhesive.

8.0 STRUCTURAL DESIGN ANALYSIS

After feasibility of the key components was established and the material properties were defined, a detailed structural analysis of the blade design was conducted. Several designs and analyses were made prior to the establishment of the final blade configuration. The detailed structural analysis described herein was that for the iteration immediately preceeding the final design. Subsequent blade modifications were minor so that a detailed analysis was not repeated for the final design. The blade configuration for which the structural analysis is detailed herein will be referred to as the "stress analysis" configuration.

The structural design analysis, as described herein, defines the blade loads considered, the stresses generated by the loads, and the margins of safety against failure from the generated stresses. The calculations also establish the overall structural characteristics of the blade. The analysis is described first for the primary blade structure and then for the hub attachment.

8.1 Primary Blade Structure

The blade chord lengths, thicknesses and external geometry of the "stress analysis" blade configuration were the same as for the final design (Table I and fig. 10). The thickness of some of the internal structural members had not been finalized at this time (they were later increased slightly to improve safety margins). The major loads on the blade structure were taken for two general conditions: normal continuous operation, and periodic events such as rapid shutdown or hurricane gusts which occur at low frequency during the operating life of the blade.

Normal operation loads. - The blade loads during normal operation are variable, with mean and cyclic components as shown schematically in figure 7. In the flatwise orientation, the loads are due to the effects

of thrust from aerodynamic lift, centrifugal force due to blade coning, and cyclic lift forces caused by wind gradients and tower wake flow. In the edgewise blade orientation, the dead-weight gravity moment is the major working load. The load calculations also included the option of the addition of a 50-pound weight at the blade tip for blade balancing or fine-tuning of natural frequency.

Blade bending moments for the maximum normal operating condition of 40 mph wind speed and 40 rpm rotational speed were calculated at NASA LeRC using the MOSTAB-WTE computer code (ref. 17). This is a single blade, one-degree-of-freedom code in which the blade may execute one flapping mode with deflections parallel to the axis permitted. Rotor speed is constant, and the rotor shaft is assumed to be rigidly supported. The code contains two empirical constants obtained from earlier Mod-0 test data. These constants were introduced to adjust the resultant blade bending moment curves for loads induced by additional tower and nacelle motions, and to increase the general level of calculated blade bending moments on the basis of nominal-plus-σ measured loads. For additional conservatism, load augmentation factors of 1.25 and 1.1 were used to increase the calculated cyclic flatwise and edgewise moments, respectively.

Bending moments were revised using MOSTAB-WTE during the evolution of the blade design. Results of the last of these calculations are shown in figures 38(a) and (b). Maximum bending moments (cyclic and steady) at the blade hub for normal operation are 12.43×10^4 ft-lb flatwise and 7.93×10^4 ft-lb edgewise. The addition of a 50-pound weight at the blade tip had a small effect on maximum moments. The largest change attributable to the tip weight was an increase in edgewise maximum moment from 7.93×10^4 to 8.3×10^4 ft-lb.

Hurricane loads. - One of the critical loads that can be imposed on the blade results from wind gusts of hurricane proportions. When strong winds occur, the blades are feathered, but they are still subject to aerodynamic loading. A fixed aerodynamic load of 50 lb/ft^2 was specified as the estimated load for this condition. This load corresponds to the maximum lift force on the blade (average maximum C_L approximately 1.39) for a wind gust of 120 mph. Bending moments were calculated by integrating the unit pressure over the planform area of the blade (total load, 10,730 lb). The bending moment produced by this aerodynamic load is shown in figure 39. The maximum moment of 29.0×10^4 ft-lb, flatwise, is more than twice that resulting from normal operation (fig. 38).

Shutdown loads. - Another critical static load case occurs during an emergency shutdown of the rotor due to rotational overspeed. During emergency shutdown, the blades are feathered through negative pitch to halt blade rotation. In so doing, the blades go through maximum negative lift. The case analyzed for emergency shutdown was a rotational speed of 45 rpm, a wind speed of 40 mph, and all blade sections experiencing maximum negative lift at the same time. The variation of maximum negative lift coefficient was presented earlier in figure 14(a). The spanwise variation in aerodynamic loading resulting from the emergency shutdown condition is shown in figure 40(a).

In addition to the aerodynamic moment, the moment created by the action of centrifugal force on the blade (7° coning angle plus elastic deflection) was also calculated. The moment distributions from only the aerodynamic load and the combined centrifugal and aerodynamic loads are shown in figure 40(b). In the calculations for the total moment given in figure 40(b), no iteration was made for the interaction between the air and centrifugal loads.

As can be seen in figure 40(b), the maximum bending moment of 38.0×10^4 ft-lb is greater than that from the hurrican gust case (fig. 39). The emergency shutdown thus becomes the critical limit load condition for the blade design. In this regard, it is noted that the model for the load is conservative, since maximum negative lift at the same instant everywhere along the blade span is not likely. Data from Mod-0A field service confirms this, in that emergency shutdown peak load values tend to be around 70 percent of what the analytical model predicts.

Bending stresses. - The variation of bending stresses along the blade span was determined using conventional beam bending theory. Steady, cyclic, and total stresses were determined. Geometric properties of eight blade cross sections along the span for the "stress analysis" configuration were determined by dividing the members of the cross section into a number of essentially rectangular elements. Summations of the elements produced the weight per foot of span, the local center of gravity, shear center, neutral axis, and the moments of inertia, I, about the flatwise and edgewise axes. Section stiffness, EI, was also determinted, based on the elastic moduli of the components of the cross section. The blade cross section elements for the selected spanwise stations are shown in figure 41.

Design stresses for the safety margin calculations are the flatwise values and the combined values. The combined stress, which assumes that the peak flatwise and edgewise moments are concurrent, represents the most severe situation. It is given by

$$\sigma^* = \sqrt{\sigma^2_{\text{flatwise}} + \sigma^2_{\text{edgewise}}} \qquad (1)$$

Wind turbine blades normally operate close to the combined stress condition.

The calculated bending stresses for the "stress analysis" configuration are listed in Table III as a function of spanwise station for the principal loading conditions. The greatest stresses occurred at the blade root for the emergency shutdown case. The effect of the addition of a 50-pound weight at the tip is most pronounced for the flatwise stresses in normal operation.

Margin of safety. - For blade bending, the critical strength property is compression (fiber crushing). The equation used for the margin of safety against failure in compression at a spanwise location along

the blade due to normal operation moments was:

$$M.S. = \frac{1}{\frac{\sigma_c}{\sigma_e} + \frac{\sigma_s}{\sigma_u}} - 1 \qquad (2)$$

where

σ_c = design cyclic bending stress at the station

σ_s = design mean bending stress at the station

σ_e = allowable fatigue stress of the wood in compression at blade design conditions

σ_u = allowable ultimate stress of the wood in compression at blade design conditions

For the static loads of the gust and shutdown cases, the equation was

$$M.S. = \frac{\sigma_u}{\sigma_s} - 1 \qquad (3)$$

Allowable stresses were determined from the nominal strength properties of the wood (Douglas fir and birch) with appropriate adjustment (knockdown) factors. As established in the section on MATERIAL PROPERTY DATA, the nominal compressive strength of Douglas fir is 7,500 psi, and the endurance stress at 4×10^8 cycles was taken as 0.3 x 7,500 = 2,250 psi. For normal cyclic operation, as indicated in the MATERIAL PROPERTY DATA section, the knockdown factor for temperature and moisture content was 0.9. Thus, the allowable fatigue stress, σ_e, was taken as 2,025 psi, and the allowable ultimate compressive stress, σ_u, was taken as 6,750 psi.

For the static (non-cyclic) loads of the hurricane gust and emergency shutdown cases, the knockdown factor for temperature and moisture content was established previously as 0.8. It was also necessary for these cases to add a further adjustment for the veneer joints and any material imperfections. This factor was taken as 1/1.2. Thus, the allowable ultimate compressive stress for the gust and shutdown design cases was 5,000 psi.

Margin of safety was calculated for the stresses determined for the blade configuration used for the detailed stress analysis (Table III). Results of the safety margin calculations are listed in Table IV as a function of spanwise location for the design loading conditions. All values are positive, with the emergency shutdown case showing the smallest values. A more graphic view of the safety margins is given in figure 42. For normal cyclic operation, as seen in figure 42(a), the lowest

margins occur at Station 150 when the combined moment is considered, and near the blade tip when the 50-lb tip load is added. For the static load cases (fig. 42(b)), relatively low margins are observed from Stations 150 to 500 for the emergency shutdown case. Even though some conservatism is contained in the moment and stress calculations, somewhat larger safety margins were desirable for the emergency shutdown case. Consequently, several of the internal structural members of the blade were increased in size.

Along with the basic blade sections, the internal joints in the root and tail were analyzed for stress and load carrying ability. Adequate margins of safety were found in all cases. Details of these calculations are not presented herein.

8.2 Hub Attachment

The load of concern for the hub attachment at the root end of the blade (fig. 15) is the maximum tensile force on the bonded stud resulting from the maximum bending moment at Station 32. As indicated previously by the single-stud tests, pull-out or fatigue failure of the stud bond can occur from excessive values of tensile load on the stud. Thus, the margin of safety calculation for the hub attachment is conducted in terms of tensile load on a stud instead of bending stress as for the primary blade structure (i.e., substitute tensile load, P, for stress, σ, in equations (2) and (3)). The load margin of safety involves the calculation of the design tensile loads on the stud and the determination of the allowable ultimate and fatigue loads. Safety margin determinations for the hub attachment were made for the same three design bending moment cases as before: normal operation, hurricane gust, and emergency shutdown.

Design loads. - The tensile load on a stud resulting from the blade bending moment at the root (Station 32) was obtained from the equation

$$P = \frac{4M}{D_b N_s} \tag{4}$$

where M is the bending moment, D_b is the bolt circle diameter, and N_s is the number of studs. For the blade design, $D_b = 18.625$ inches, and $N_s = 24$. Thus, with P in pounds and M in foot-pounds, equation (4) becomes

$$P = 0.1074\ M \tag{5}$$

For the normal operating condition, the design combined moment at the blade root (Station 32) is obtained from figure 38. The root combined cyclic moment is 10.87×10^4 ft-lb, while the root combined mean moment is 3.87×10^4 ft-lb. The corresponding design cyclic and mean tensile loads on the studs were then obtained from equation (5), respectively, as

$$P_c = 11{,}680 \text{ lb} \qquad \text{and} \qquad P_s = 4{,}160 \text{ lb} \tag{6}$$

The maximum combined load was thus 15,840 pounds.

The most severe case for the static design loads occurred for the emergency shutdown situation. According to figure 40(b), the moment at the blade root for this case was 38.0×10^4 ft-lb. Thus, the maximum static design tensile load on the stud was

$$P = 40{,}810 \text{ lb} \tag{7}$$

Margin of safety. - The margin of safety against failure of the design stud was determined from the single-stud test results mentioned in the section on KEY COMPONENTS TESTS. The Mod-0A design stud configuration of figure 37 was not tested in the single-stud strength investigation described in reference 16. However, its configuration was sufficiently close to the geometry of the tapered studs used in the tests, so that the test results were considered applicable to the design stud.

In consideration of the results of the previously mentioned pull-out load tests on single tapered studs (ref. 16), the design value of ultimate load for the design stud configuration was taken as 70,000 lb. Thus, if a knockdown factor of 0.8 is used as before for elevated temperature effects, and an additional factor of 0.9 is taken for defects and load asymmetry, the allowable ultimate load for the design stud is of the order of

$$P_u = 0.8 \times 0.9 \times 70{,}000 = 50{,}400 \text{ lb} \tag{8}$$

This value, in conjunction with the design load for the emergency shutdown case (eq. (7)), produced a margin of safety value (eq. (3) with $\sigma \rightarrow P$) of 0.23. This value was considered quite adequate, in view of the conservatism in the load calculation.

Margin of safety against failure in fatigue was also estimated from the test results of the single-stud investigation. As indicated previously, the tapered studs achieved a life of about 3×10^6 cycles at an applied load of 35,000 pounds. Reference 16 (fig. 33 in ref. 16) extrapolated the fatigue data to a maximum load at 4×10^8 cycles of about 28,000 pounds. However, because of the limited test data involved, other extrapolated values could be reasonably established. A maximum load of as low as 25,000 pounds could be taken. Thus, if a knockdown factor of, say, 0.7 were used, the allowable maximum load in fatigue, P_e, could vary from 19,600 to 17,500 pounds. Furthermore, from considerations of epoxy shear stress analysis, the blade design contractor estimated the allowable maximum load on the design stud at 4×10^8 cycles to be about 17,100 pounds. As indicated from equation (6), the design value of combined maximum load on the stud was 15,840 pounds. Thus, for these two values, the margin of safety against fatigue failure in the hub attachment during normal operation to 4×10^8 cycles is 0.08.

The calculated low margin of safety in fatigue for the blade hub attachment was considered acceptable in view of the conservatism factors contained in the calculation procedure. These conservatism factors include: inclusion of augmentation of the calculated design loads in the computer program; peak edgewise and flatwise loads do not really occur simultaneously; peak loads do not occur at all times (closer to 10 percent of time); and allowable fatigue load was taken inversely proportional to calculated peak shear stress in the epoxy. Nevertheless, it was decided to increase the thickness of the laminated nose piece at the root of the blade for the final design. An increased wood thickness around the imbedded stud would reduce the peak shear stress in the epoxy and consequently, improve the fatigue strength of the bond.

8.3 Overall Structural Properties

As indicated previously, the blade section elements of figure 41 were also used to determine the weight, stiffness, natural frequency, and tip deflection of the blade for the configuration used for the detailed stress analysis.

Weight. - The density values used for the weight estimation are:

Douglas fir laminate (nose): 42 lb/ft^3

Sawn fir: 36 lb/ft^3

Birch ply: 42 lb/ft^3

Honeycomb: 1.67 lb/ft^3

Tail panel, net: 13 lb/ft^3

Honeycomb bonding material: 80 lb/ft^3

Surface coating: 90 lb/ft^3

The weight distribution along the span is shown in figure 43. The total weight of the wood blade configuration of figure 41 plus the steel studs was calculated as 2,080 pounds. The addition of lightning protection would raise the weight value to around 2,100 pounds.

Stiffness. - The stiffness distribution along the blade span is given by the spanwise variation of the product of the modulus of elasticity and moment of inertia, EI, as shown in figure 44. The stiffness increases toward the axis for the airfoil section portion of the blade, with the edgewise stiffness considerably greater than that in the flatwise direction. The stiffness then tends to converge as the cross section departs from the airfoil shape to the root end configuration. The larger edgewise stiffness is expected to result in a natural frequency that is larger than that in the flatwise direction.

Natural frequency. - The first-mode natural frequencies for the flatwise and edgewise orientations were calculated by the Stodola method which assumes that the mode shape is identical to the static gravity deflection of the blade. The calculated first-mode flatwise frequency was 2.25 Hz and the edgewise frequency was 3.59 Hz. Both values are within the acceptable bands defined in the specifications.

Deflection. - The deflection of the blade tip due to airload was determined for the emergency shutdown case from the summation of local deflections calculated from the average strain for the blade sections. In the calculation, the modulus of elasticity was taken as 0.9 of the reference value to allow for elevated temperature effects. To this value of deflection, the deflection effect of centrifugal force due to coning was added to give a total tip deflection of 74.4 inches. With the static clearance between blade and tower given as 103 inches, the minimum operating clearance was 28.6 inches. This value is well above the minimum allowable clearance of 12 inches.

9.0 FINAL BLADE DESIGN

The overall geometry and dimensions of the final blade design were the same as those of the iteration that was used for the stress analysis. The geometric characteristics of the final blade design are given in Table I and figures 10 and 11. As a result of the analysis of blade stress margins of safety, it appeared desirable to increase the internal thickness of the nose section of the blade along the span. In particular, the thickness of the root section containing the studs was increased from 4.0 to 4.8 inches. The number of the fir veneers was, therefore, increased for the final design, with the final spanwise variation of nose thickness as shown in figure 45. Also, the inner stringer (1 in. x 5/8 in.) in the tail panel was extended to the full length of the blade. To compensate for the added weight of these additions, the shear web blocking piece (fig. 41) was reduced to a maximum of 2 x 1.5 inches in cross section. An additional stress analysis of the final blade configuration was waived in view of the small changes involved.

The other major change for the final blade design was the use of an intermediate spool piece between the hub spindle and blade root end, as shown in figure 15. This spool piece was necessary because the flange of the wind turbine hub spindle, which was designed to mate with a flange on the aluminum blade, was not believed to be sufficiently stiff to permit direct attachment to the wood blade studs. However, because of the length of the spool piece, it was necessary to reduce the blade span by 18 inches. This was done by cutting 18 inches off the blade tip.

An overall planform view of the blade design, with the upper half of the blade removed, is shown in figure 46. The figure also shows the various sections of the span that are detailed in succeeding figures. The heavy arrows indicate the stations for which detailed cross sections are presented. The station locations in figure 46 are those of the earlier stress analysis configuration. As indicated above, the tip of

the final blade design was reduced by 18 inches to allow for the addition of the spool piece at the blade root. Thus, in terms of distance from the rotor axis, the root of the final design configuration would be at 50 inches, and the tip would be at 750 inches.

The detailed construction of the individual spanwise sections shown in figure 46 is shown in figures 47(a) through (e). The light dashed arrows indicate the desired grain direction for the members involved. In general, grain or face grain of all parts were to be oriented longitudinally to the blade unless otherwise specified. All plywood was to be aircraft quality birch.

Several blade cross sections are detailed in figure 48(a) through (h). The sections shown in these figures, which are from the lower half of the mold, represent the low-pressure surface of the airfoil. The construction of the high-pressure side is the same, except that the outer blade contour differs from the blade contour of the low-pressure side. Figure 48(a) for the root end of the blade does not show the birch plywood end cap that covers the open end of the blade.

A detailed weight analysis was made of the final blade configuration. The revised calculated weight was 2,430 pounds, compared to the previous estimate of 2,080 lbs. The increase in weight was attributed mainly to the design construction changes mentioned above and to the addition of lightning protection. The application of the lightning protection screen required the use of a thick layer of thixotopic material to fill the mesh and establish full contact between the outer plywood and the covering glass changes. Approximately half of the weight increase was due to the structural changes. The weights of the first two blades constructed were 2,470 and 2,603 pounds, with a center of gravity approximately 224 inches from the face of the blade root. The blade weights and center of gravity were balanced by blade ballasting the lighter blade with thickened epoxy resin.

10.0 COST ANALYSIS

The blade cost data presented contain two general types of information. The first is the estimated costs for large-quantity production initially generated by the contractor at the conclusion of the final design of the Mod-0A blade configuration. This is then updated with cost data from laminated wood blades that have been designed or fabricated since that time. Cost projections for laminated wood blades from 60 to 250 feet in length are also presented based on designs for a 200-foot blade, as well as for the 62.5-foot Mod-0A design. Finally, a comparison is given of estimated costs for large-span blades constructed from different materials.

10.1 Mod-0A Blades

Cost estimates were made for the 100th and 1000th blade of the Mod-0A design at the completion of the final design configuration.

These estimates were expressed in terms of 1977 U. S. dollars, as required by contract specifications. Blade costs were determined from production rates of 120 and 960 blades per year. These cost estimates were based on the construction of a new fabrication plant. The plant is designed around a basic manufacturing module illustrated in figure 49(a). This module is capable of producing 120 blades per year on a one-shift basis, and 240 blades per year with two shifts. Increased rates of production to 960 blades per year (with two shifts) would then be obtained through the addition of similar manufacturing modules, as shown in figure 49(b). The plant is to be located 30 to 50 miles north of Bay City, Michigan, to tap a basically agrarian labor market.

The details of the blade cost analysis conducted by the contractor are given in Appendix A. The analysis indicated an estimated cost of $4.33 per pound of blade weight for the 100th blade, and $2.81 per pound for the 1,000th blade in 1977 dollars. In regard to figure 2, the original specifications required a cost-weight factor less than 100. The estimated cost-weight factor for the 100th blade is 57.5, and for the 1,000th blade it is 37.3. These values are substantially below the indicated limit.

Estimated blade costs were projected to current years in Appendix A based on a fixed blade design and material specification, but with improvements in labor efficiency, manufacturing methods, and material selection and purchasing. According to Appendix A, the Mod-0A blade cost per pound in 1982 dollars was projected to increase to about $6.2 to $7.8 for the 100th blade (absolute cost, $14,900 to $18,700 for a 2,400-lb blade). For the 1,000th blade, the unit cost in 1982 dollars extrapolates to $4.0 to $5.0 per pound. It is likely, however, that refinements and improvements in blade design and construction will occur with time. Present work by the contractor indicates that materials cost can be reduced significantly by replacing sliced fir veneers with rotary-cut veneers, and by replacing the tail-panel honeycomb with all-wood composite construction. Although economies can be expected with time, there is also the general consideration that initial cost estimates tend to be optimistic. Thus, the use of a "fixed" configuration for the cost projections may not be far out of line.

Several sets of wood blades have been constructed for the Mod-0A wind turbine based on the final design and fabrication concepts detailed herein. Purchase price was of the order of $45,000 each in 1980 dollars, or about $18.8 per pound. The original aluminum blades cost about $200,000 each. However, both of these cases are basically prototype or single-item fabrications, which are always more costly than large-quantity production runs. The $18.8 per pound actual cost for the several essentially prototype wood composite blades built for the Mod-0A wind turbines compares to an estimated cost per pound of from $5.4 to $6.2 in 1980 dollars for a production rate of 100 blades per year (Appendix A). This cost reduction appears entirely realistic.

10.2 Other Blade Data

It is also currently possible to construct a variation of estimated blade cost as a function of blade span (turbine rotor radius). These data are obtained from the cost analysis for the 62.5-foot Mod-0A blade detailed in Appendix A and a more recent analysis of wood blades for the Mod-5A wind turbine design conducted by the General Electric Company (ref. 18) from data supplied by Gougeon Bros., Inc. The results of these analyses are shown in figure 50 in terms of cost per pound of blade weight for the 100th blade in 1980 dollars. The value for the Mod-0A blade was established based on a 10 percent yearly cost increase. The blade designs for the two machines are not exactly comparable, since the Mod-5A blade is a teetered configuration with tip span pitch control. Also, the Mod-5A wood blade was based on utilization of less costly rotary-cut fir veneers. However, it is believed that the effect of these differences is not large compared to the overall effect of increased blade span.

The design studies for the Mod-5A wind turbine outlined in reference 18 also contained a comparison of estimated weights and costs for blades constructed of stainless steel, fiberglass, and wood composite. A comparison of results is shown in figure 51. For a given length of span, the wood composite blade produced the lowest estimated weight and cost. A very promising potential therefore exists for the development of low-cost blades constructed of wood composite.

11.0 SUMMARY OF RESULTS

The design analysis of a wood composite blade for the Mod-0A wind turbine (125-ft diam. rotor) has produced the following major results:

1. A blade structural concept was developed which satisfied the design specifications. The design concept includes a primary spar (nose) section constructed of Douglas-fir veneers laminated with epoxy adhesive, and a tail section composed of honeycomb cored plywood panels. The attachment of the wood blade to the rotor hub was through steel load-take-off studs bonded into the root of the blade.

2. A cost effective fabrication concept was developed for the blade construction. It consisted of assembling the structural components in a two-part female mold. The two assembled halves would then be trimmed, prior to bonding together, by a band saw set on tracks on the outer perimeter of the mold.

3. Laboratory tests conducted on specimens of butt-jointed Douglas-fir veneers, and on single steel stud configurations bonded in laminated Douglas-fit blocks, demonstrated the feasibility and structural integrity of these two key components.

4. Stress analysis of the wood composite blade configuration was conducted for both the primary blade structure and the hub attachment.

Adequate margins of safety (i.e., >0) were obtained against failure in ultimate strength during an emergency shutdown, or in fatigue strength during normal cyclic operations for the design life of the blade ($4x10^8$ cycles).

5. Detailed design drawings of the wood composite blade concept were made. No problems or unacceptable characteristics were found. Blade weight was estimated to be 2,430 pounds.

6. A cost analysis for blades in quantity production showed the cost of the wood composite blade to be very competitive with other methods of manufacture. Production cost was estimated to be from $15,000 to $18,000 per blade in 1982 dollars for a production rate of 100 blades per year.

12.0 CONCLUDING REMARKS

The design development program described herein has resulted in a wood composite blade design and fabrication concept that can lead to blades which can be manufactured at relatively low cost. Actual wood composite blades built for the Mod-0A wind turbines cost much less than the original aluminum blades. Estimated blade costs for quantity production were well within the desired cost range. The practicality of the construction system developed herein is based on proven construction techniques. However, actual experience in volume production of wood composite blades will be required to develop the envisioned manufacturing techniques so that the projected blade costs can be achieved.

The weakest aspect of the blade design was found to be the attachment of the blade root to the hub spindle. Uncertainty in the estimated fatigue strength of the bond of the studs imbedded in the blade root produced relatively low calculated margins of safety for the normal cyclic operating moments (about 0.08). However, due to a large degree of conservatism in both the calculated applied loads and the selected material allowable loads, the performance of the attachment should be acceptable. This assessment is basically confirmed by actual operation of wood composite blades in the Mod-0A wind turbine in Hawaii. At the time of writing, these blades have been operated trouble-free for over 6,000 hours (about $2x10^7$ cycles).

The design development has also pointed up some aspects of the design analysis which may warrant further investigation. For example, the emergency shutdown load was found to be the principal design driving load. If this load could be reduced by a different operating procedure or by a different aerodynamic blade form or cross-section, system structure stresses and weight could be decreased. Another area that requires more attention is the determination of allowable loads, material strength properties, and performance adjustment factors. In particular, further analysis and tests are recommended to determine more accurately the fatigue strength of the stud bond and its major influencing parameters. Calculations would be useful for assessing the sensitivity of the resulting margins of safety to the variability or uncertainty in the values of the inputs (e.g., material strength properties and adjustments factors). Such calculations are indicated for the primary blade structure,

the steel stud, and the stud bond. Finally, the potential improvement in margin of safety that can result for the hub attachment from changes in stud overall geometry should be investigated.

13.0 APPENDIX A

COST ANALYSIS FQR QUANTITY PRODUCTION OF BLADES

The analysis is conducted for the 100th and 1,000th blade of the Mod-0A design in terms of 1977 dollars. Costs are determined from production rates of 120 blades/year and 960 blades/year as obtained from a new manufacturing plant (fig. 49). Factors detailed are the labor, material, and capital costs.

Labor Cost

The labor payroll cost was determined from the estimated plant manning for the production rates of 120 and 960 blades/year. The estimated direct labor man-hours for fabrication of the 100th blade at 120 blades per year is detailed in Table V. With the inclusion of crew chiefs, the total is 256 man-hours. A mold train in the manufacturing module (fig. 49) produces a blade every two shifts (8 hr/shift). Thus, 16 men are required per shift on the production line for the 120/yr production rate. For the 1,000th blade with the four-module plant operating two shifts (960 blades/yr), it was assumed that further experience and refinements would allow the manpower on a production train to be reduced from 16 to 10. Thus, with four trains and two shifts, 80 men would be required per day on the production line.

The complete plant manpower requirements and resulting total labor cost per blade are shown in Table VI. The production line cost is seen to decrease considerably for the 960 blades/year rate compared to the 120 blades per year rate. Also, with the expanded operation, fewer auxilliary personnel are required per production train. Thus, as indicated in Table VI, a considerable reduction in payroll cost per blade is to be expected for the higher blade production rate.

Materials Cost

The estimated materials cost for the production of the 100th blade is obtained from the breakdown of Table VII. These values were determined in 1979 dollars and then converted to 1977 dollars. The respective materials cost per blade for the 100th blade are 1.738 dollars/lb in 1979 dollars and 1.512 dollars/lb in 1977 dollars (15 percent inflation increase from 1977 to 1979). For the 1,000th blade at 960 blades/year, it was determined that design and manufacturing refinements would result in a 15 percent reduction in materials cost. Thus, for the 1,000 blade, the cost of materials per blade in 1977 dollars is 1.285 dollars/lb.

Capital Costs

The estimated capital costs for the new blade manufacturing plant of figure 49 are listed in Table VIII in 1977 dollars. The capital cost (plant and tooling) for the 960 blades per year production rate (four

manufacturing modules) is less than four times the one-module rate. Depreciation is not computed for the cost of the land. The depreciation costs per blade for the 100th and the 1,000th blade are $920 and $417, respectively.

Total Costs

The estimated total cost per blade and the cost per pound of blade is given in Table IX. Materials, payroll, and depreciation costs are taken from Tables VII, VI, and VIII. Labor overhead, which includes such items as plant utilities, maintenance, taxes, insurance, fringe benefits, etc., was determined as 95 percent for the 120 blades per year and 85 percent for the 960 blades per year (reduced because of two-shift operation). General and administrative costs include the usual items such as office supplies and utilities, telephone, transportation, legal, accounting, etc.

The total estimated cost per pound of blade weight was then obtained as 4.33 dollars/lb for the 100th blade and 2.81 dollars/lb for the 1,000th blade in 1977 dollars. In terms of absolute cost, the respective values are around $10,400 and $6,700 per blade.

A projection of blade cost per pound of weight into present and future years is given in Table X for three cost increase rates due to inflation. In these calculations, it was assumed that the blade design, materials, and fabrication remain unchanged. Thus, in 1982 dollars, blade cost per pound might run from about $6.2 to $7.8 for the 100th blade, and from $4 to $5 for the 1,000th blade. The absolute cost for a 2400-lb blade is then projected to range from $14,900 to $18,700 for the 100th blade.

Blades fabricated for the operating Mod-0A wind turbines were purchased for around $45,000 each in 1980. In comparison, from Table X in terms of 1980 dollars, the cost of the 100th blade in quantity production would have been about $5.4/lb to $6.2/lb. Total cost for a 2400-pound blade would then have been in the range from $13,000 to $14,900. It is also noted that the cost of the aluminum blades originally installed on the Mod-0A wind turbines (about $200,000) was considerably greater than the cost of the later wood composite blades.

14.0 REFERENCES

1. Thomas, R. L., and Baldwin, D. H.: The NASA Lewis Large Wind Turbine Program. DOE/NASA/20305-7, NASA TM-82761, 1981.

2. Lieblein, S., Londahl, D. S., Furlong, D. B., Peery, D. J., and Dreier, M. E.: Evaluation of Feasibility of Prestressed Concrete for Use in Wind Turbine Blades. DOE/NASA/5906-79/1, NASA CR-159725, Sept. 1979.

3. Lieblein, S., Ross, R. S., and Fertis, D. G.: Evaluation of Urethane for Feasibility for Use in Wind Turbine Blade Design. DOE/NASA/7653-79/1, NASA CR-159530, April 1979.

4. Gewehr, H. W.: Design, Fabrication, Test, and Evaluation of a Prototype 150-Foot Long Composite Wind Turbine Blade. DOE/NASA/0600-79/1, NASA CR-159775, Sept. 1979.

5. Eggert, Walter S., Jr.: Design and EValuation of Low-Cost Blade for Large Wind Driven Generating Systems. DOE/NASA/0129-1, NASA CR-165491.

6. Gougeon, M., and Zuteck, M.: The Use of Wood for Wind Turbine Blade Construction. Page 293 in Large Wind Turbine Design Characteristics and R&D Requirements, S. Lieblein, Editor. NASA Conf. Publ. 2106, DOE Publ. CONF-7904111, 1979.

7. Linscott, B. S., and Shaltens, R. K.: Blade Design and Operating Experience on the MOD-0A 200 kW Wind Turbine at Clayton, New Mexico. Page 225 in Large Wind Turbine Design Characteristics and R&D Requirements, S. Lieblein, Editor. NASA Conf. Publ. 2106, DOE Publ. CONF-7904111, 1979.

8. Donham, R. E.: Evaluation of an Operating MOD-0A 200 kW Wind Turbine Blade. Page 239 in Large Wind Turbine Design Characteristics and R&D Requirements, S. Lieblein, Editor. NASA Conf. Publ. 2106, DOE Publ. CONF-7904111, 1979.

9. Weingart, Oscar: Design, Evaluation, and Fabrication of Low Cost Componsite Blades for Intermediate Size Wind Turbine. DOE/NASA/0100-1, NASA CR-165342, Sept. 1981.

10. Puthoff, R. L.: Fabrication and Assembly of the ERDA/NASA 100-kW Experimental Wind Turbine. NASA TM X-3390, 1976.

11. Linscott, B. S., Glasgow, J., Anderson, W. D., and Donham, R. E.: Experimental Data and Theoretical Analysis of an Operation 100 kW Wind Turbine. DOE/NASA/1028-78/16, NASA TM-72883, Jan. 1978.

12. Abbott, I. H., von Doenhoff, A. E., and Stivers, L. S., Jr.: Summary of Airfoil Data. NACA Report No. 824, 1945.

13. Bankaitis, H.: Evaluation of Lightning Accomodation Systems for Wind-Driven Turbine Rotors. DOE/NASA/20320-37, NASA TM-82784, March 1982.

14. Anon.: Wood Handbook; Wood as an Engineering Material. Forest Products Lab. Forest Serv., U. S. Dept. of Agriculture. Agriculture Handbook No. 72, Revised August 1974.

15. Kommers, W. J.: The Fatigue Behavior of Wood and Plywood Subjected to Repeated and Reversed Bending Stresses. Forest Products Lab, Forest Serv., U. S. Dept. of Agriculture No. 1327, 1944.

16. Faddoul, James R.: Test Evaluation of a Laminated Wood Wind Turbine Blade Concept. DOE/NASA/20320-30, NASA TM-81719, May 1981.

17. Spera, David A.: Comparison of Computer Codes for Calculating Dynamic Loads in Wind Turbine. DOE/NASA/1028-78/16, NASA TM-73773, 1977.

18. Anon.: Conceptual Design Review Report, MOD-5A Wind Turbine Generator. NASA Contract No. DEN3-153, General Electric Co., May 1, 1981.

TABLE I. - FINAL DESIGN BLADE GEOMETRY

Station, in.	Chord length, in.	Maximum thickness, in.	$\frac{\text{Thickness}}{\text{chord length}}$, percent	Twist, deg
32	22.5	22.3	----	0
102	47.5	20.9	----	0
150	62.4	19.8	31.7	0
300	52.8	15.3	29.0	.6
400	46.4	12.3	26.5	1.0
500	40.0	9.3	23.3	1.7
600	33.6	6.3	18.7	2.6
700	27.2	3.3	12.1	3.9
750	24.0	1.8	7.5	4.8

TABLE II. - PROPERTIES OF WEST SYSTEM EPOXY WITH VARIOUS HARDENERS AND FILLERS

Hardener	Filler	Density, lb/ft^3	Elastic modulus, lb/in^2	Specific[a] modulus ft^3/in^2
205	None	71.0	327 000	4,610
	Asbestos	69.5	350 000	5,040
	Colodial silica	63.6	260 000	4,090
	Microballoons	39.0	147 000	3,770
	Microspheres	38.2	208 000	5,450
	1/8-in. graphite fibers	60.9	549 000	9,020
	1/4-in. graphite fibers	63.2	454 000	7,180
	Graphite fiber mat	59.5	527 000	8,860
206	None	73.8	296 000	4,010
206	Asbestos	72.2	333 000	4,610
206	Microspheres	39.7	166 000	4,180

[a]Specific modulus is defined as the ratio of modulus to density.

TABLE III. - CALCULATED BLADE BENDING STRESSES[+]

[Stress analysis configuration.]

Stress condition	Spanwise station, in.							
	32	102	150	300	400	500	600	700
(a) Normal operation								
Flatwise								
Steady	306	298	334	360	423	544	655	303
Cyclic	863	857	955	957	964	963	987	283
Peak	1,169	1,155	1,289	1,317	1,387	1,507	1,642	586
Edgewise								
Steady	178	243	364	233	161	95	56	12
Cyclic	495	665	977	689	564	346	257	47
Peak	673	908	1,341	922	725	441	313	59
Combined								
Steady	354	385	494	429	453	552	657	303
Cyclic	995	1,085	1,366	1,179	1,117	1,023	1,019	287
(b) Normal operation with 50-pound tip weight								
Flatwise								
Steady	334	338	386	411	622	847	1,268	1,041
Cyclic	819	819	928	981	1,011	1,048	1,145	1,422
Peak	1,153	1,157	1,314	1,392	1,633	1,895	2,413	2,463
Edgewise								
Steady	181	258	393	336	216	134	119	67
Cyclic	526	709	1,050	903	667	494	398	237
Peak	707	967	1,443	1,239	883	628	517	304
Combined								
Steady	380	425	406	531	658	858	1,274	1,043
Cyclic	973	1,083	1,401	1,333	1,211	1,158	1,212	1,442
(c) Hurricane gust								
Flatwise, steady	2,729	2,590	2,842	2,568	2,410	2,366	2,283	996
(d) Emergency shutdown								
Flatwise, steady	3,576	3,578	4,021	4,174	4,213	4,237	3,610	1,795
Flatwise, steady + 50 lb tip weight	3,599	3,597	4,070	4,130	4,105	3,999	3,073	1,468

[+]Values in psi.

TABLE IV. - BENDING STRESS MARGIN OF SAFETY

[Stress analysis configuration.]

Stress condition	Spanwise station, in.							
	32	102	150	300	400	500	600	700
Normal operation								
Flatwise	1.121	1.140	0.919	0.902	0.856	0.798	0.711	4.41
Combined	.839	.687	.337	.549	.616	.704	.664	4.36
Normal operation + 50-lb tip weight								
Flatwise	1.203	1.200	.940	.834	.691	.555	.327	.168
Combined	.879	.673	.293	.357	.438	.430	.270	.154
Hurricane gust, (flatwise, steady)	.832	.931	.759	.947	1.075	1.113	1.190	4.02
Emergency shutdown (flatwise, steady)	.398	.397	.243	.198	.187	.180	.385	1.79
Emergency shutdown + 50-lb tip weight (flatwise, steady)	.389	.390	.229	.211	.218	.250	.627	2.41

TABLE V. - ESTIMATED DIRECT LABOR MAN-HOURS FOR FABRICATION OF 100th BLADE AT 120 BLADES/YEAR

Item	Man-hours
Veneer preparation	50
Tail stock preparation	30
Lay gelcoat and cloth in mold	25
Mold tail and nose	30
Manufacture and install shear web and root end build up	20
Machine halves flush with bandsaw	5
Bond halves together	15
Install meatl studs in root end	20
Install lightening protection, clean up, and balance	20
Final finish	10
Prepare for shipment	10
Total	235

TABLE VI. - ESTIMATED PLANT MANPOWER AND PAYROLL COST PER BLADE

[Costs in 1977 dollars.]

Class	Number of men per day[a]	$ rate/hr	Total hours/blade	Total cost, $/blade
(a) 100th Blade at 120 blades per year[b]				
Production line	16	4.50	256	1152
Receiving and shipping	1	4.50	16	72
Maintenance	1	6.00	16	96
Office manager				
Office helper	1	4.50	16	72
Development engineer				
Quality control	1	8.00	16	128
Foreman				
Plant manager	1	12.00	16	192
Totals	21	-----	336	1712
(b) 1,000th Blade at 960 blades per year[c]				
Production line	80	4.50	160	720
Receiving and shipping	3	4.50	6	27
Maintenance	3	6.00	6	36
Office manager	1	6.00	2	12
Office helper	1	4.00	2	8
Development engineer	1	8.00	2	16
Quality control	1	8.00	2	16
Foreman	2	8.00	4	32
Plant manager	1	14.00	2	28
Totals	93	-----	186	895

[a] Eight-hour shifts.

[b] 1 Fabrication train, 1 shift; 16 men/train; 1 blade/2 days.

[c] 4 Fabrication trains, 2 shifts; 10 men/train; 4 blades/day.

TABLE VII. - ESTIMATED MATERIALS COST BREAKDOWN FOR FABRICATION OF 100th BLADE AT 120 BLADES PER YEAR

[1979 dollars.]

Item	Weight in blade, lb	Amount needed	Unit cost	Total cost, $/ blade
Douglas fir veneer, 1/16-in. thick	1,131	8,700 ft^2	15¢/ft	1,305
Steel studs	120	24	$40	960
Epoxy	445	490 lb	$1.35/lb	662
Birch aircraft plywood, 1/8-in. thick	266	700 ft^2	64¢/ft^2	448
Birch aircraft plywood, 1/16-in. thick	63	330 ft^2	56¢/ft^2	185
Lightning protection, ice detector	10	-------	--------	125
Miscellaneous paint, nose strip, etc.	16	-------	--------	100
Douglas fir sawn stock	142	91 bd ft	74¢/bd ft	67
Fiberglass, 10-ounce, 60-in. wide	30	35 yds	$1.50/yd	53
Birch aircraft plywood, 1/4-in. thick	53	69 ft^2	75¢/ft^2	52
Verticel honeycomb	28	360 ft^2	13.3¢/ft^2	48
Total	2,304	-------	---------	4,005

TABLE VIII. - ESTIMATED CAPITAL COSTS

[1977 dollars.]

Item	Years of life	Dollars	
		120 blades per year	960 blades per year
Manufacturing plant	20	522,000	1,827,000
Tooling, jigs, and fixtures	10	174,000	609,000
Mold trains	5	87,000	348,000
Total		783,000	2,784,000
Depreciation[a]		[b]110,400	[c]400,300
Land (135,000 ft^2)	---	61,000	61,000

[a]First year, sum of digits method (Gov't rules).
[b]Depreciation per blade, $920.
[c]Depreciation per blade, $417.

TABLE IX. - ESTIMATED TOTAL COST PER BLADE

[1977 dollars.]

Item	100th Blade (120 blades/yr)		1,000th Blade (960 blades/yr)	
	$	$/lb	$	$/lb
Materials	3,484	1.512	2,961	1.285
Payroll	1,712	.743	895	1.388
Labor related overhead	1,626	.706	761	.330
Depreciation	920	.399	417	.181
Sub total	7,742	3.360	5,034	2.185
15% general and administrative	1,161	.504	755	.328
Sub total	8,903	3.864	5,789	2.513
12% fee + 1 yr guarantee[a]	1,068	.464	695	.302
Total	9,971	4.328	6,484	2.814

[a]Standard Gougeon guarantee against defects in materials and/or workmanship for 1 year after installation (not to exceed 18 mo after shipment) provided Gougeon operating and maintenance instructions are followed. Does not include the cost of liability insurance; or the cost of additional paperwork and red tape over and above the Gougeon normal guaranteed quality assurance procedures; or the costs of removal from tower, shipping, re-assembly, etc.

TABLE X. - PROJECTION OF BLADE COSTS DUE TO INFLATION

Inflation rate, percent	Cost per pound of blade weight, $/lb							
	1977	1978	1979	1980	1981	1982	1983	1984
(a) 100th Blade								
7.5	4.33	4.65	5.00	5.38	5.78	6.22	6.68	7.18
10.0	4.33	4.76	5.24	5.76	6.34	6.97	7.67	8.44
12.5	4.33	4.87	5.48	6.17	6.94	7.80	8.78	9.88
(b) 1,000th Blade								
7.5	2.81	3.02	3.25	3.49	3.75	4.03	4.34	4.66
10.0	2.81	3.09	3.40	3.74	4.11	4.53	4.98	5.48
12.5	2.81	3.16	3.56	4.00	4.50	5.06	5.70	6.41

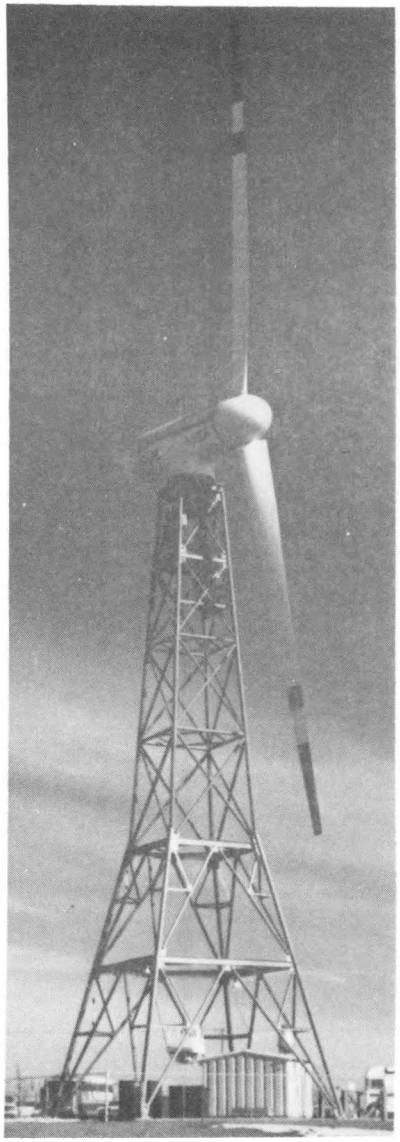

CLAYTON, NEW MEXICO

CULEBRA, PUERTO RICO

BLOCK ISLAND, RHODE ISLAND

FIGURE 1. - MOD-OA 200-KW WIND TURBINES.

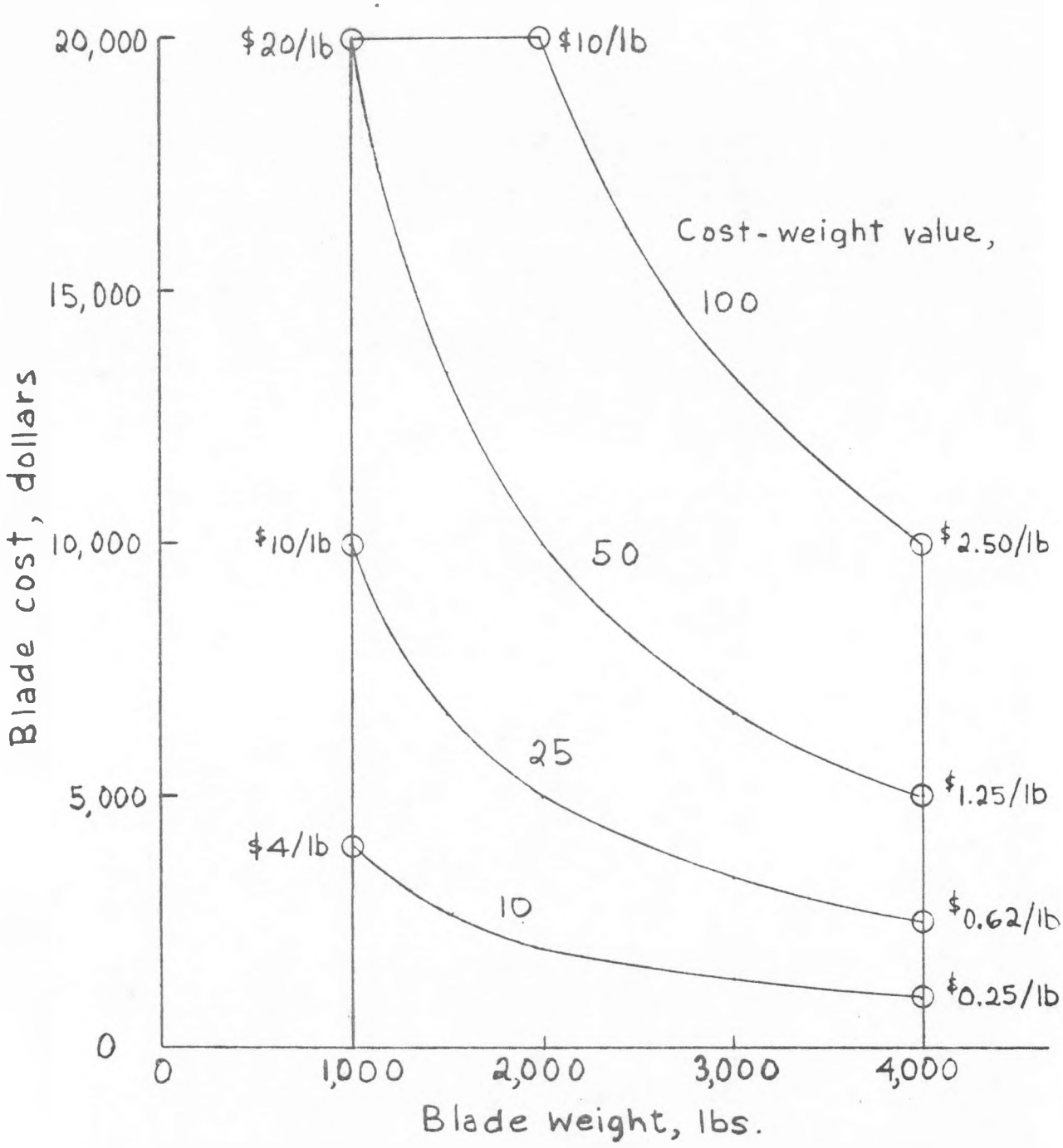

Figure 2.- Cost-weight relationship per blade showing envelope for acceptable designs for wood composite blades. Production rate, 100 blades/year.

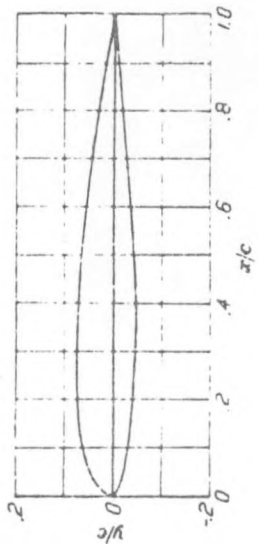

NACA 23012

[Stations and ordinates given in percent of airfoil chord]

Upper surface		Lower surface	
Station	Ordinate	Station	Ordinate
0	...	0	0
1.25	2.67	1.25	−1.23
2.5	3.61	2.5	−1.71
5.0	4.91	5.0	−2.26
7.5	5.80	7.5	−2.61
10	6.43	10	−2.92
15	7.19	15	−3.50
20	7.50	20	−3.97
25	7.60	25	−4.28
30	7.55	30	−4.46
40	7.14	40	−4.48
50	6.41	50	−4.17
60	5.47	60	−3.67
70	4.36	70	−3.00
80	3.08	80	−2.16
90	1.65	90	−1.23
95	.92	95	−.70
100	(.13)	100	(−.13)
100	.....	100	0

L. E. radius: 1.58
Slope of radius through L. E.: 0.305

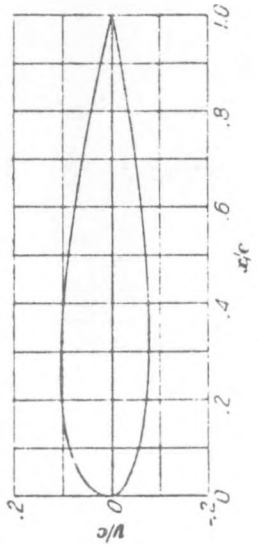

NACA 23018

[Stations and ordinates given in percent of airfoil chord]

Upper surface		Lower surface	
Station	Ordinate	Station	Ordinate
0	...	0	0
1.25	4.09	1.25	−1.83
2.5	5.29	2.5	−2.71
5.0	6.92	5.0	−3.80
7.5	8.01	7.5	−4.60
10	8.83	10	−5.22
15	9.86	15	−6.18
20	10.36	20	−6.86
25	10.56	25	−7.25
30	10.55	30	−7.47
40	10.04	40	−7.37
50	9.05	50	−6.81
60	7.75	60	−5.91
70	6.18	70	−4.82
80	4.40	80	−3.48
90	2.39	90	−1.91
95	1.32	95	−1.09
100	(.10)	100	(−.19)
100	...	100	0

L. E. radius: 3.56
Slope of radius through L. E.: 0.305

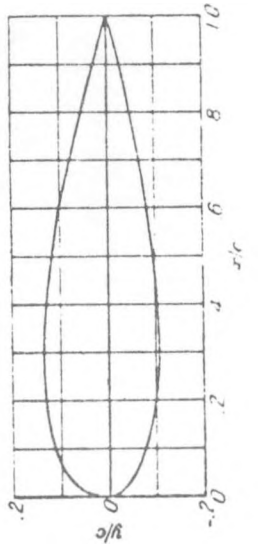

NACA 23024

[Stations and ordinates given in percent of airfoil chord]

Upper surface		Lower surface	
Station	Ordinate	Station	Ordinate
0	0	0	0
.277	4.017	2.223	−3.203
1.361	5.764	3.777	−4.172
3.853	8.172	6.247	−5.542
6.401	9.864	8.723	−6.540
9.121	11.049	10.577	−7.047
15.001	12.528	14.994	−7.572
20.253	13.267	19.747	−7.704
25.292	13.535	24.758	−7.726
30.265	13.516	29.735	−7.674
40.246	12.928	39.744	−7.279
50.235	11.990	49.766	−6.782
60.202	10.806	59.798	−6.242
70.162	9.388	69.838	−5.651
80.116	5.687	79.884	−4.833
90.068	3.135	89.936	−3.074
95.036	1.721	94.964	−1.904
100	.....	100	0

L. E. radius: 6.33
Slope of radius through L. E.: 0.305

FIGURE 3.– NACA 230-SERIES AIRFOILS (REF. 12).

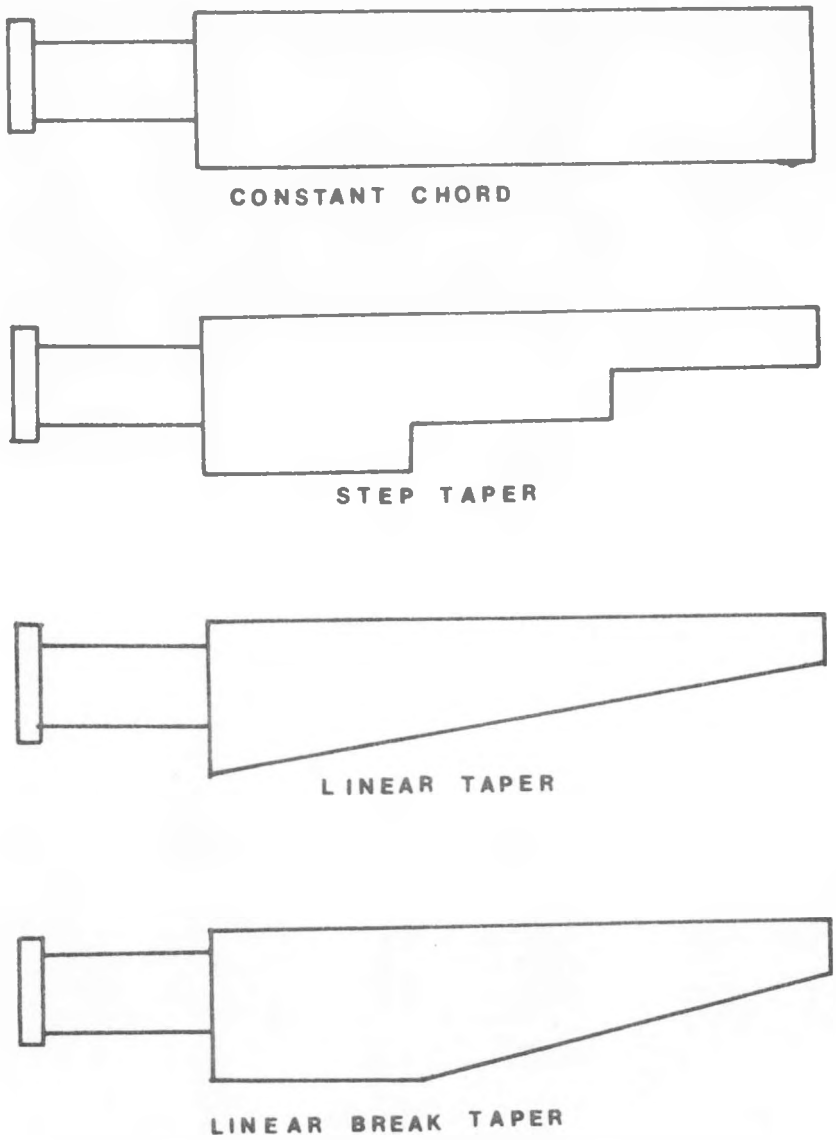

FIGURE 4.— ACCEPTABLE BLADE PLANFORMS.

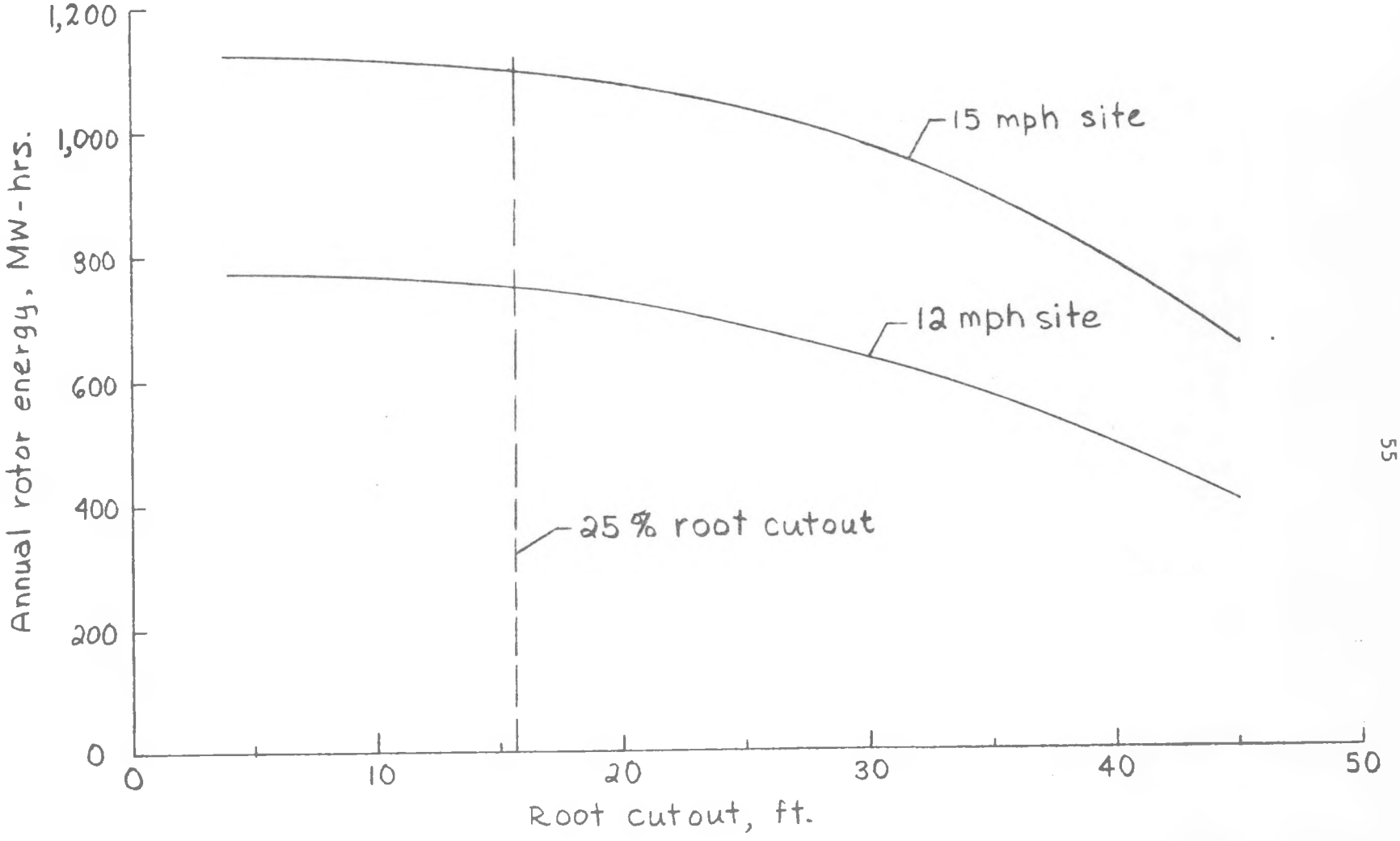

Figure 5.- Effect of root cutout on annual rotor energy. MOD-0A planform, 14° linear twist, -2° pitch, NASA 23018 blade.

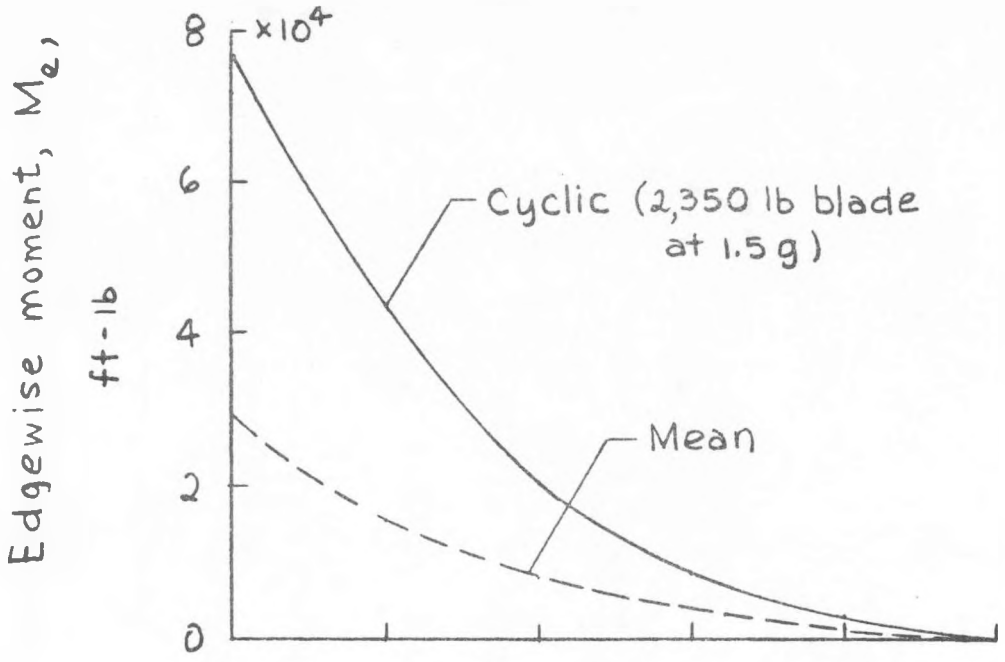

(a). Edgewise bending moments.

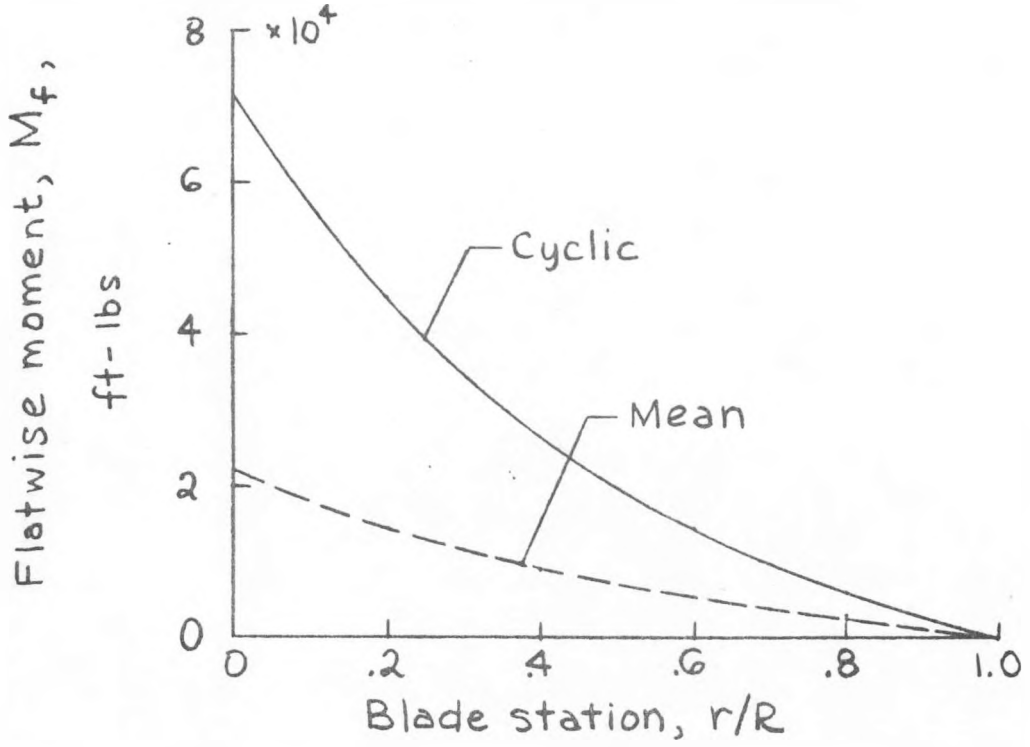

(b). Flatwise bending moments.

Figure 6.- Representative bending moment distributions for MOD-0A blade. Moment vectors are parallel and perpendicular to chord at r/R = 0.75.

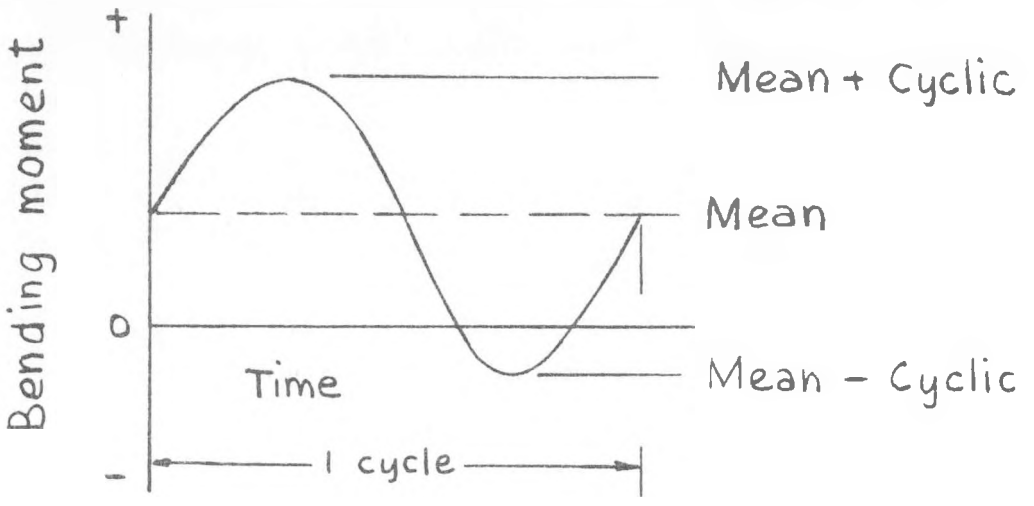

Flatwise moment:

$+M_f$, compression in high pressure side

Edgewise moment:

$+M_e$, compression in leading edge

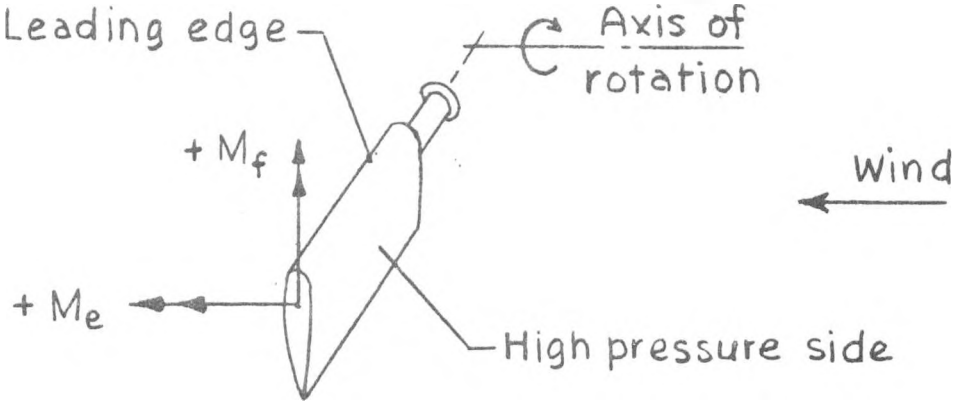

Figure 7.- Bending moment definitions and conventions.

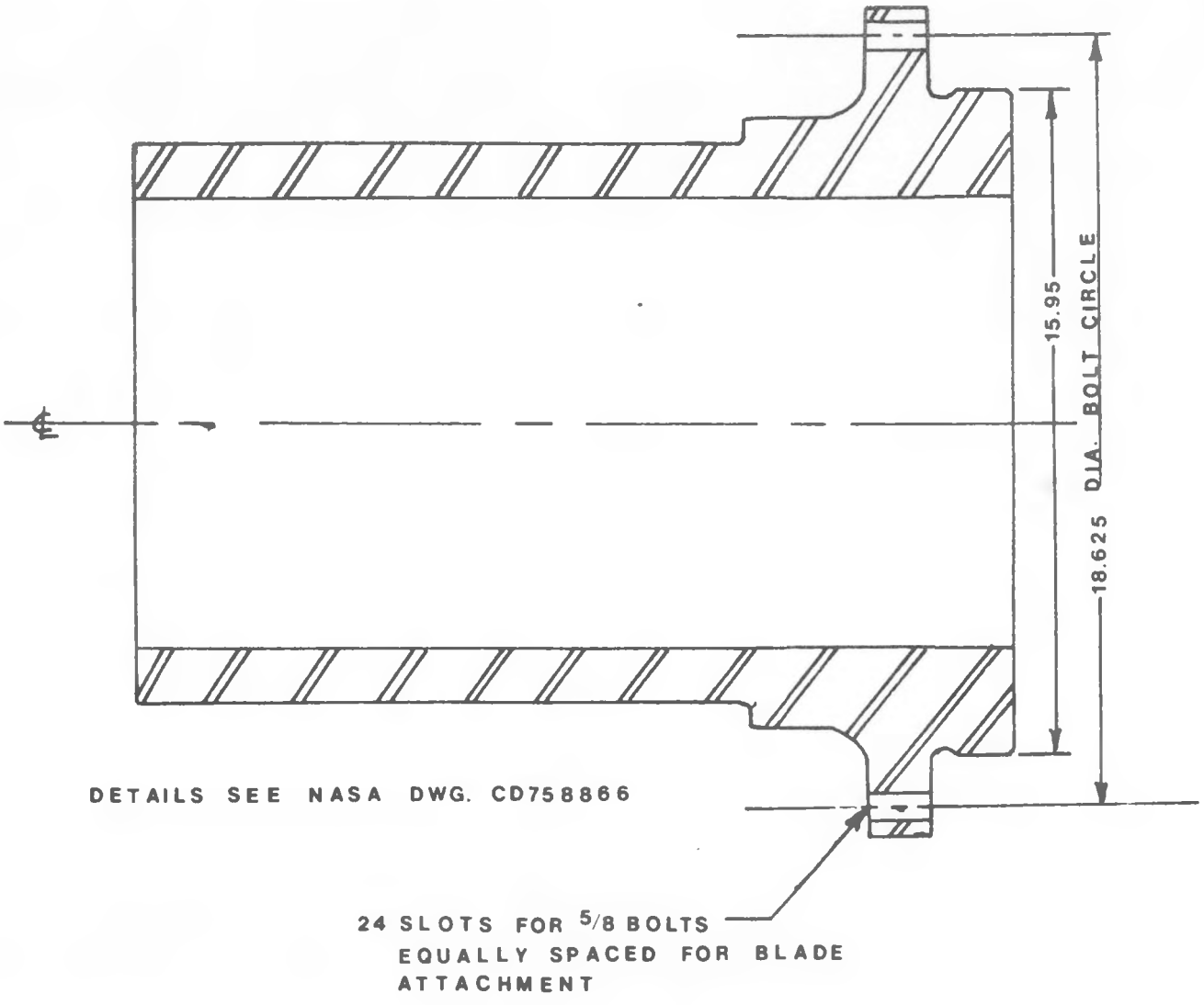

FIGURE 8.- PITCH CONTROL HUB (DIMENSIONS IN INCHES).

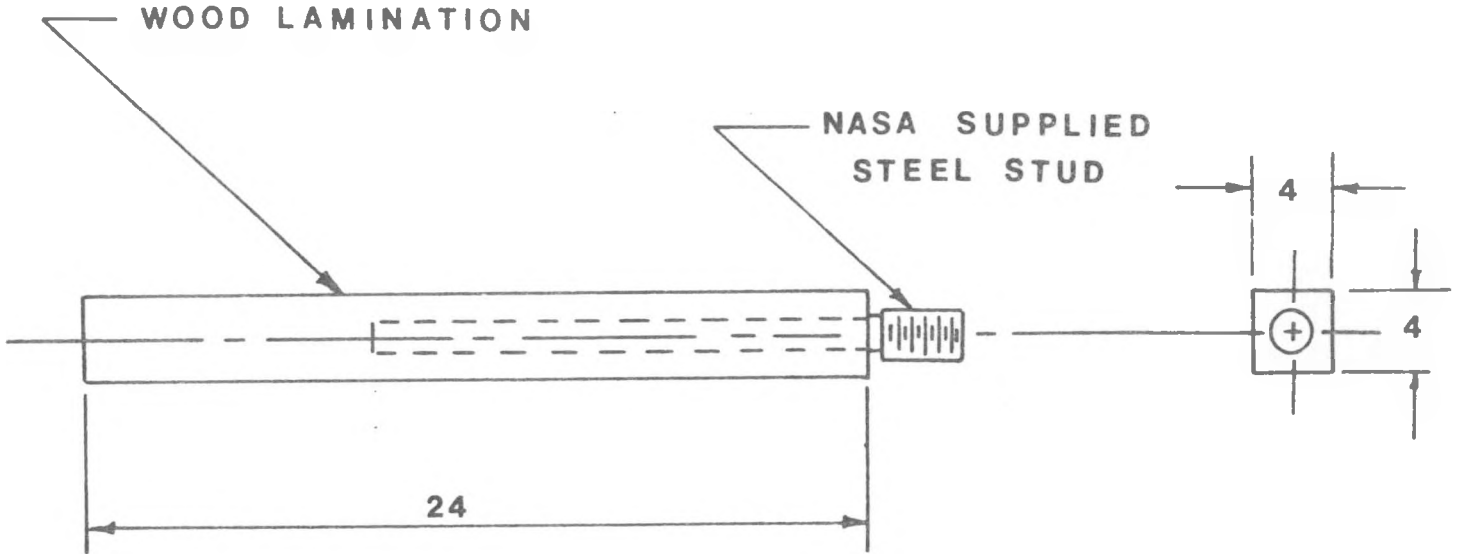

FIGURE 9. - LOAD TAKE-OFF STUD TEST SPECIMEN (DIMENSIONS IN INCHES).

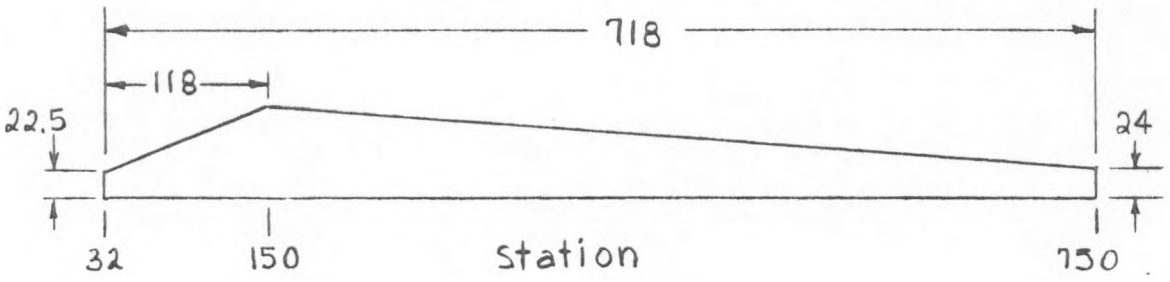

(a). Planform.

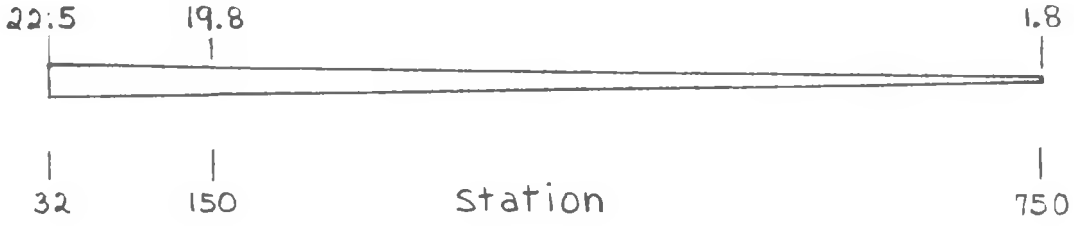

(b). Thickness.

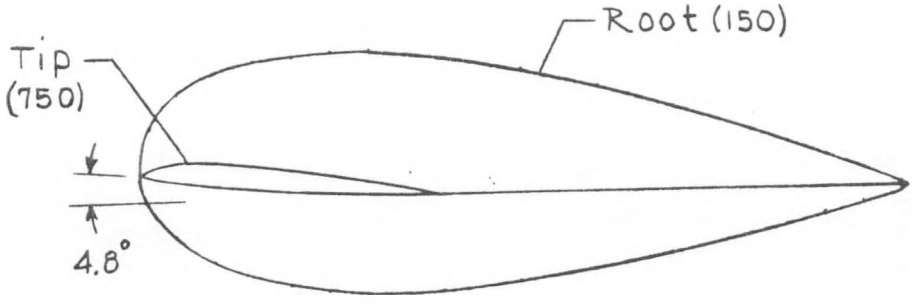

(c). Cross sections.

Figure 10.- External geometry of Mod-0A wood composite blade. (Dimensions in inches.)

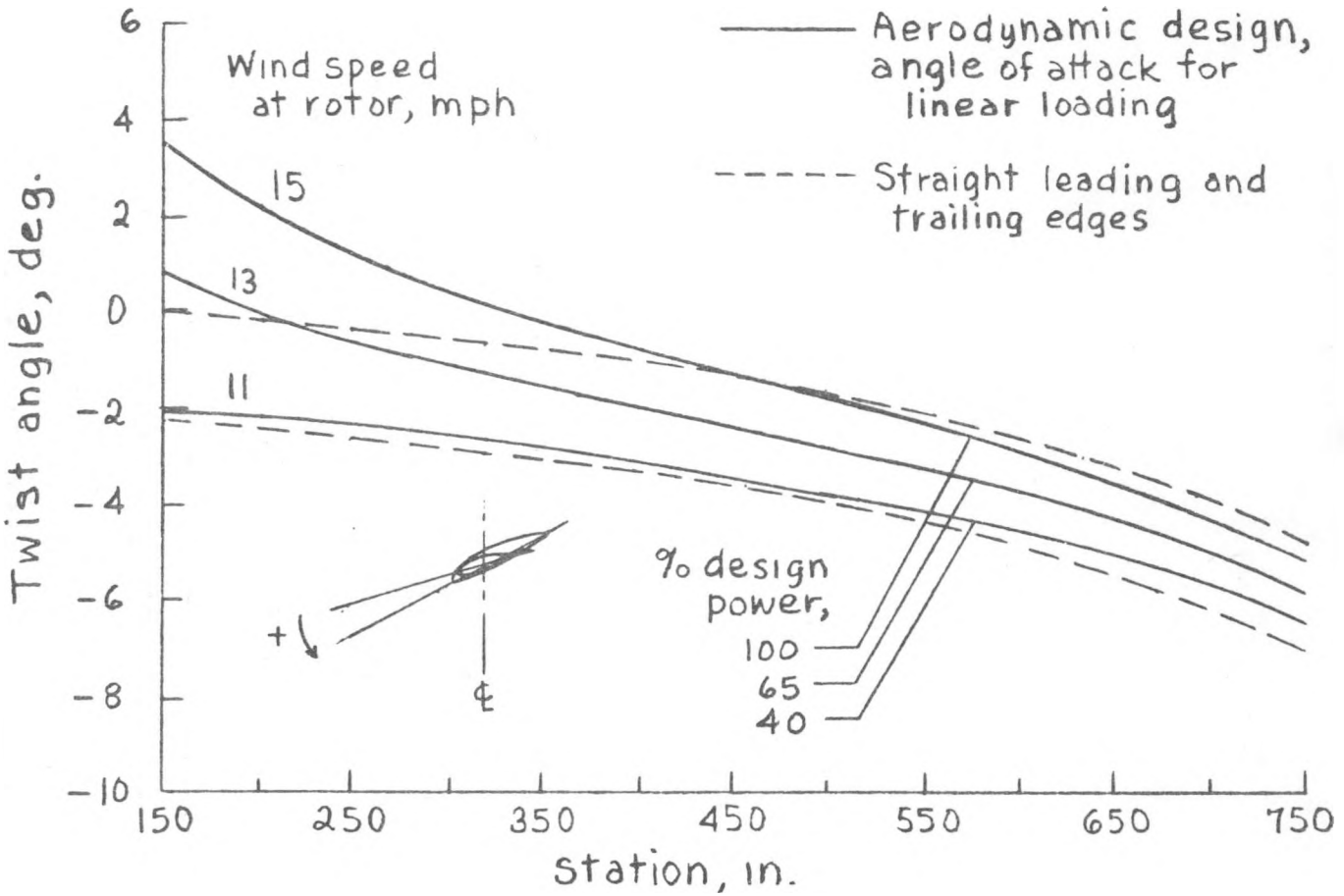

Figure 11.- Spanwise variation of local twist angle.

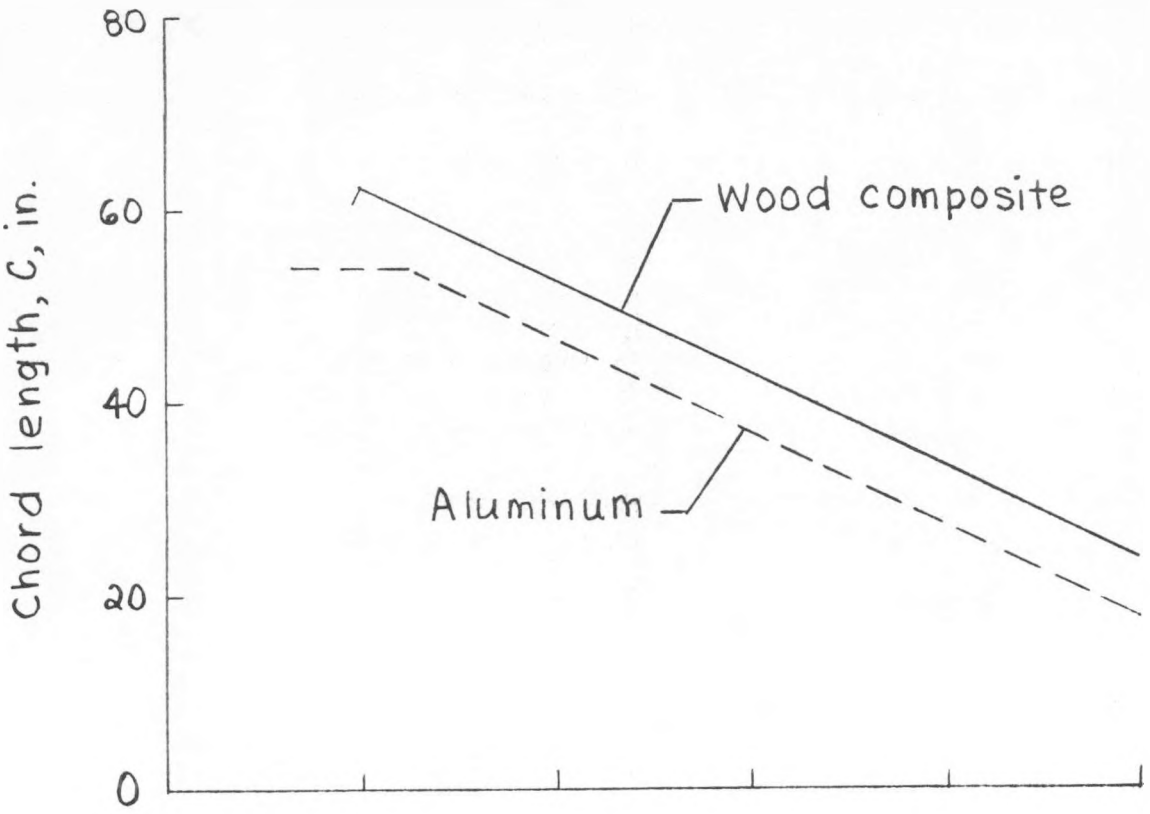

(a). Chord length.

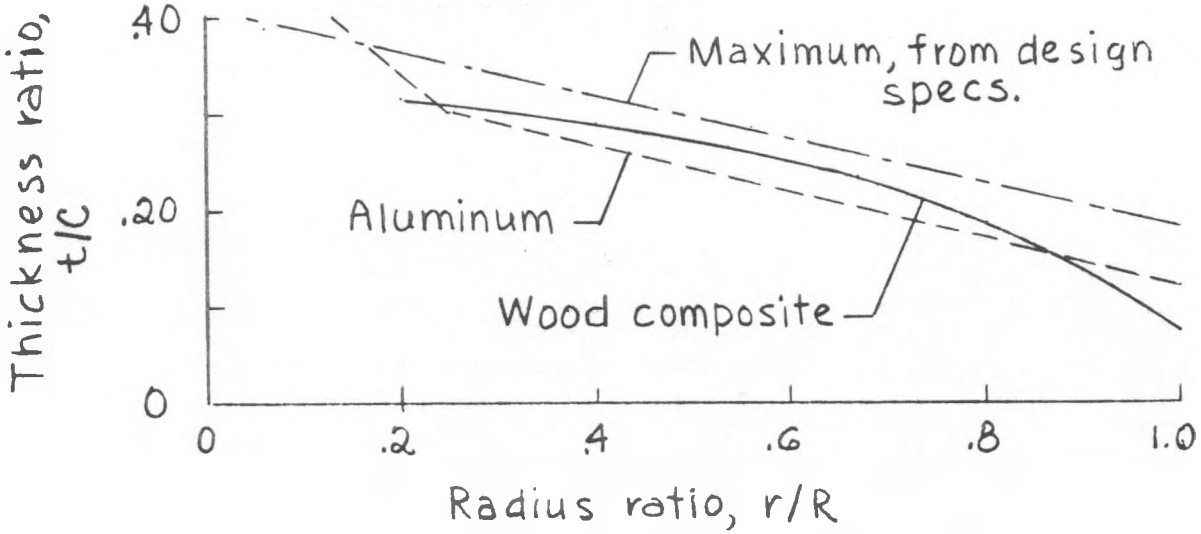

(b). Maximum thickness ratio.

Figure 12.- Comparison of blade geometries for Mod-0A wind turbine.

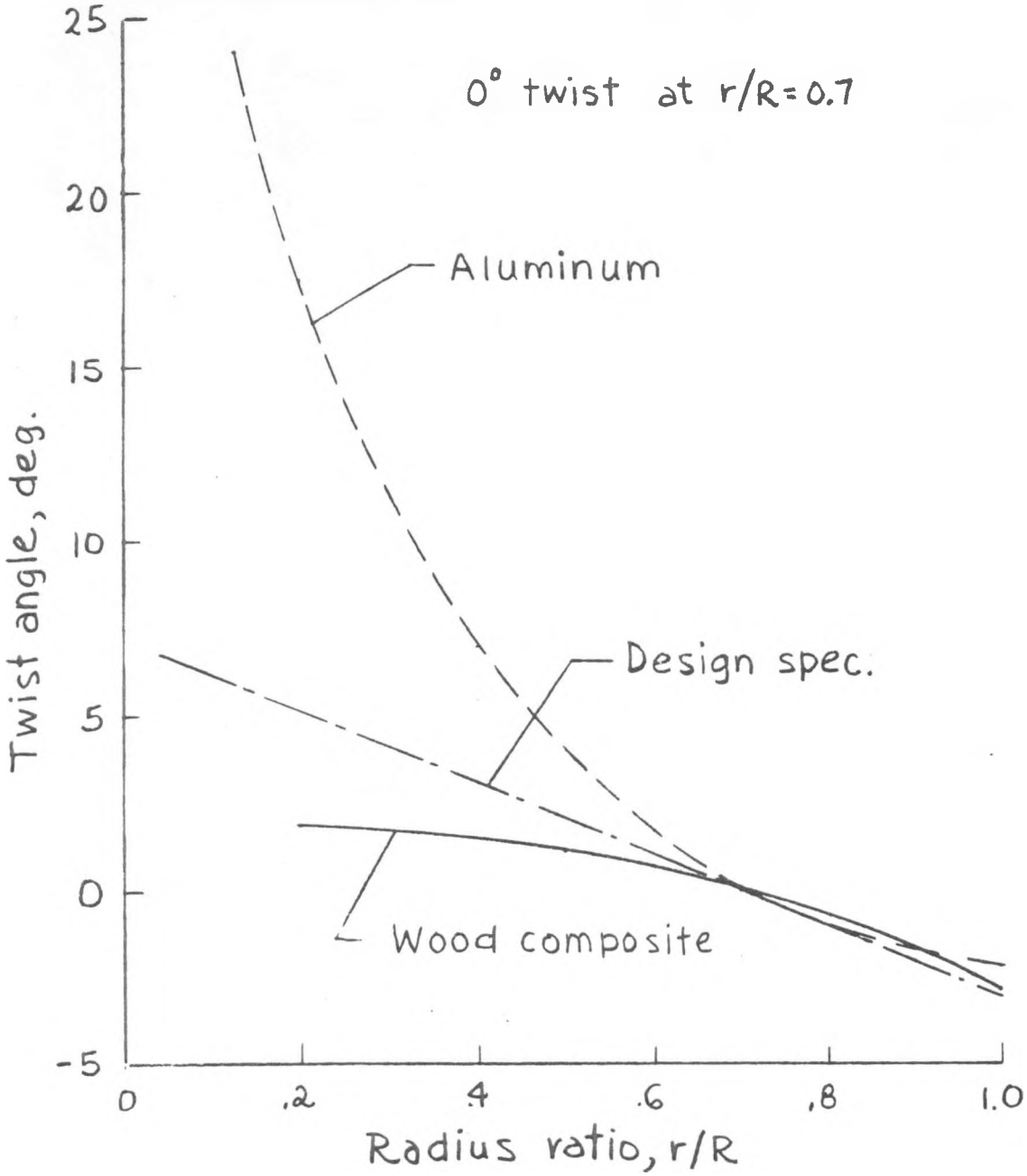

(c). Degree of twist.

Figure 12.- Concluded.

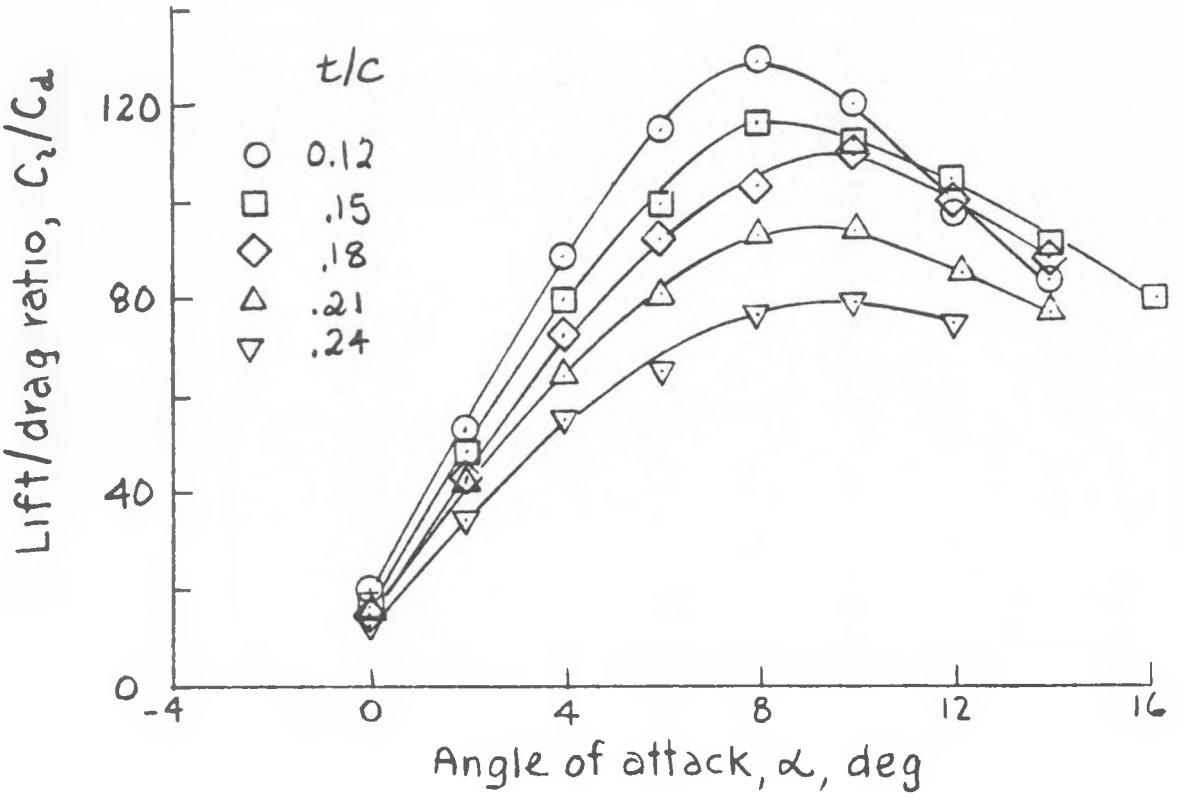

Figure 13.- Lift/drag characteristics of NACA 230-series airfoil sections, $R_e = 6 \times 10^6$. Data from ref. 12 .

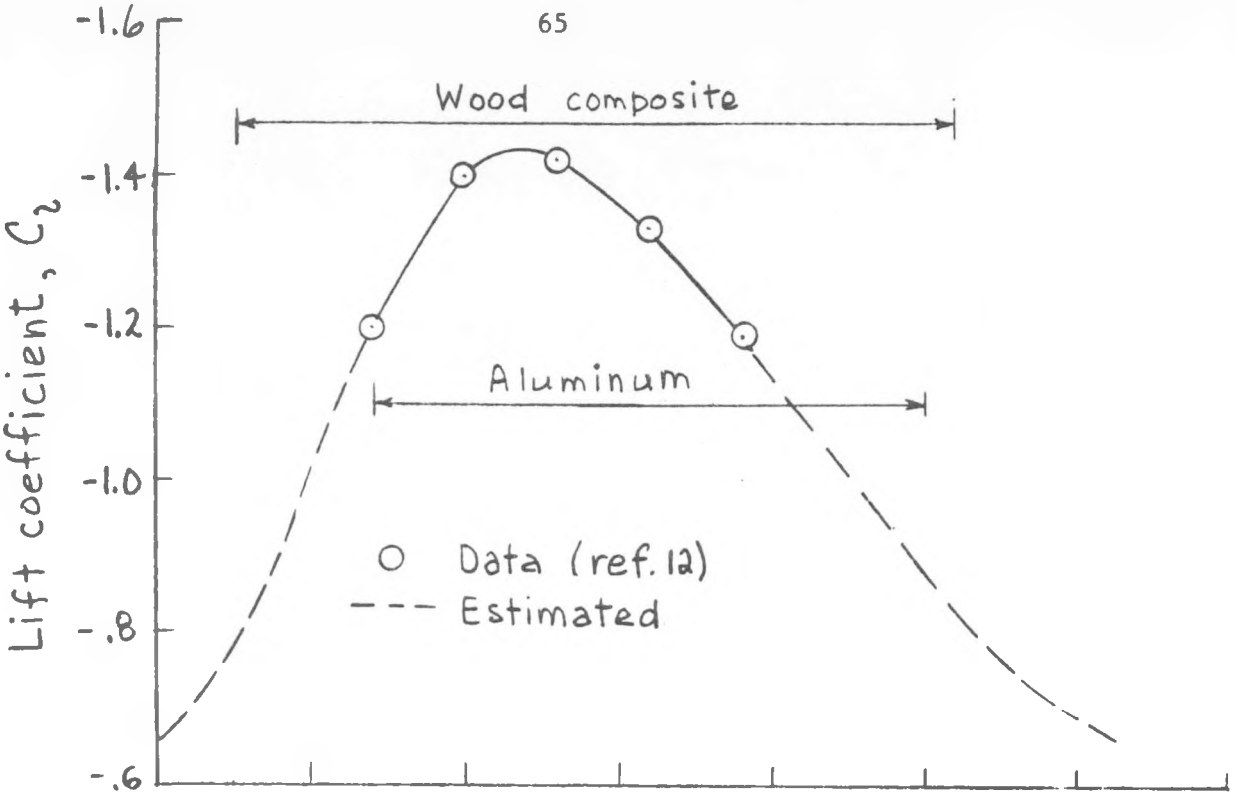

(a). Maximum negative lift coefficient

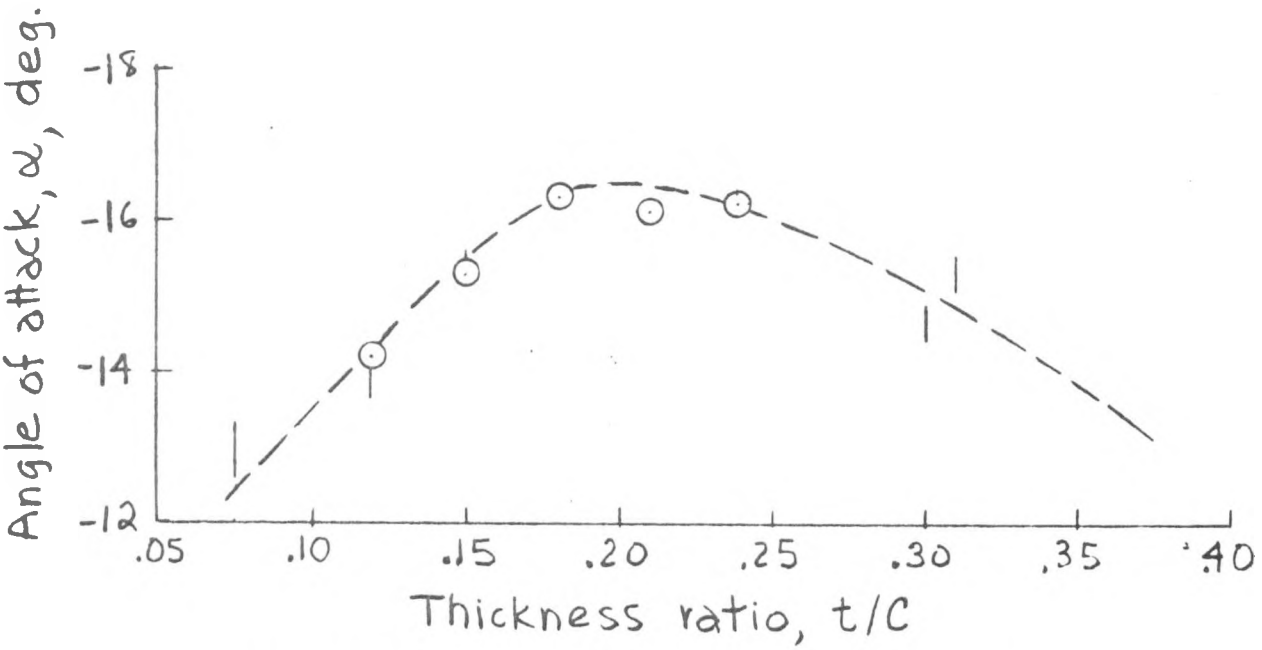

(b). Angle of attack at maximum C_l.

Figure 14. - Negative stall characteristics of NACA 230-series airfoil sections, $R_e = 6 \times 10^6$.

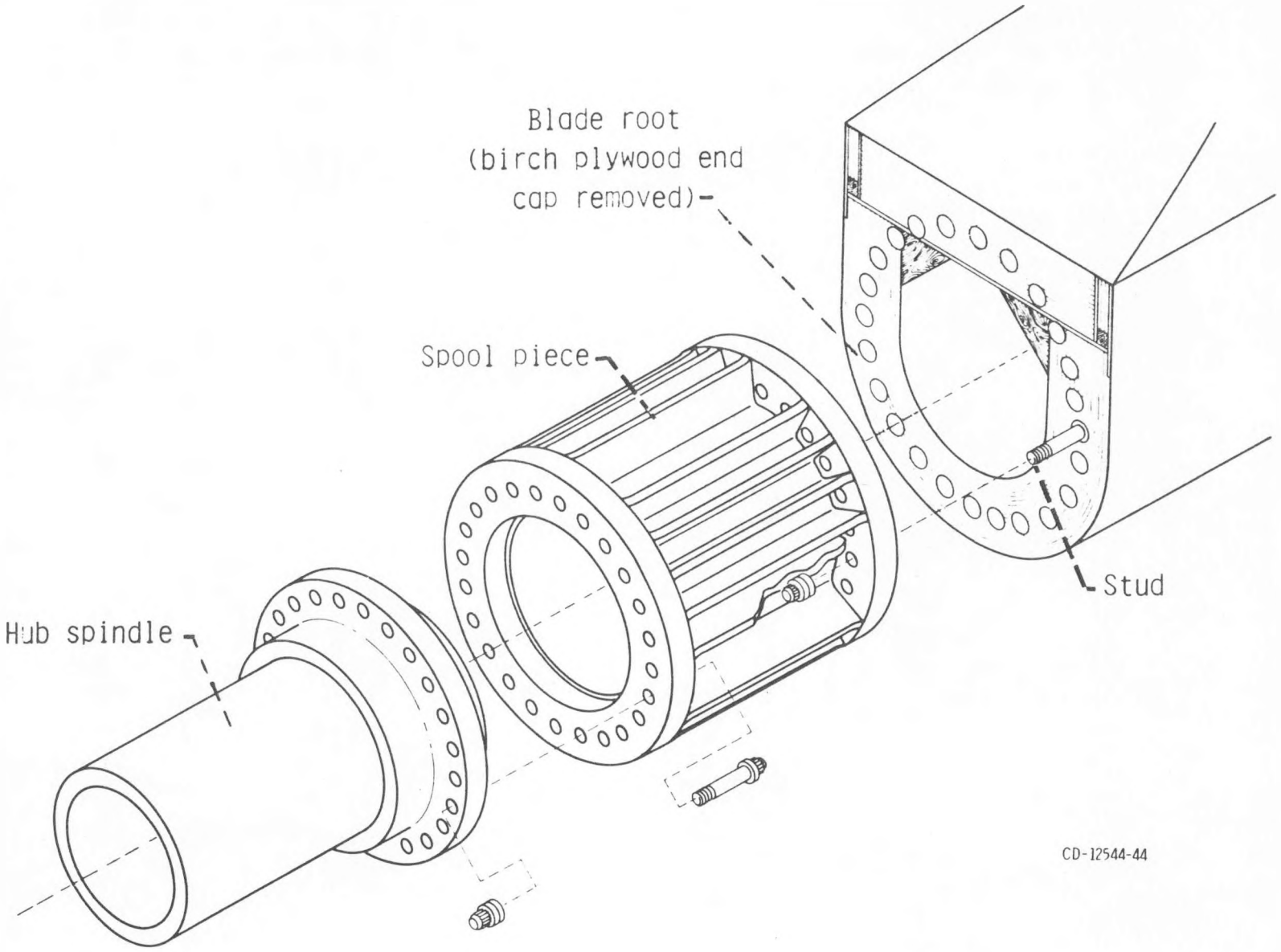

Figure 15. - Schematic of hub attachment concept for wood blade.

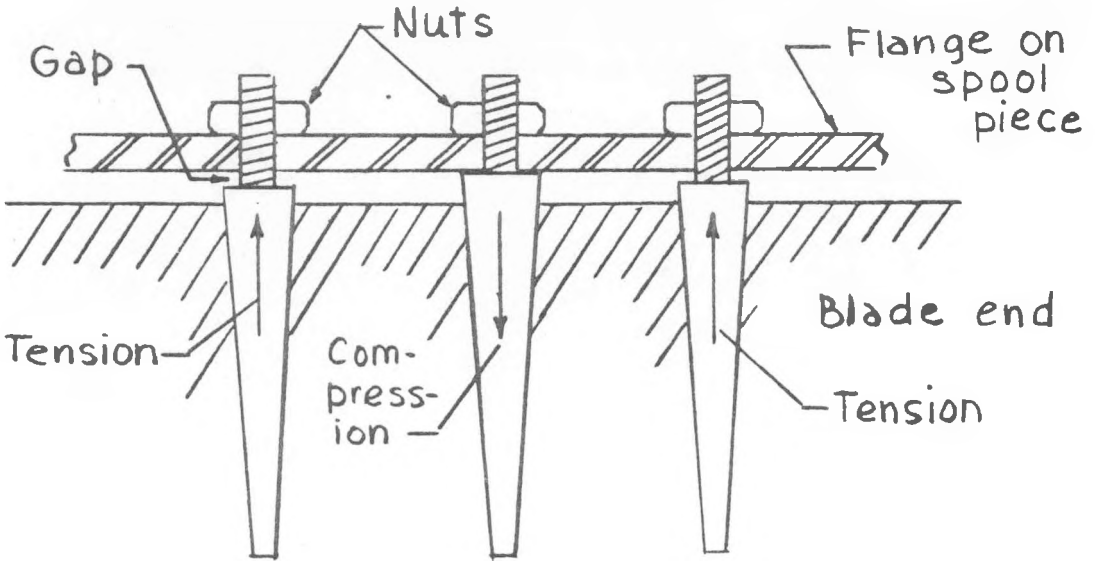

Figure 16.- Stud prestress in blade/hub attachment.

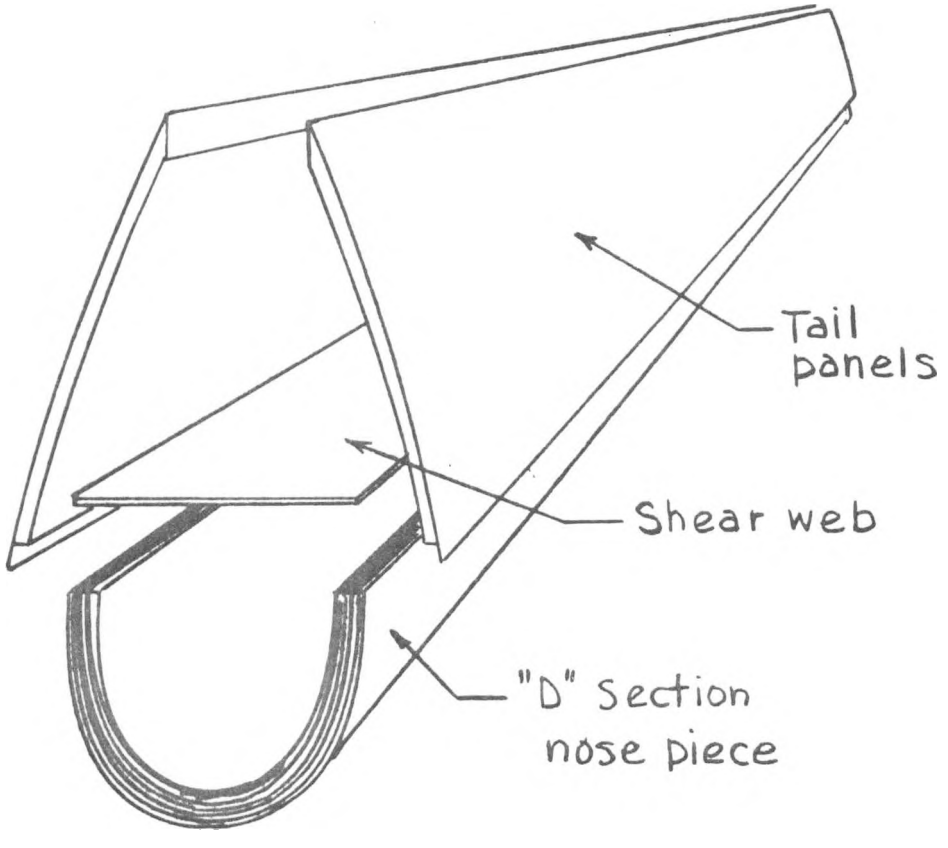

Figure 17.- Early fabrication concept with three molded sections (nose piece and each tail panel).

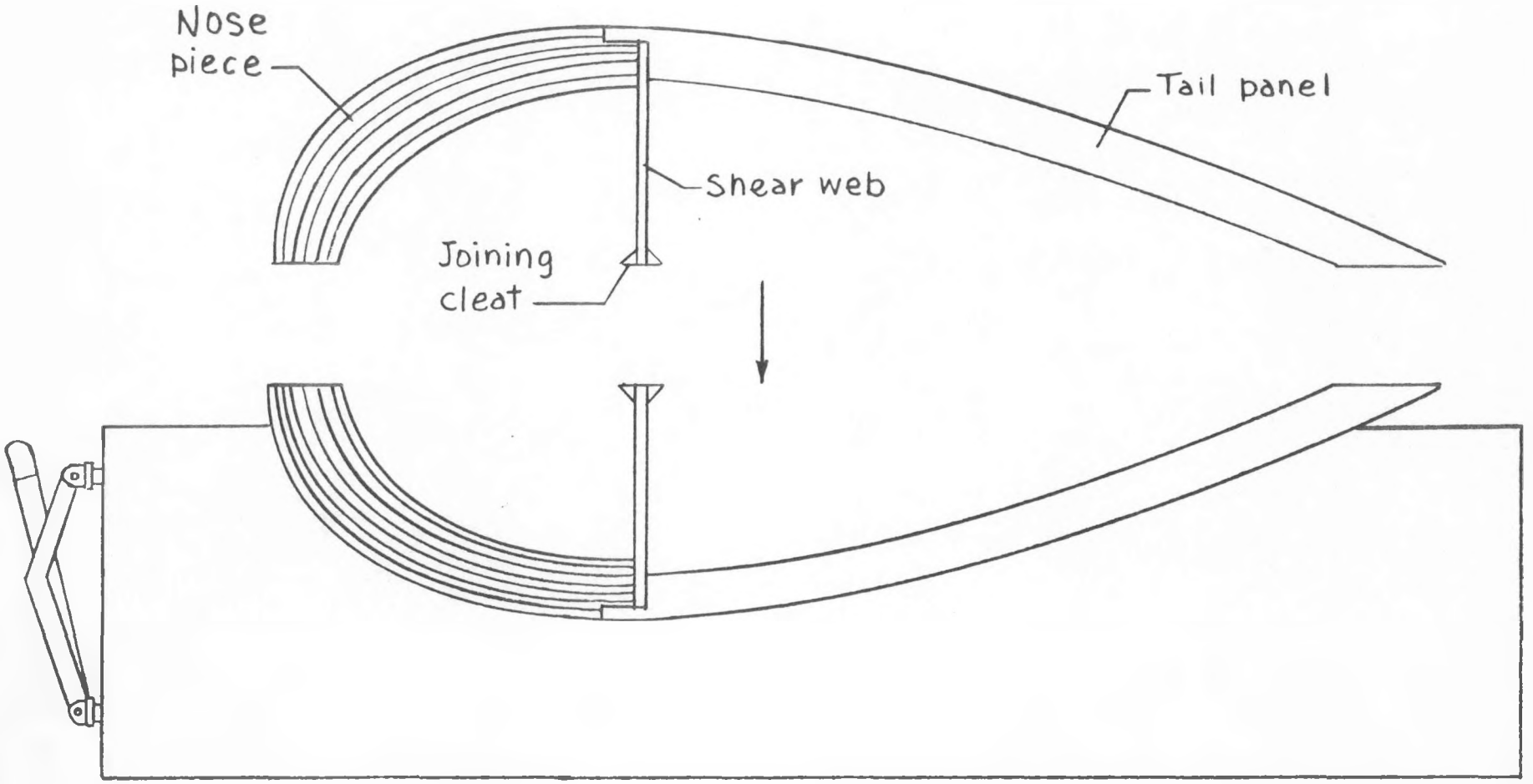

FIGURE 18. — TWO-PART HALF-SHELL MOLD METHOD.

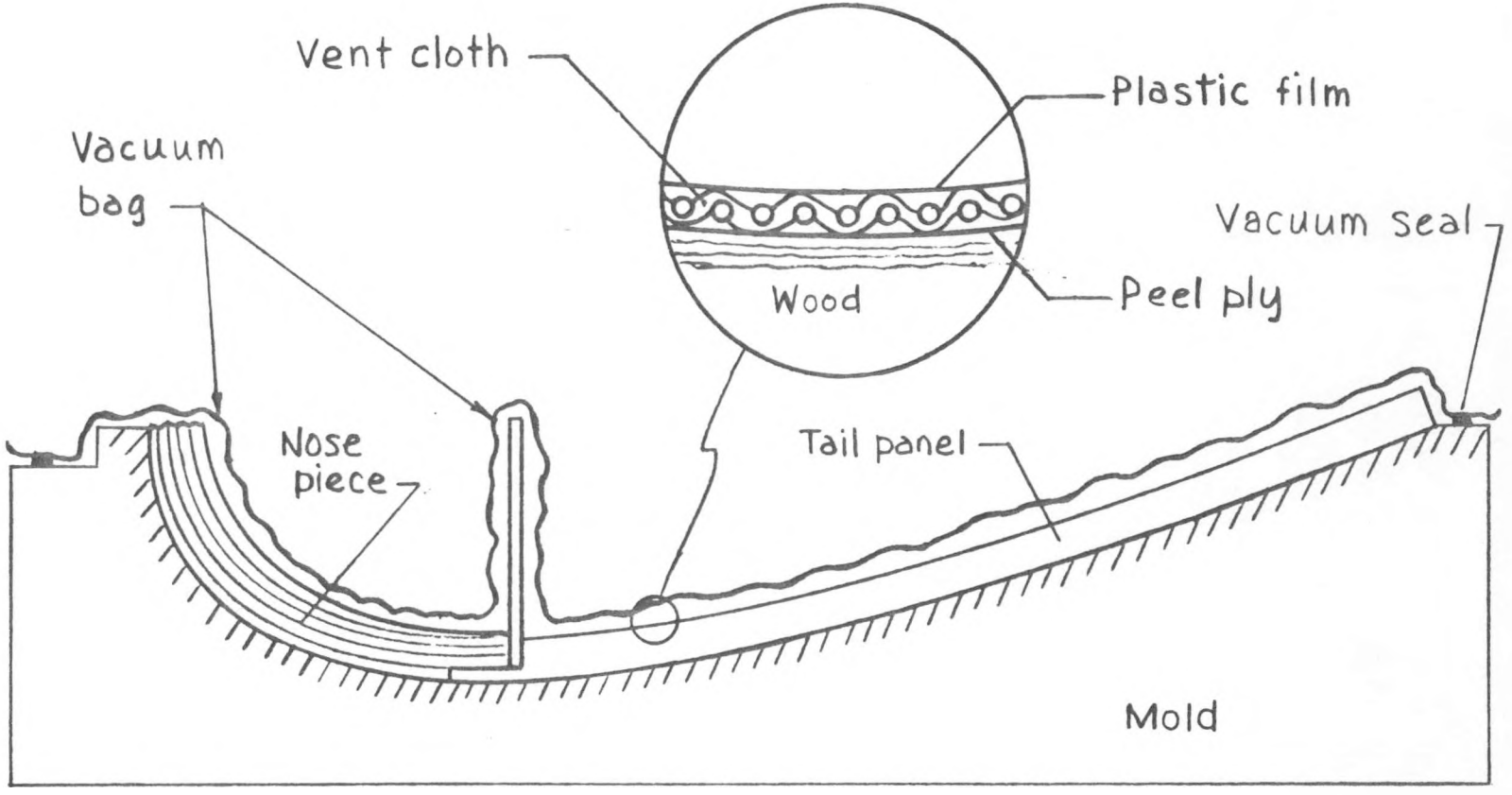

FIGURE 19. - FEMALE MOLD SHOWING VACUUM BAG COMPACTION CONCEPT.

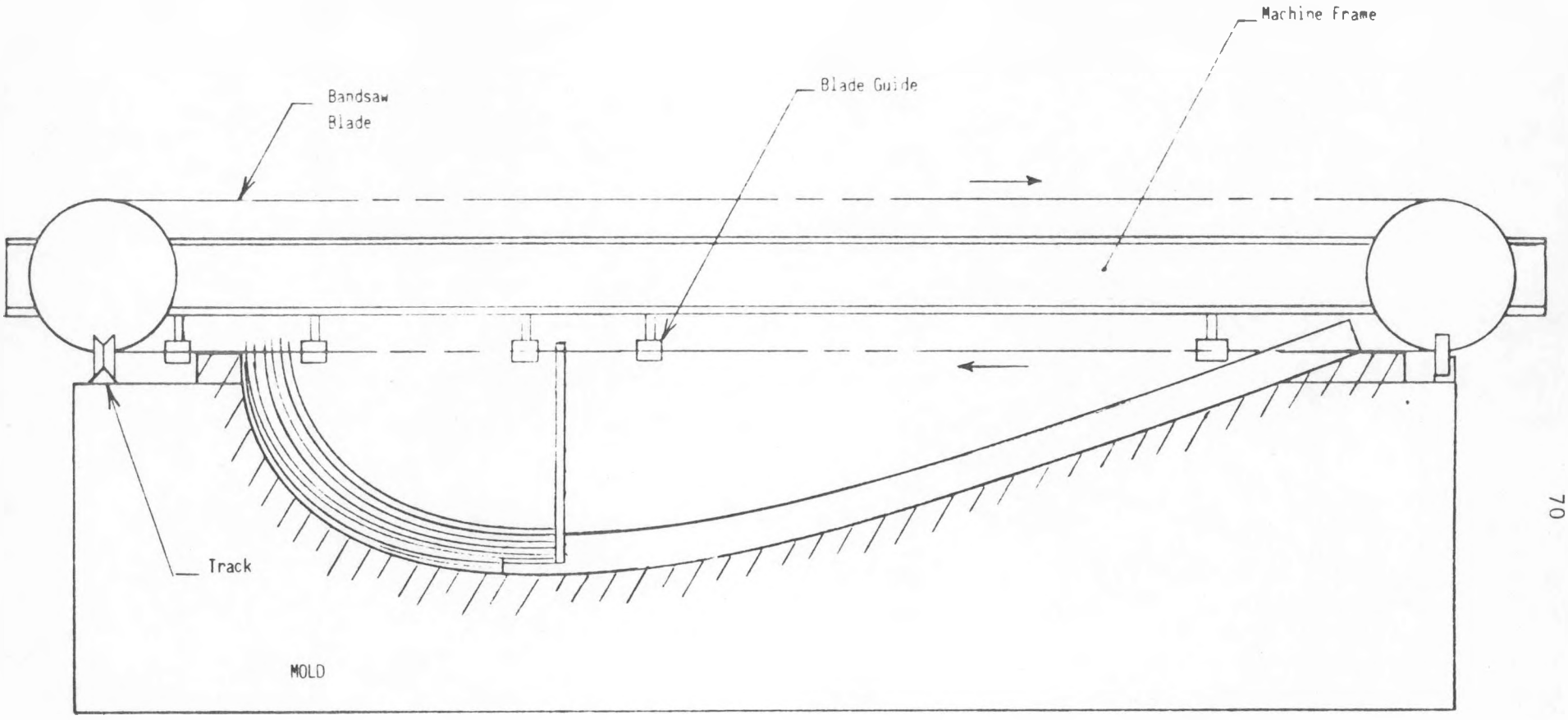

FIGURE 20. - BANDSAW CONCEPT FOR CUTTING BLADE HALF-SHELLS.

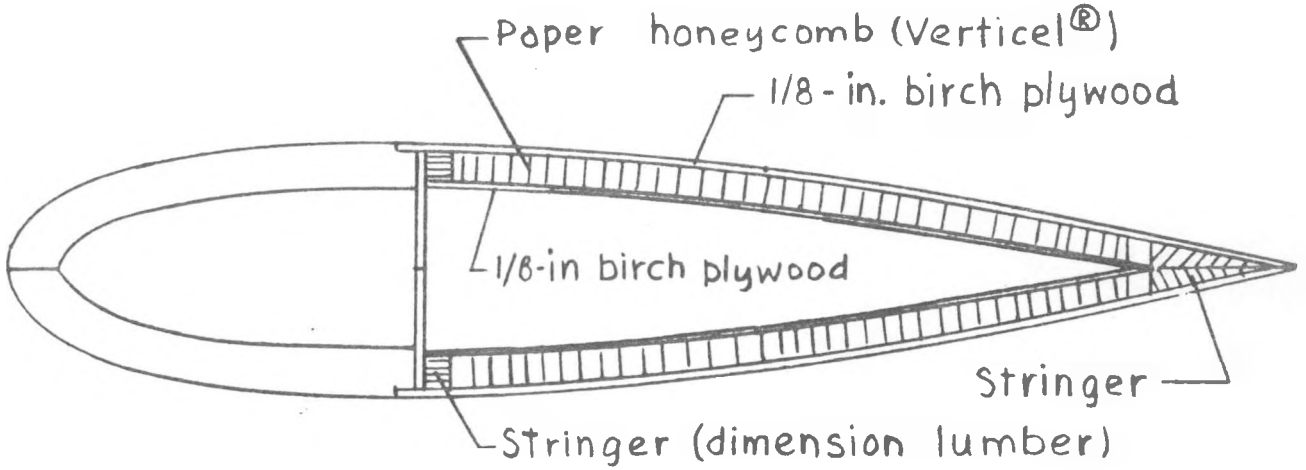

FIGURE 21. - FULLY-SUPPORTED CORED TAIL PANEL CONCEPT.

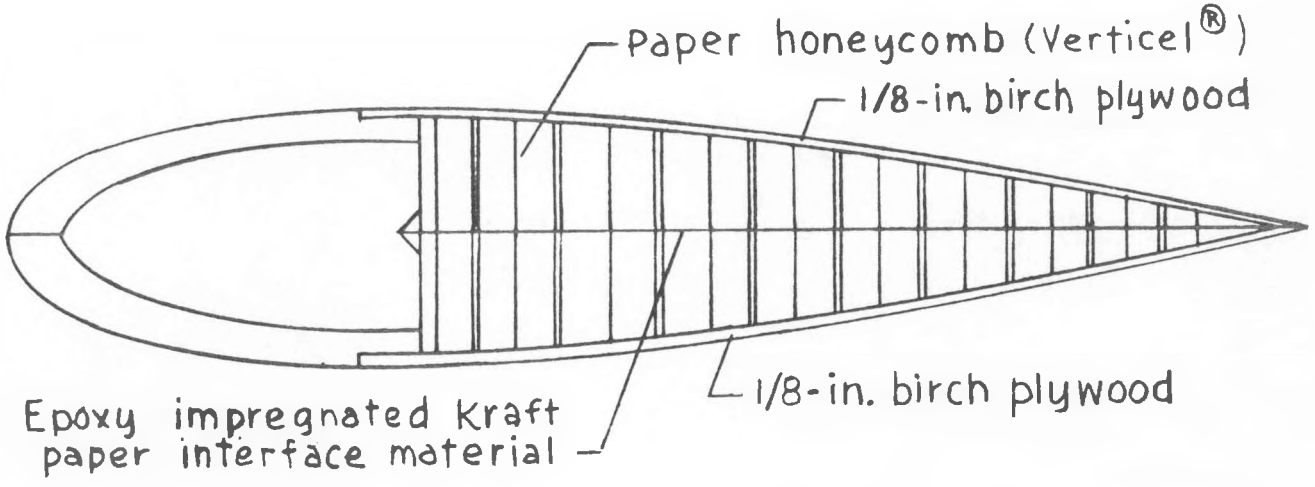

FIGURE 22.— FULLY-CORED SECTION AT OUTER TIP OF BLADE.

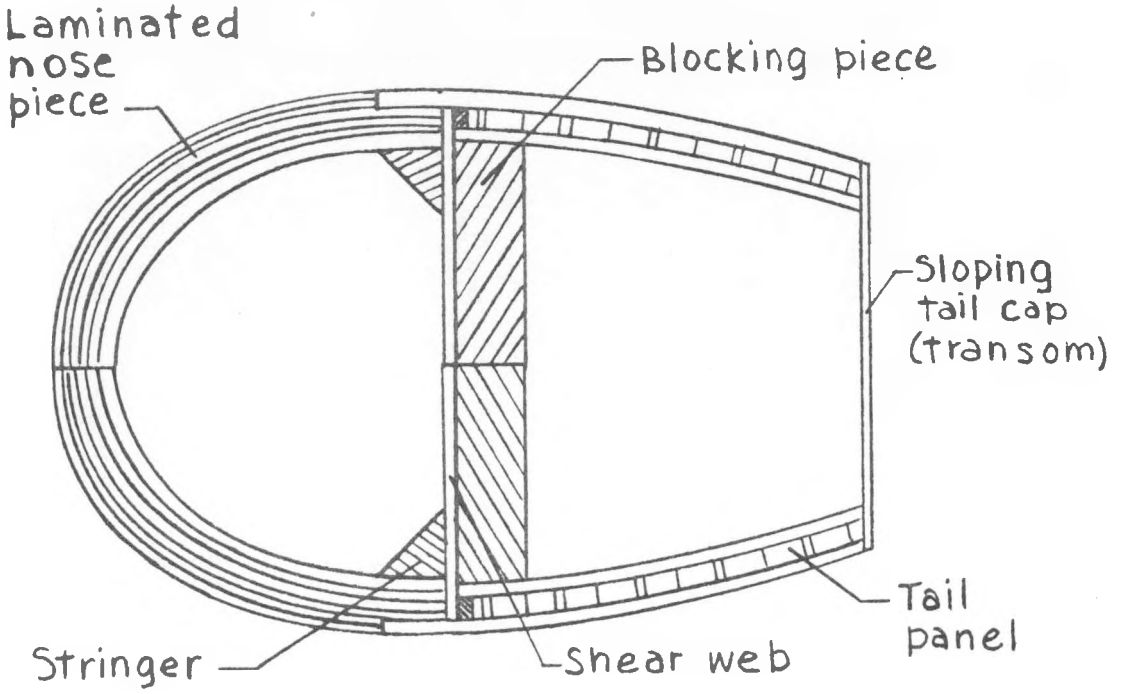

Figure 23.- Blade root build up from blade root end to station 150.

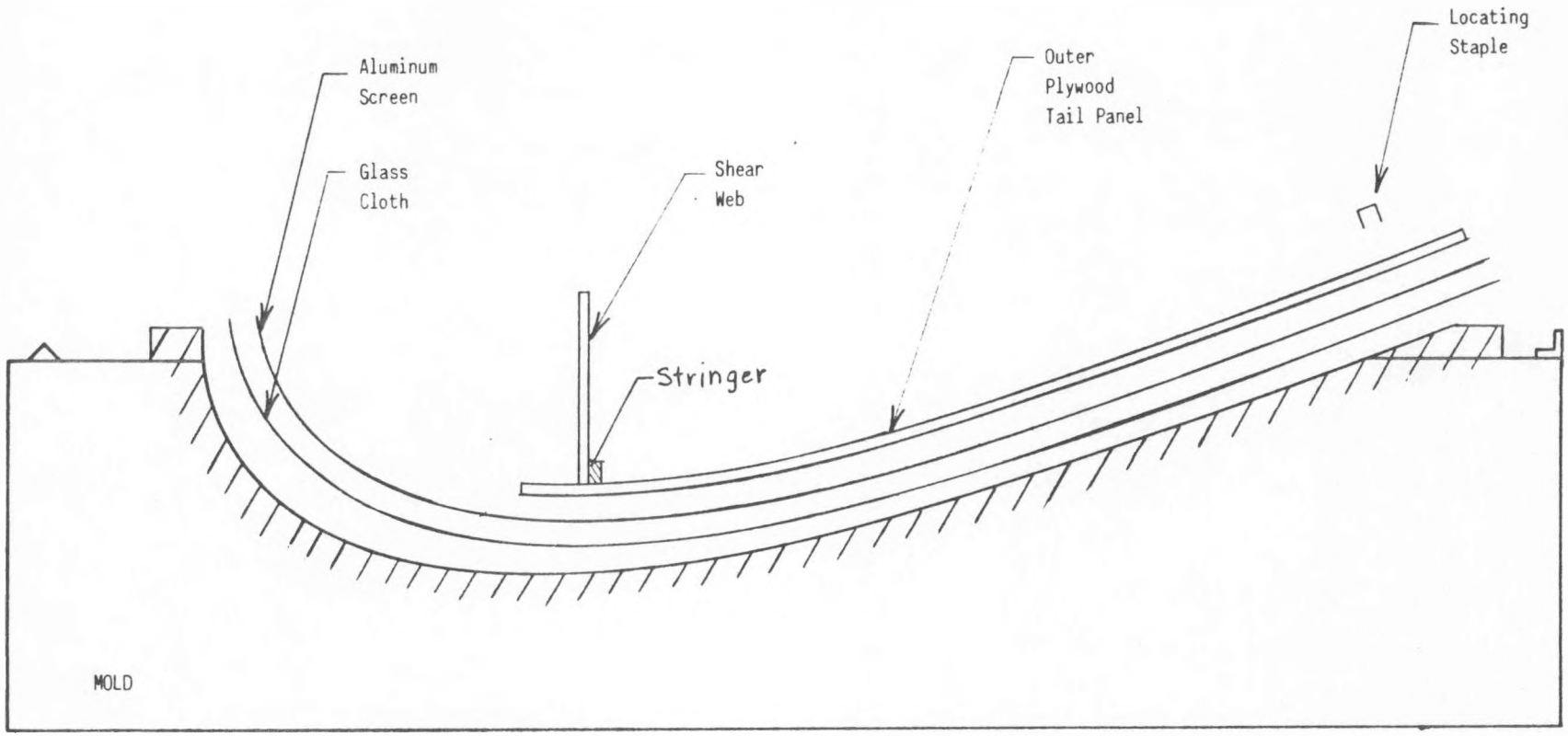

FIGURE 24.— MATERIAL INSERTION IN HALF MOLD.

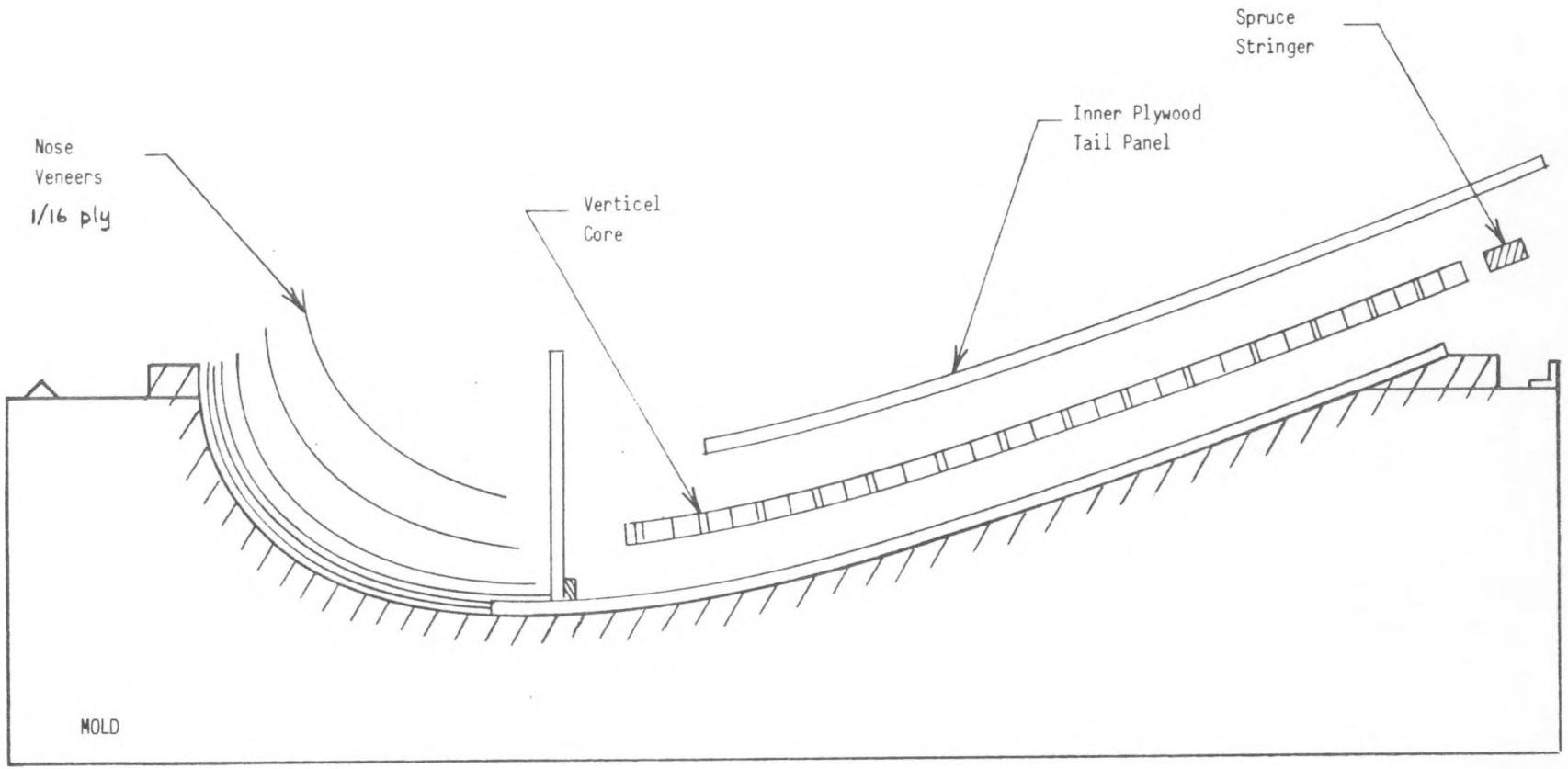

FIGURE 25. INSERTION OF REMAINING MATERIAL IN HALF-MOLD.

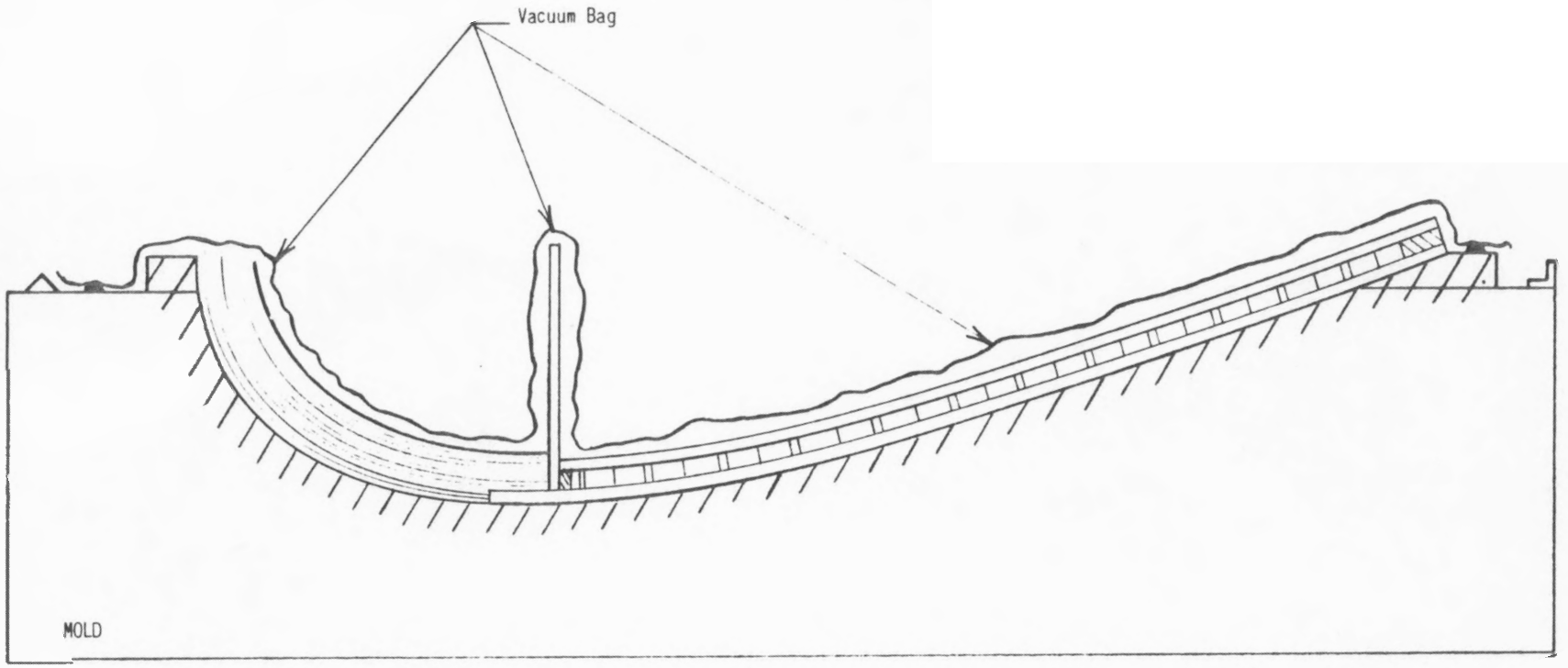

FIGURE 26.- VACUUM BAG APPLICATION.

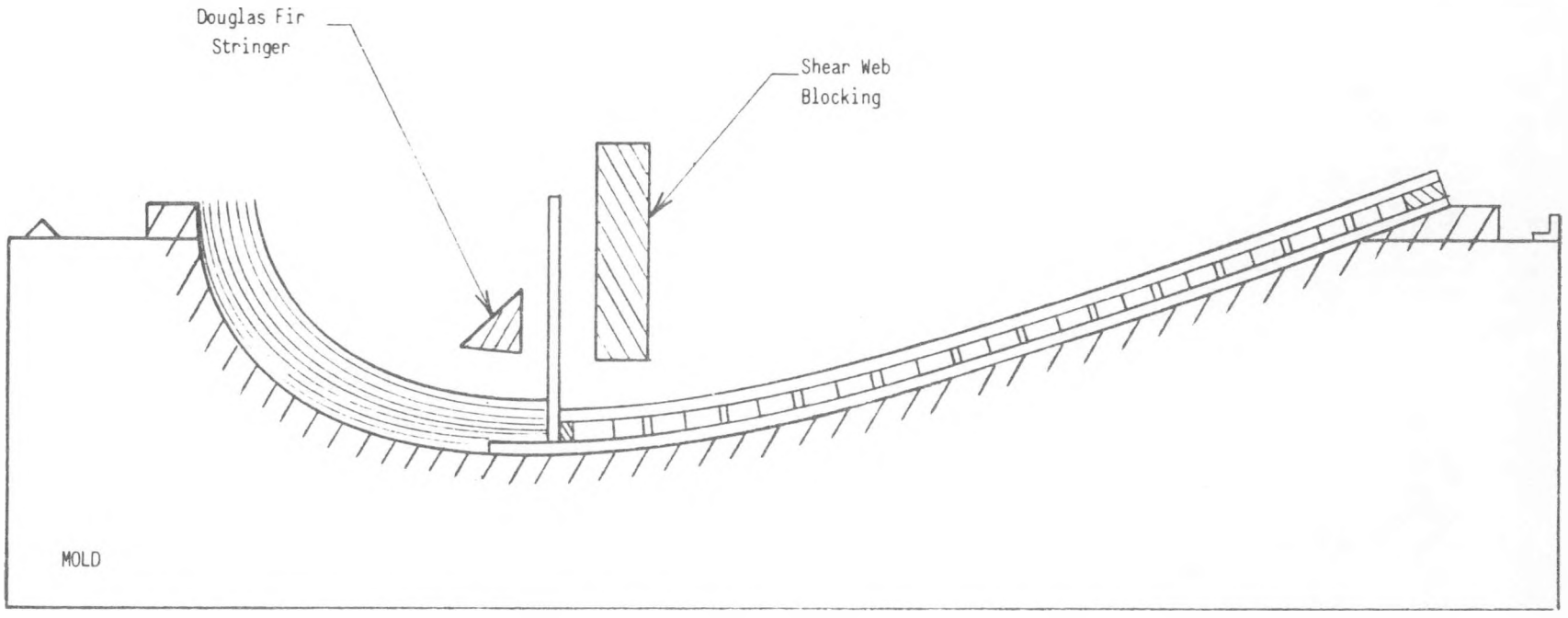

FIGURE 27.— ADDITION OF BUILDUP OF SHEAR WEB FOR ROOT SECTION.

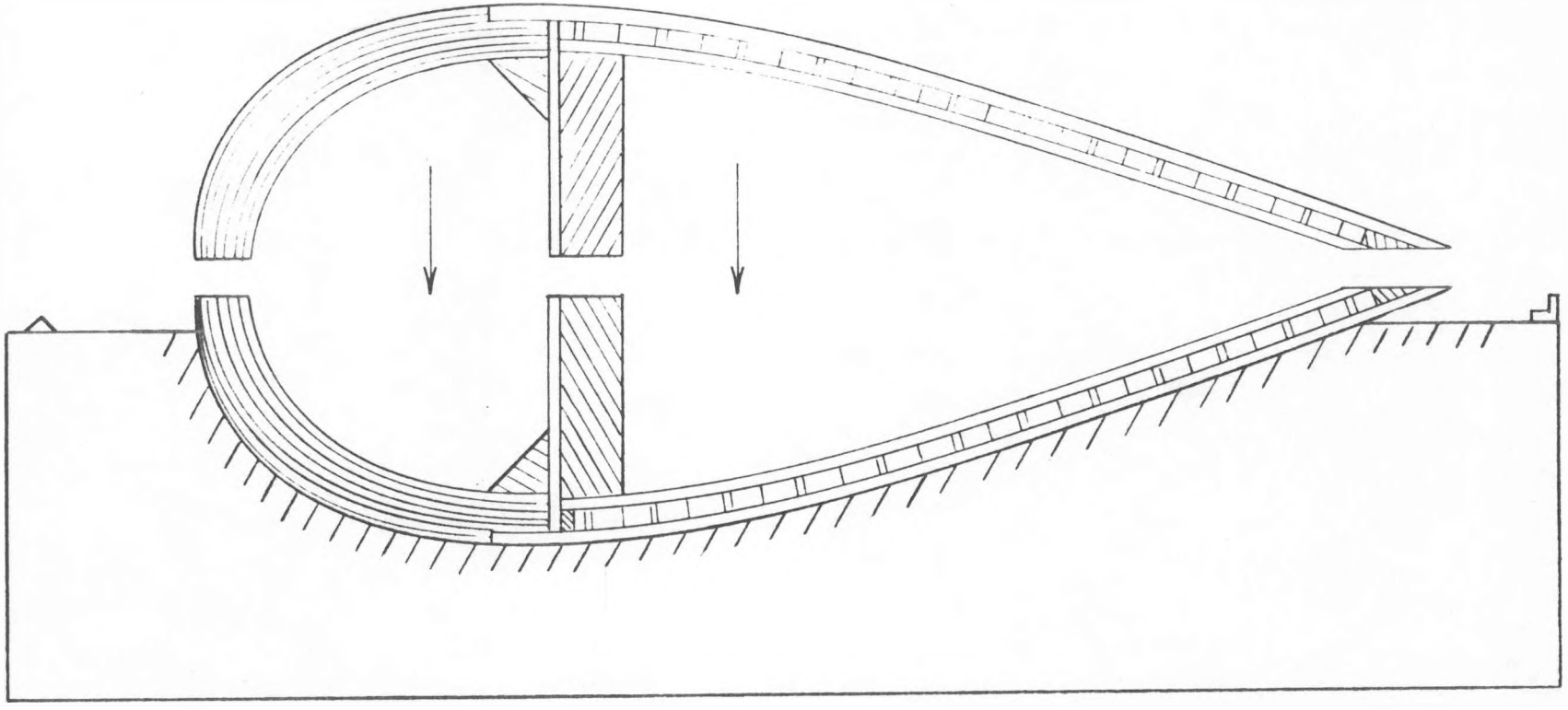

FIGURE 28.— BONDING OF THE TWO BLADE HALVES.

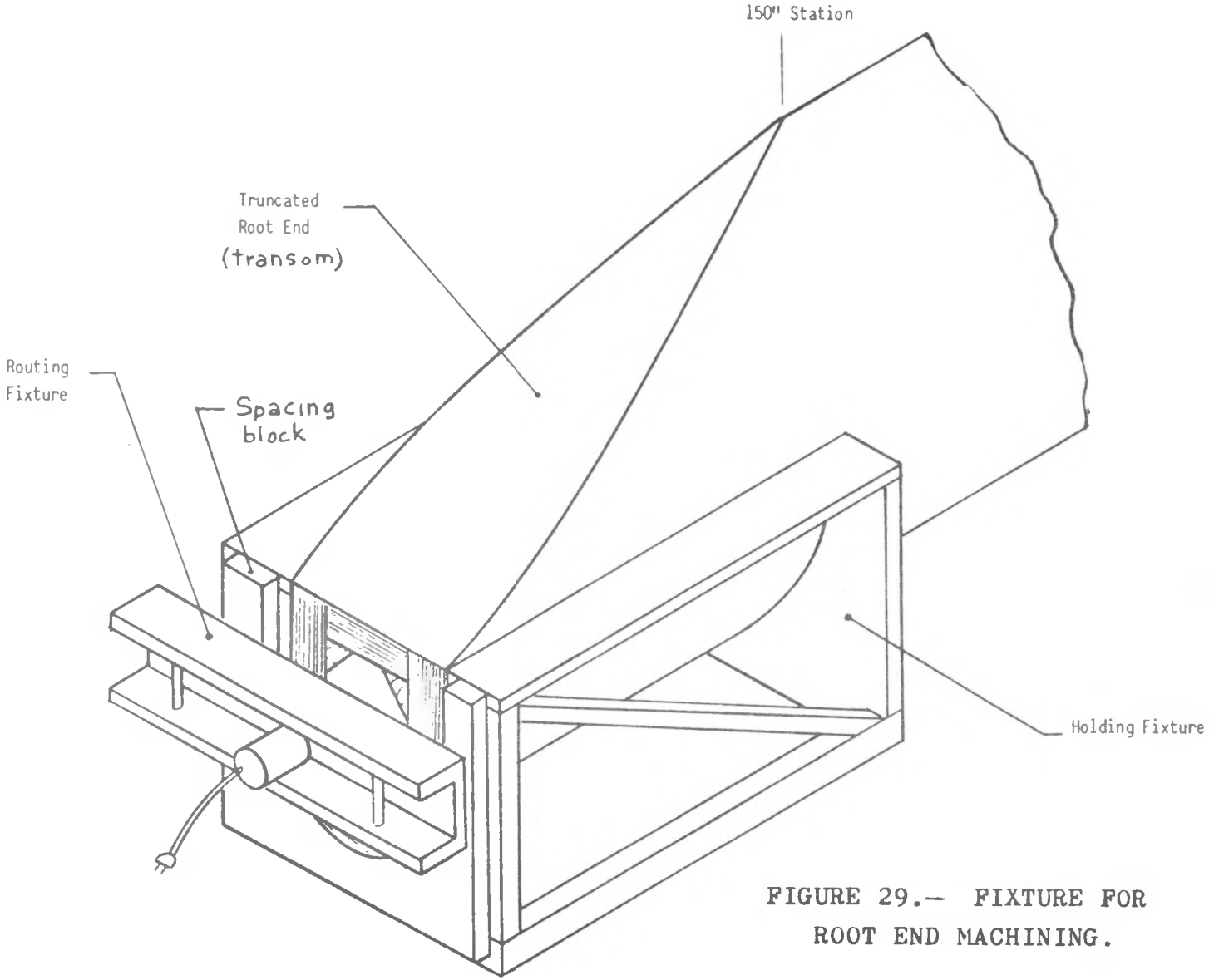

FIGURE 29.— FIXTURE FOR
ROOT END MACHINING.

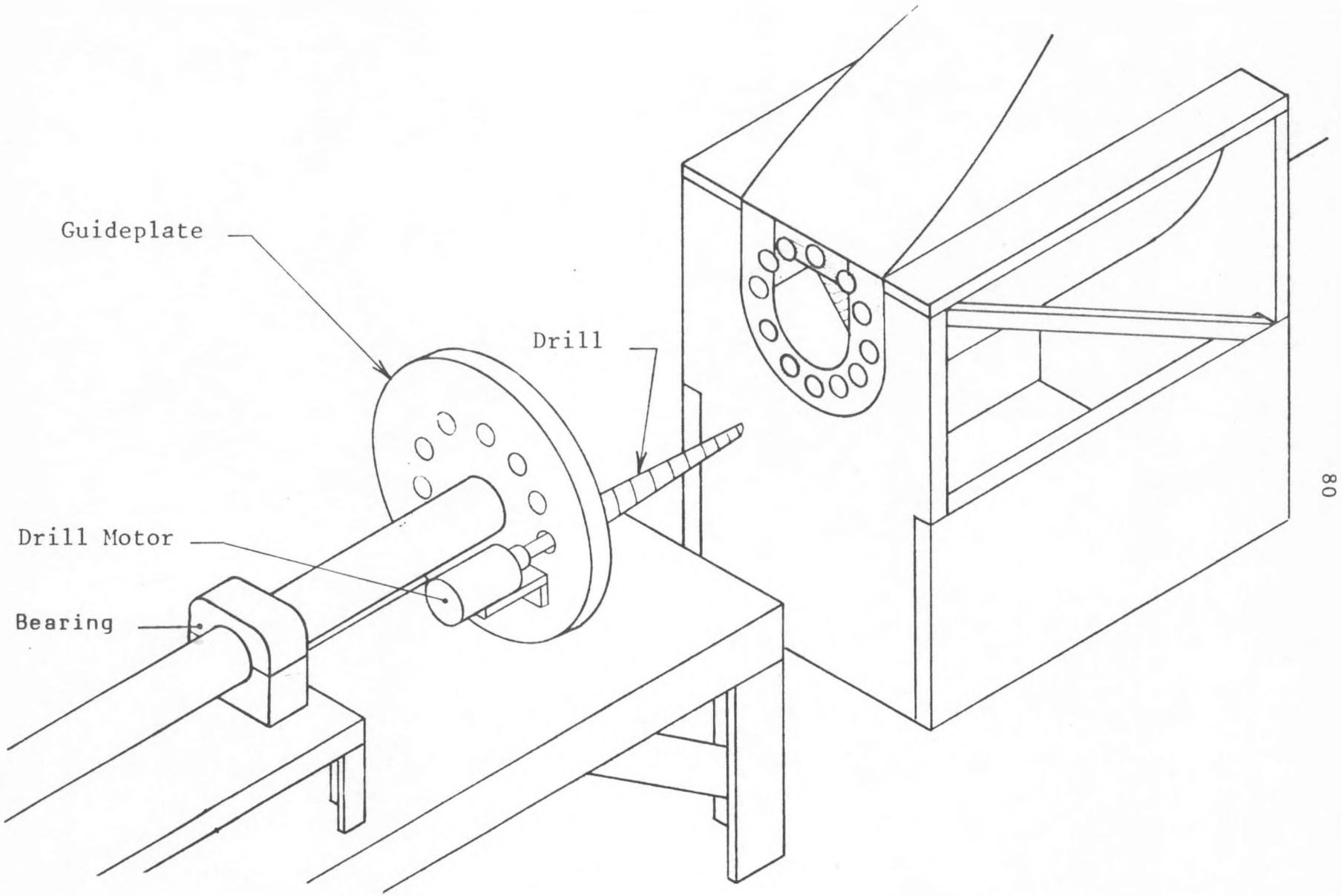

FIGURE 30.— DRILLING FIXTURE FOR STUD HOLES.

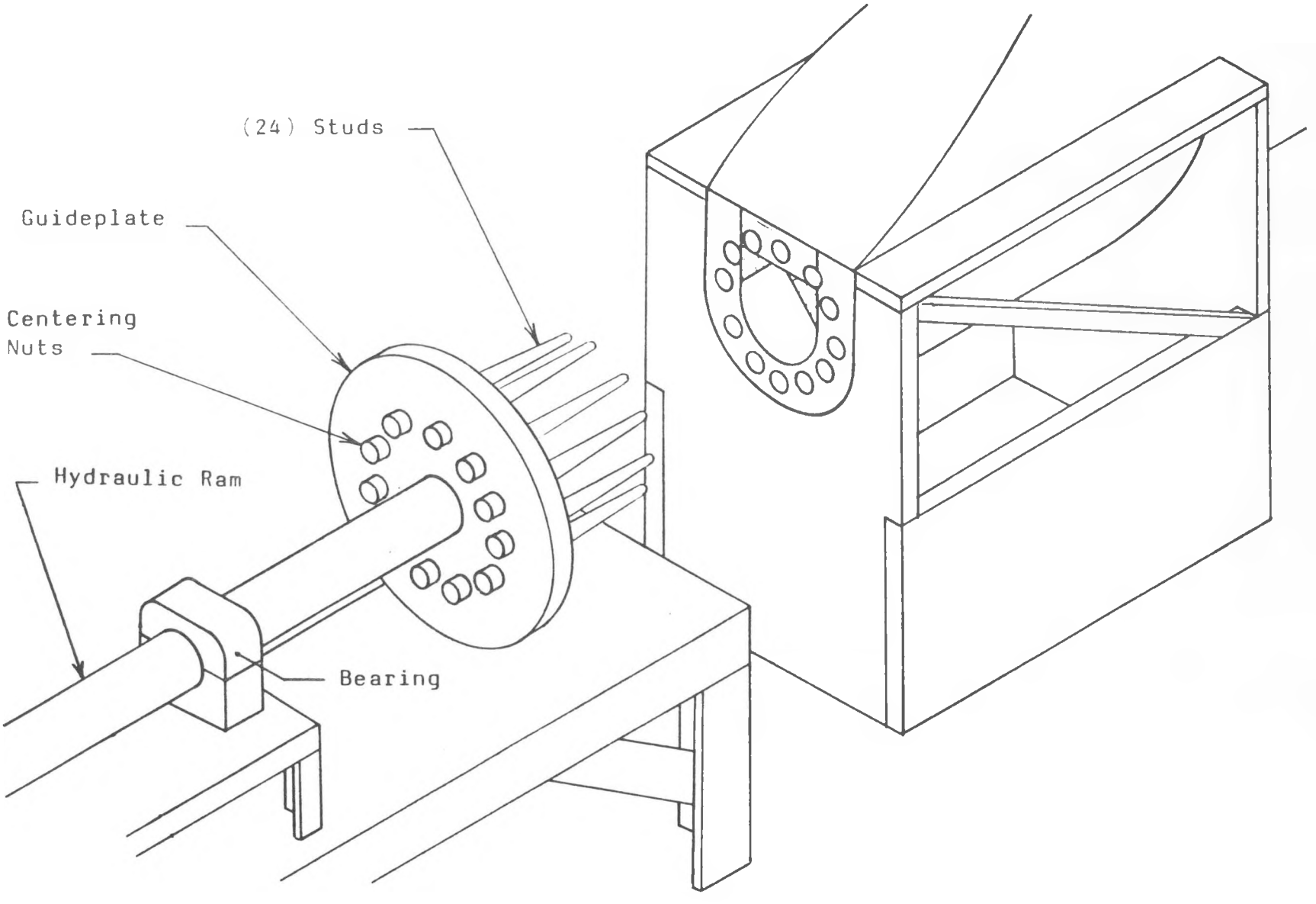

FIGURE 31. STUD INSERTION FIXTURE.

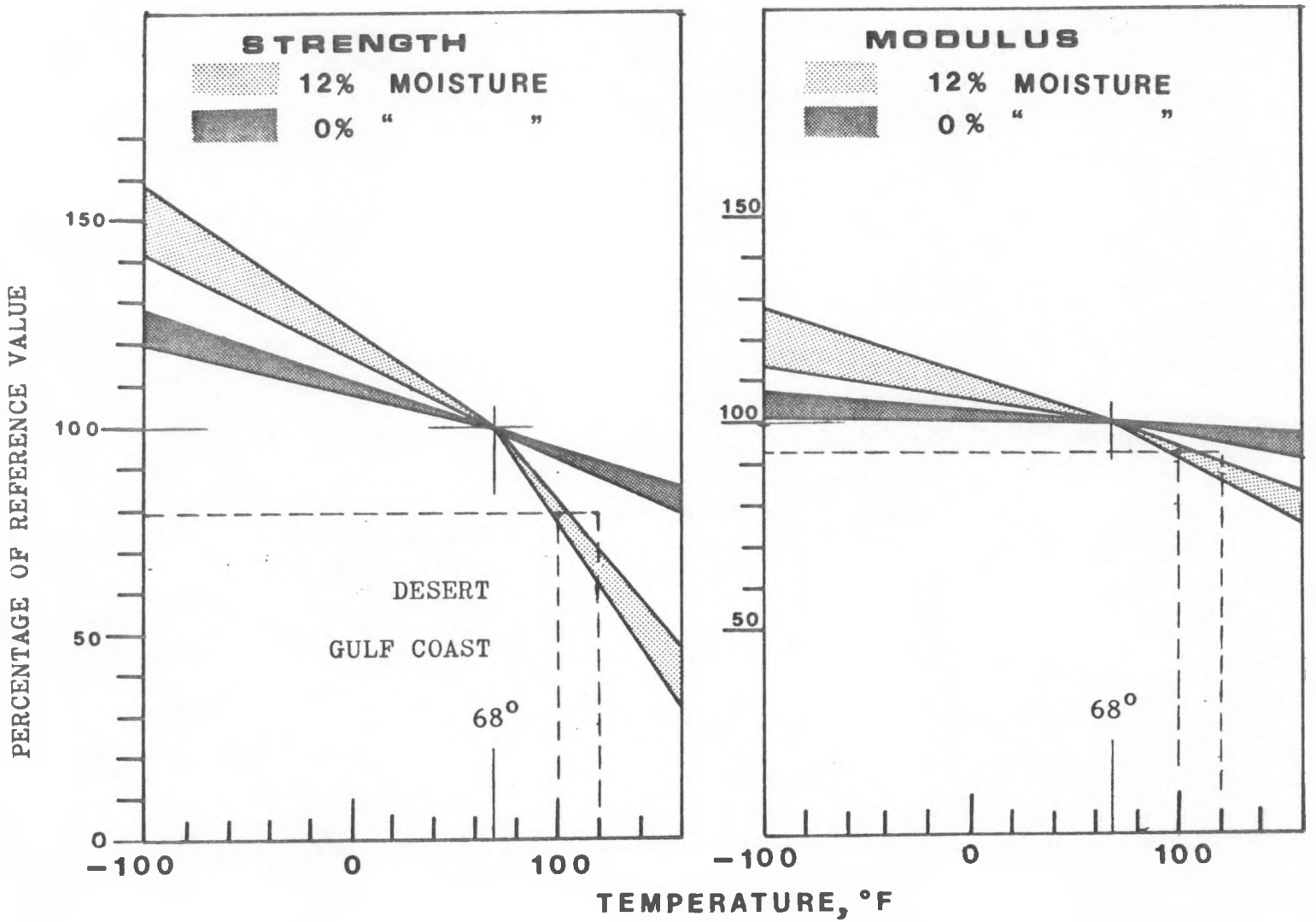

FIGURE 32.— EFFECT OF TEMPERATURE ON MECHANICAL PROPERTIES OF WOOD. (FROM REFERENCE 14)

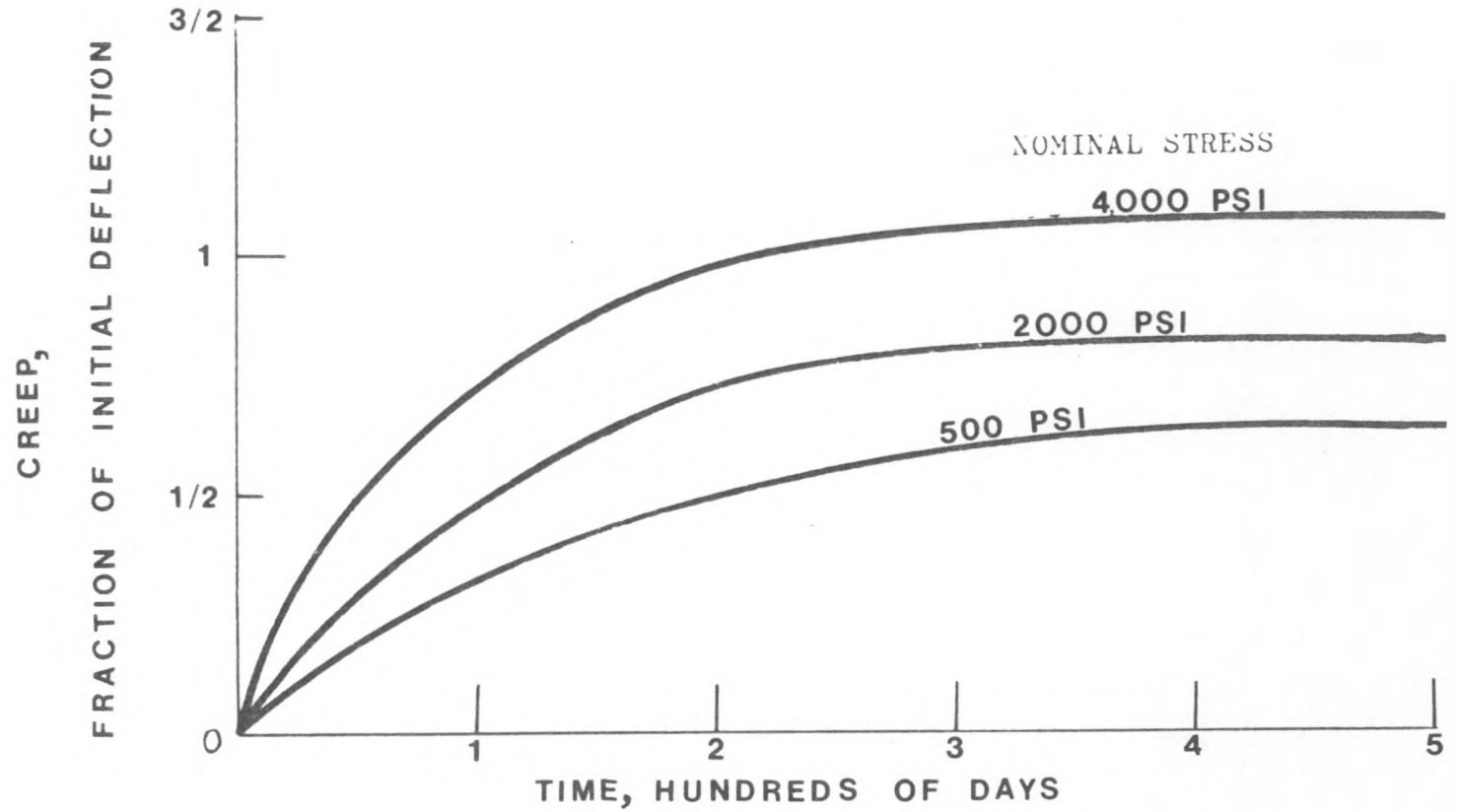

FIGURE 33. - CREEP PROPERTIES OF WOOD (FROM REF. 14).

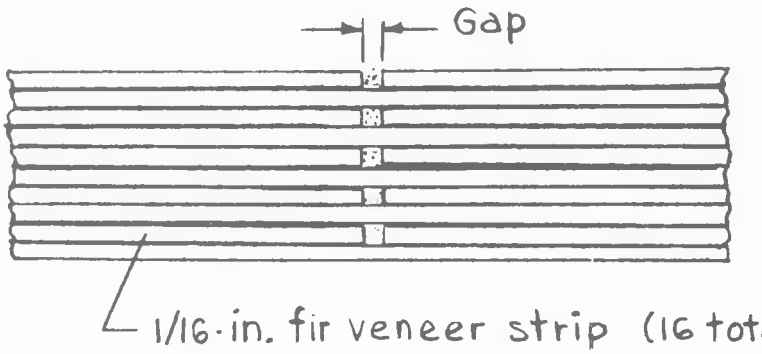

(a). Test sample for veneer joint strength.

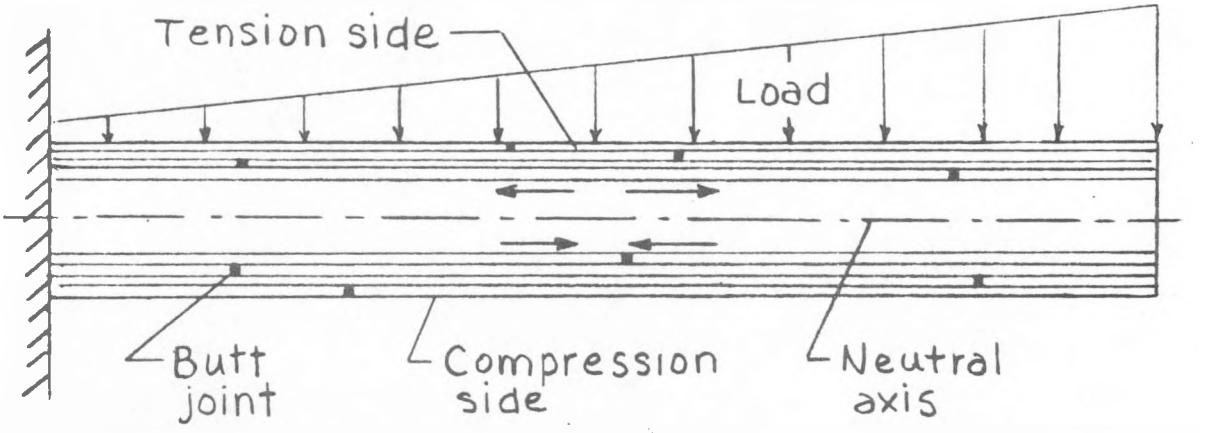

(b). Blade as laminated cantilever beam with butt joined strips.

Figure 34.- Laminated sections with butted veneer joints.

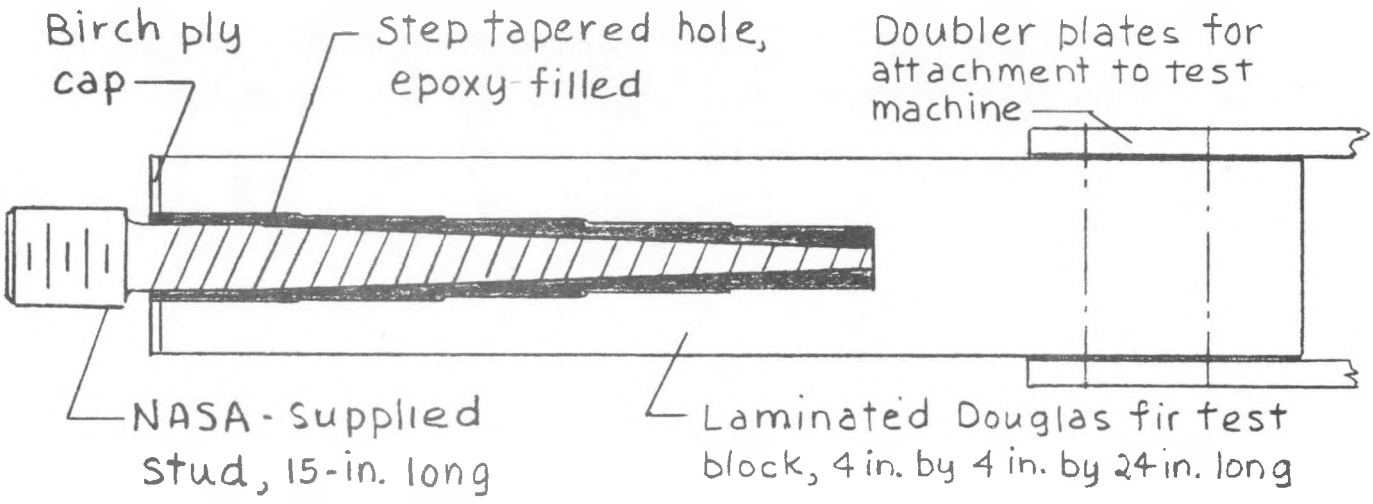

Figure 35.- Baseline specimen for test of bond strength.

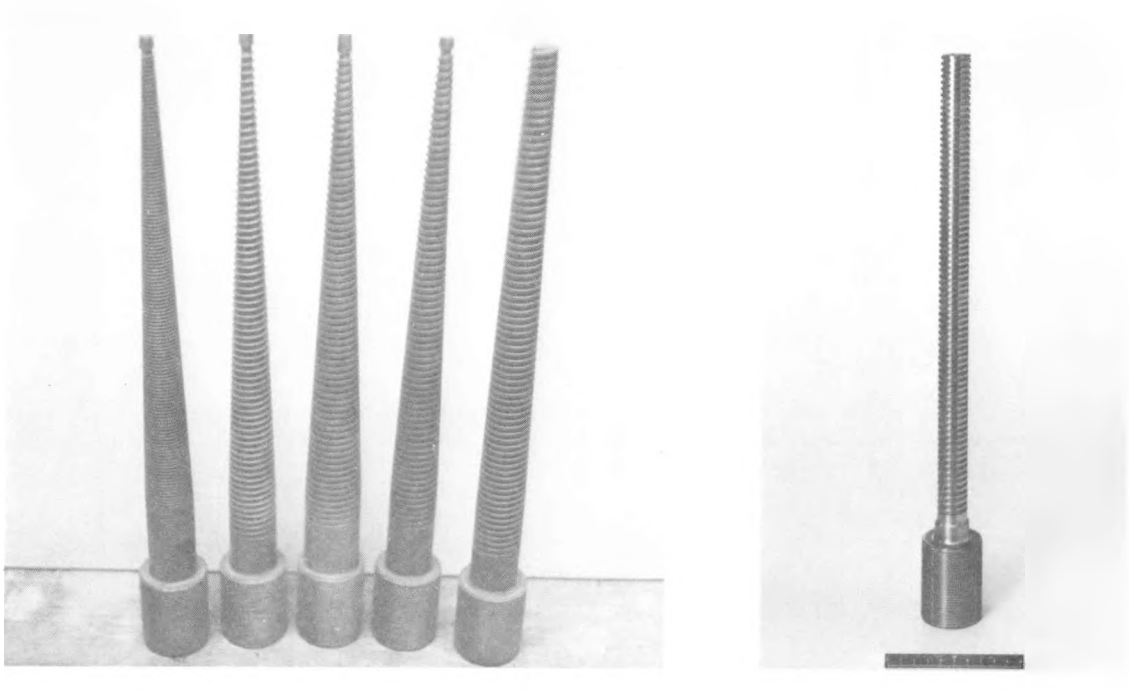

Figure 36.- Sample studs used in single-stud tests.

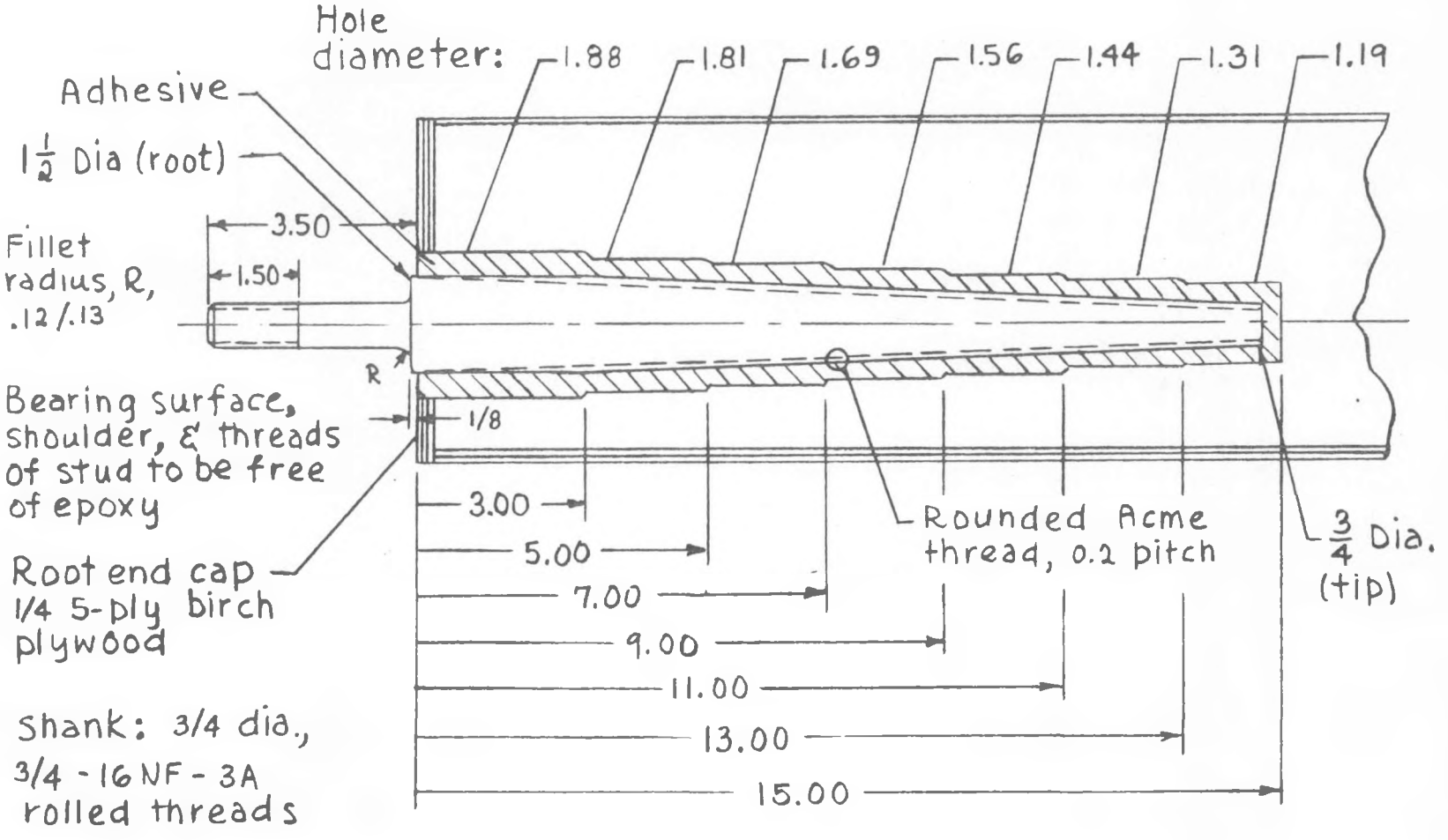

Figure 37.- Final stud design configuration (dimensions in inches).

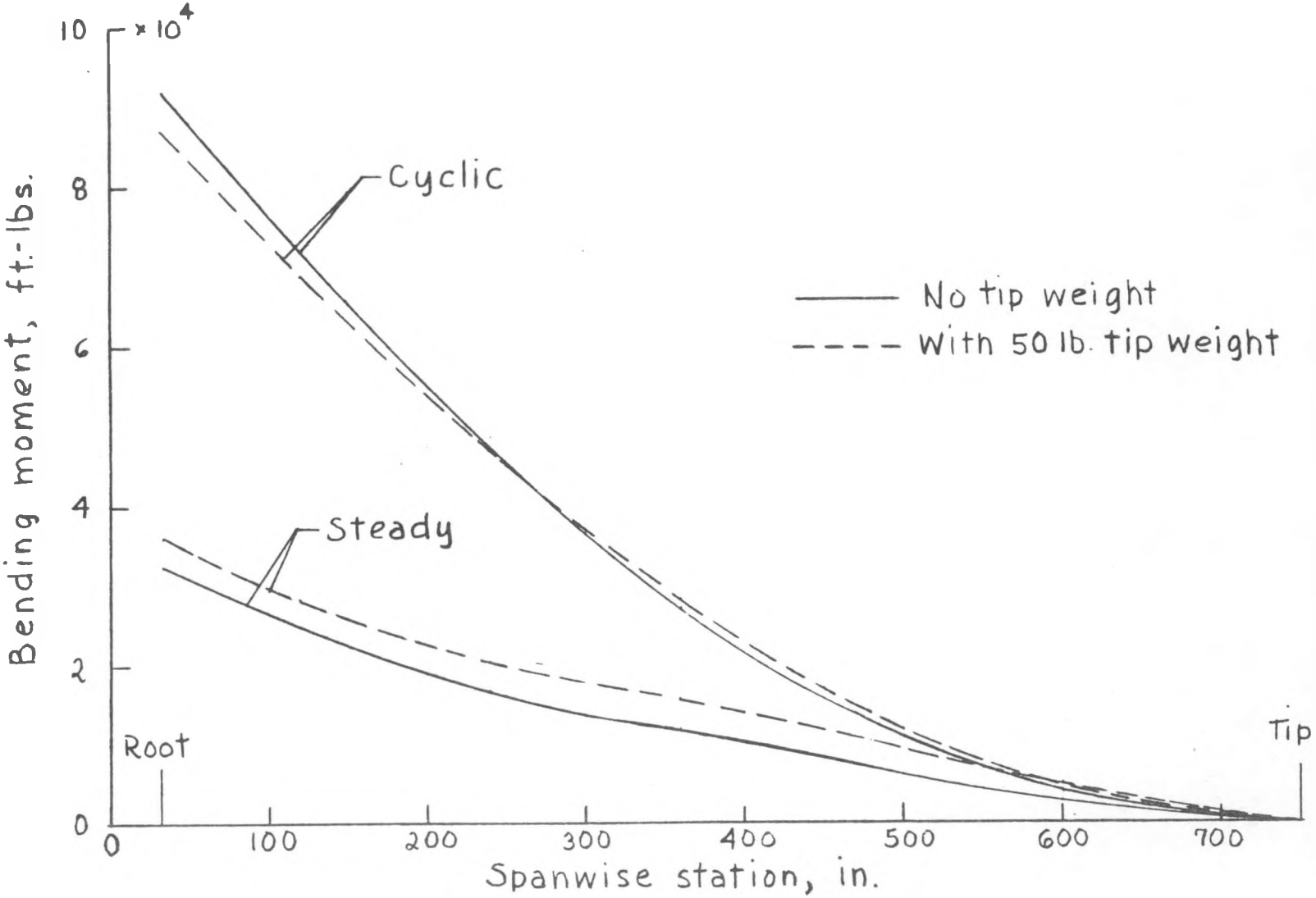

(a). Flatwise bending moment.

Figure 38.- Calculated bending moments for stress analysis configuration. Normal operation. Wind speed, 40 mph; rotor speed, 40 rpm; coning angle, 7°.

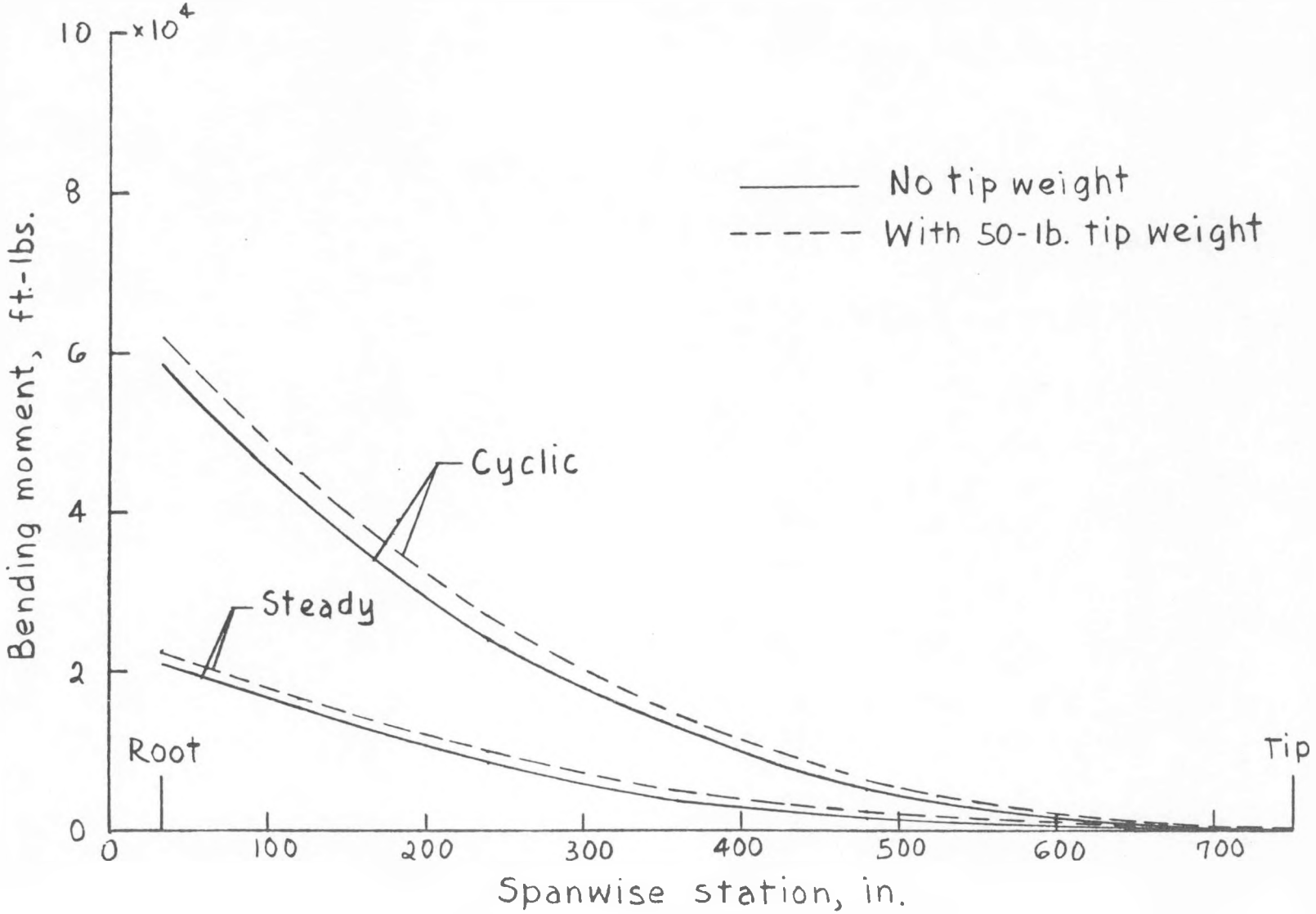

(b). Edgewise bending moment.

Figure 38.- Concluded.

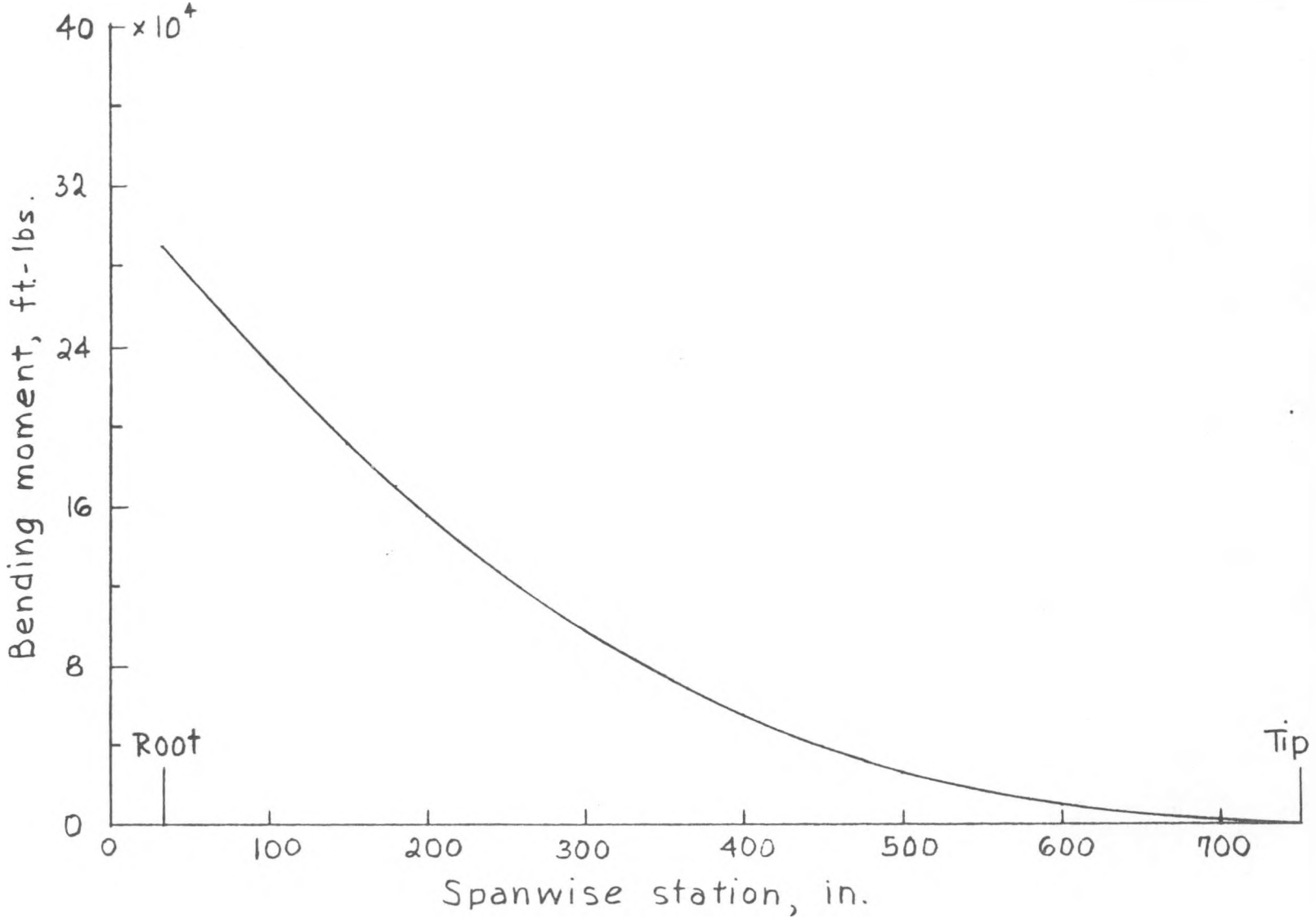

Figure 39.-Hurricane wind condition. Bending moment distribution from air load of 50 lbs/sq. ft.

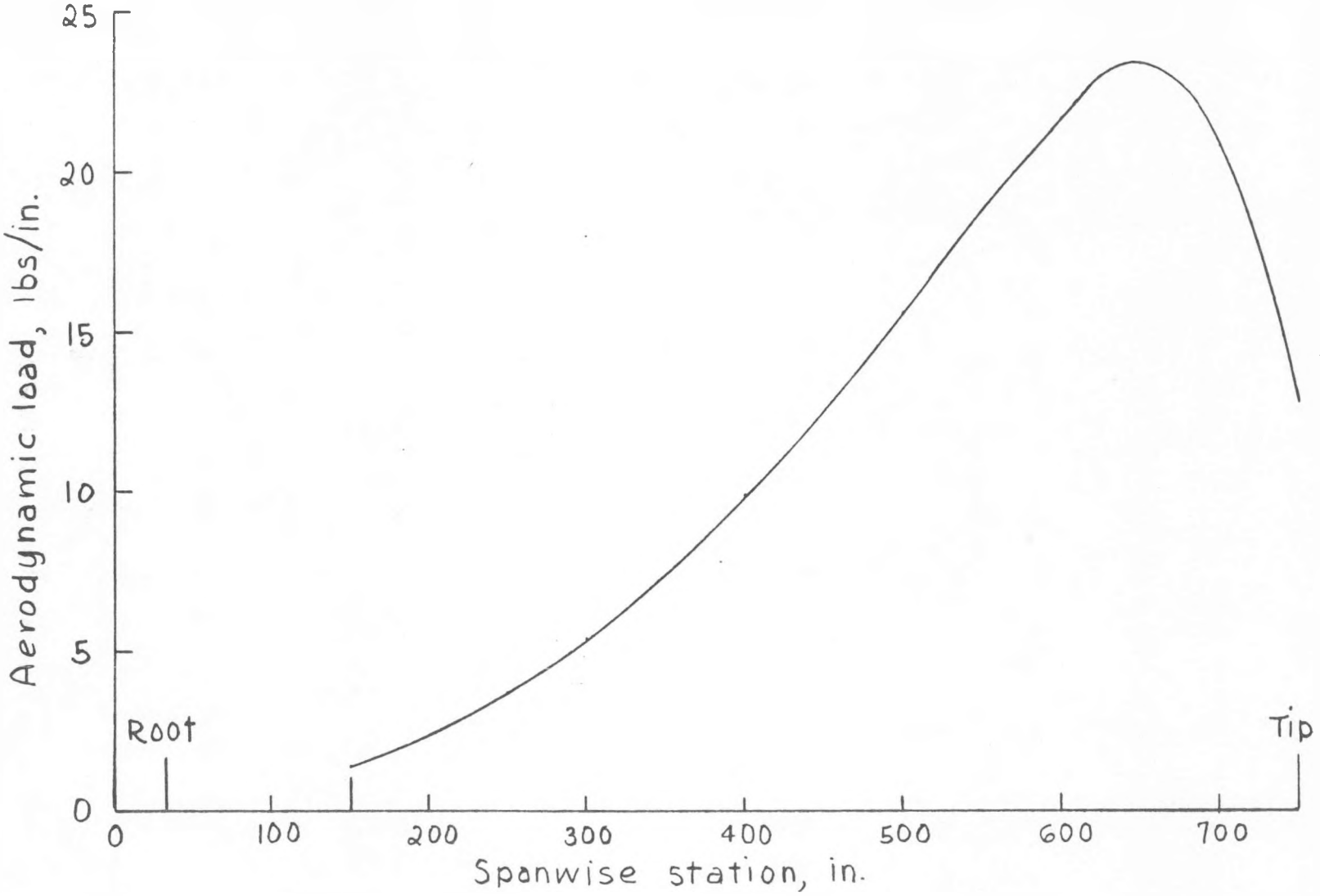

(a). Aerodynamic load variation.

Figure 40.- Emergency shutdown condition. Wind speed, 40 mph.; rotor speed, 45 rpm; all blade sections at maximum negative lift.

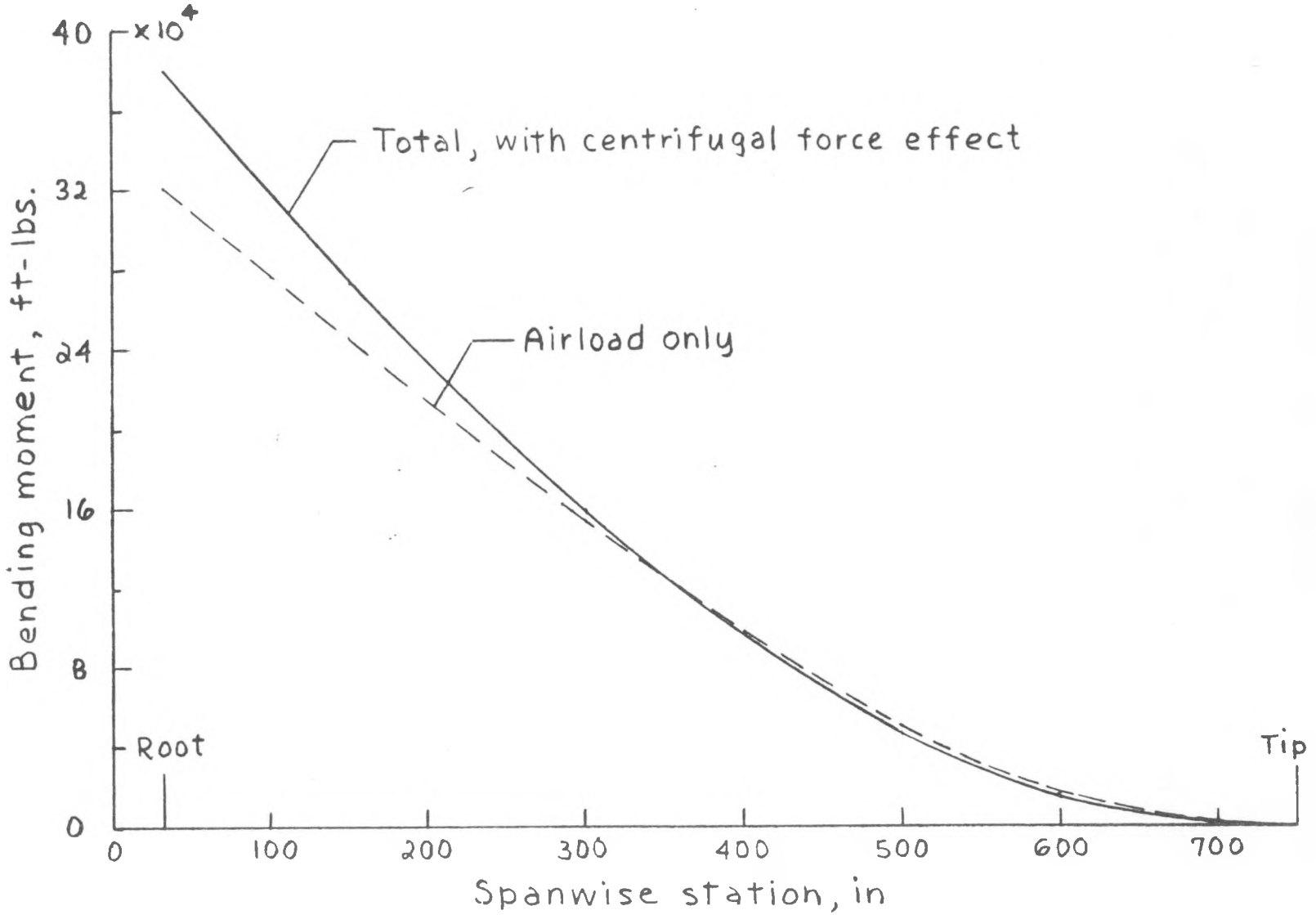

(b). Bending moment distribution.

Figure 40.- Concluded.

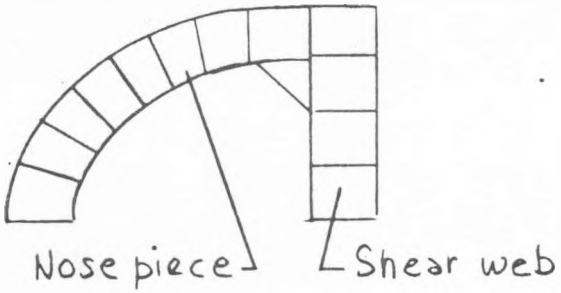

(a). Station 32.

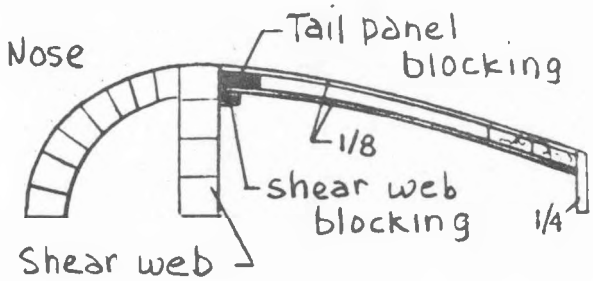

(b). Station 102.

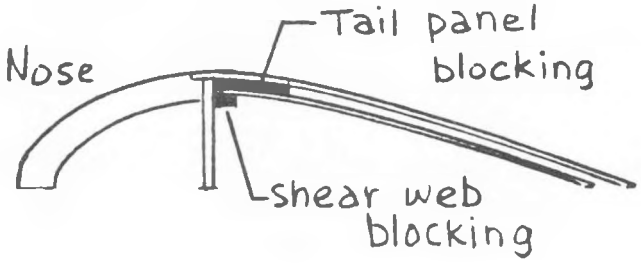

(c). Station 150 to 500

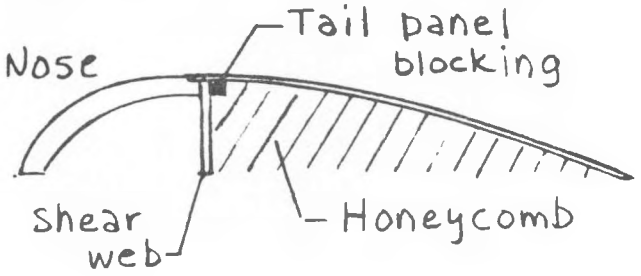

(d). Station 600 to 750.

Station	Nose thickness	Shear web thickness	shear web blocking	Tail panel blocking
32	4.0	4.0	—	—
102	3.38	2.38	2 × 4	3/4 × 8
150	3.25	0.25	2 × 4	3/4 × 8
300	2.50	.25	1 1/4 × 4	3/4 × 8
400	2.00	.25	1 × 2	3/4 × 6
500	1.563	.25	1/2 × 2	3/4 × 4
600	1.063	.25	0	1/2 × 2 3/4
700	0.625	.25	0	0
750	.438	.25	0	0

Figure 41.— Internal structure of blade cross sections used for detailed stress analysis. (Dimensions in inches.)

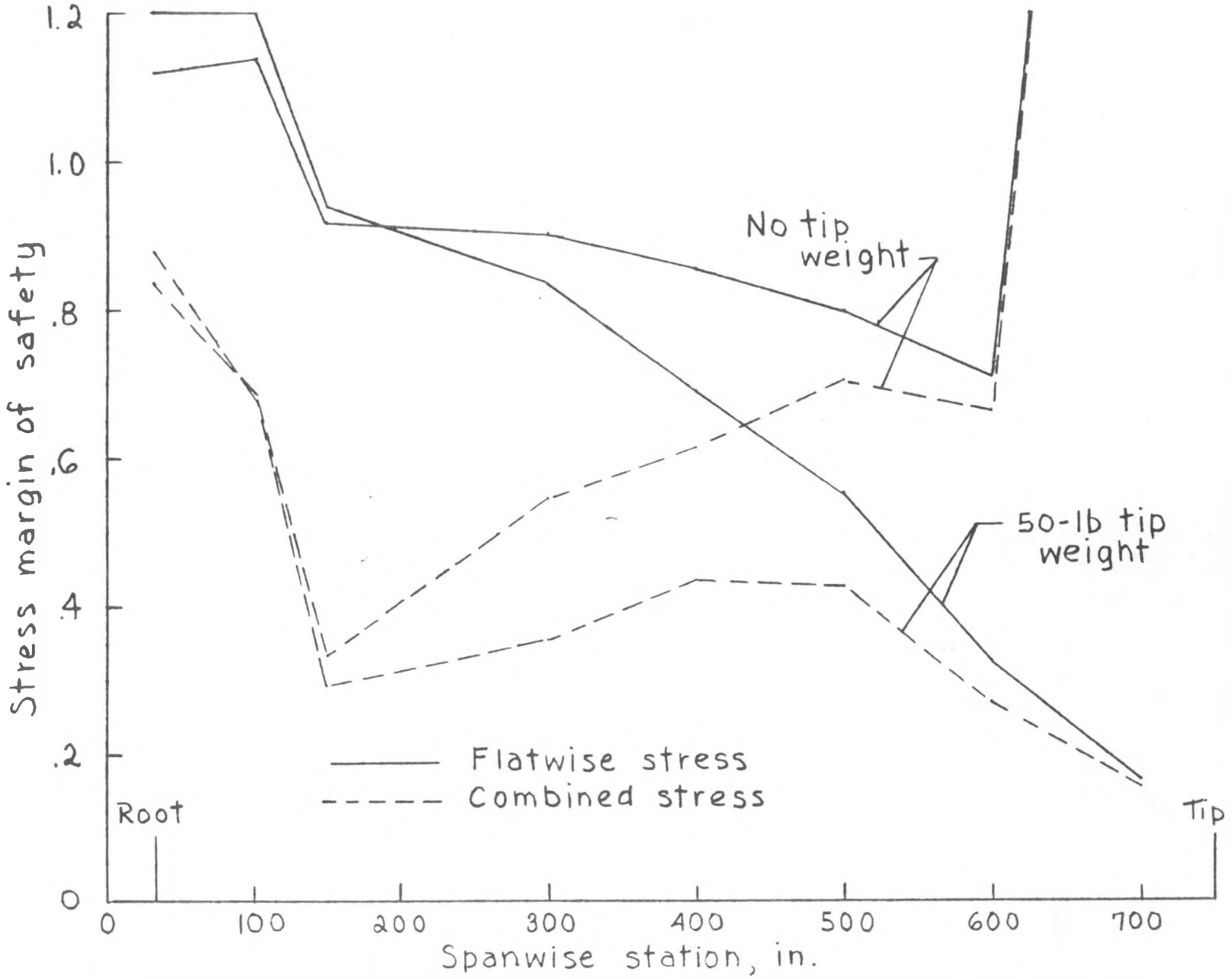

(a). Normal operation case, 4×10^8 cycles (compression, fatigue).

Figure 42.- Margin of safety for bending stress. Stress analysis geometry.

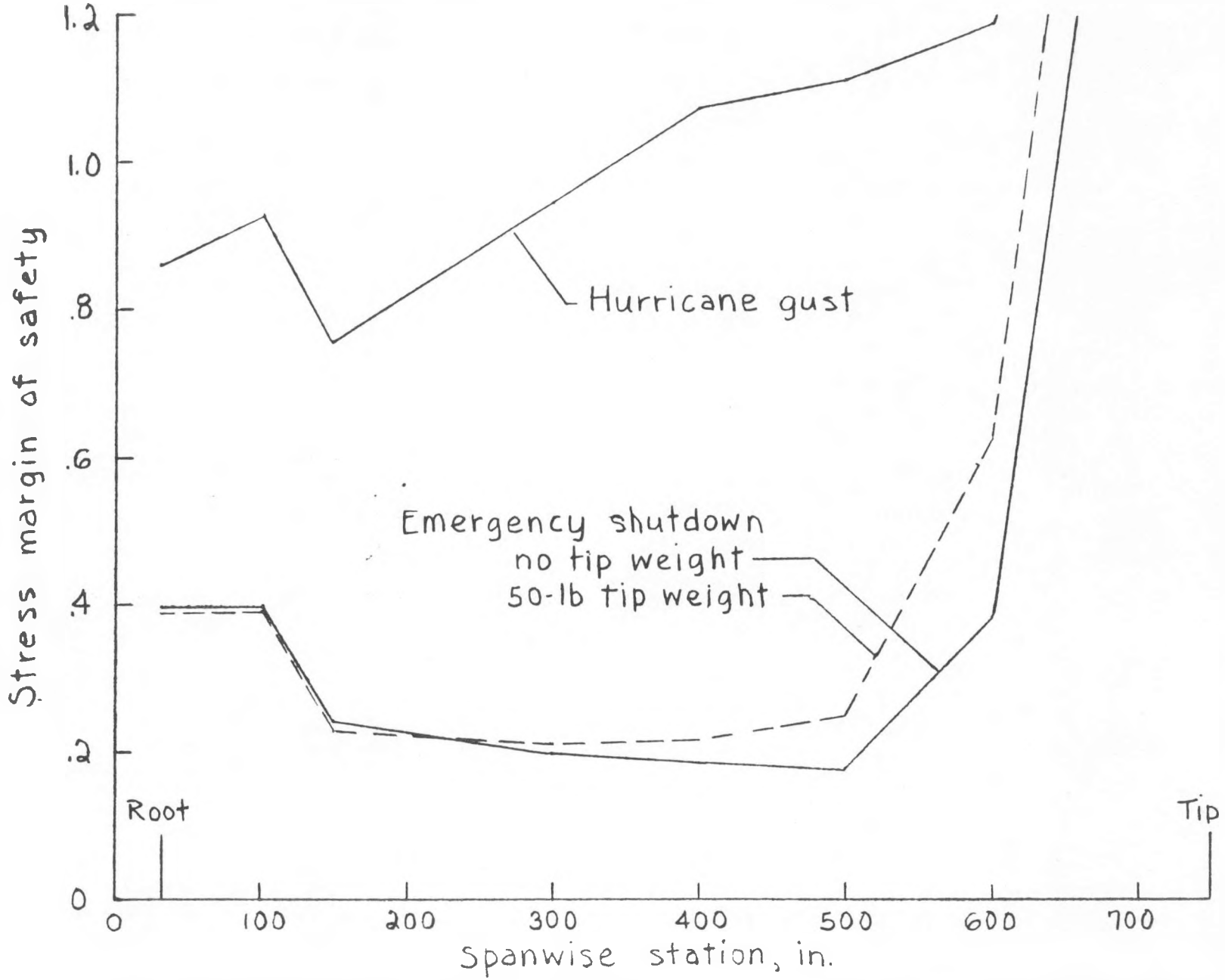

(b). Shutdown and gust cases, flatwise stress (compression, static).

Figure 42.- Concluded.

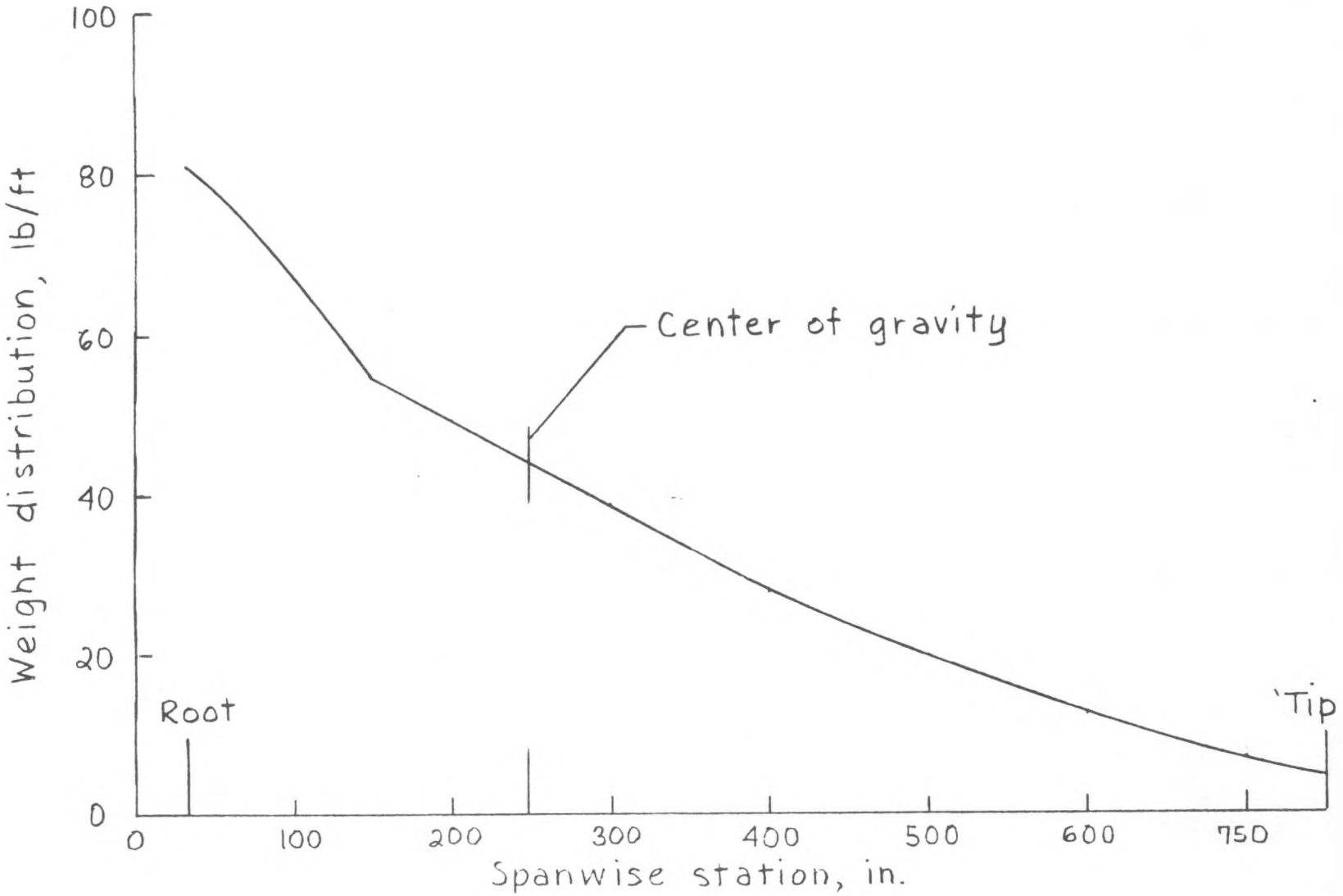

Figure 43.- Calculated spanwise weight distribution. Stress analysis configuration.

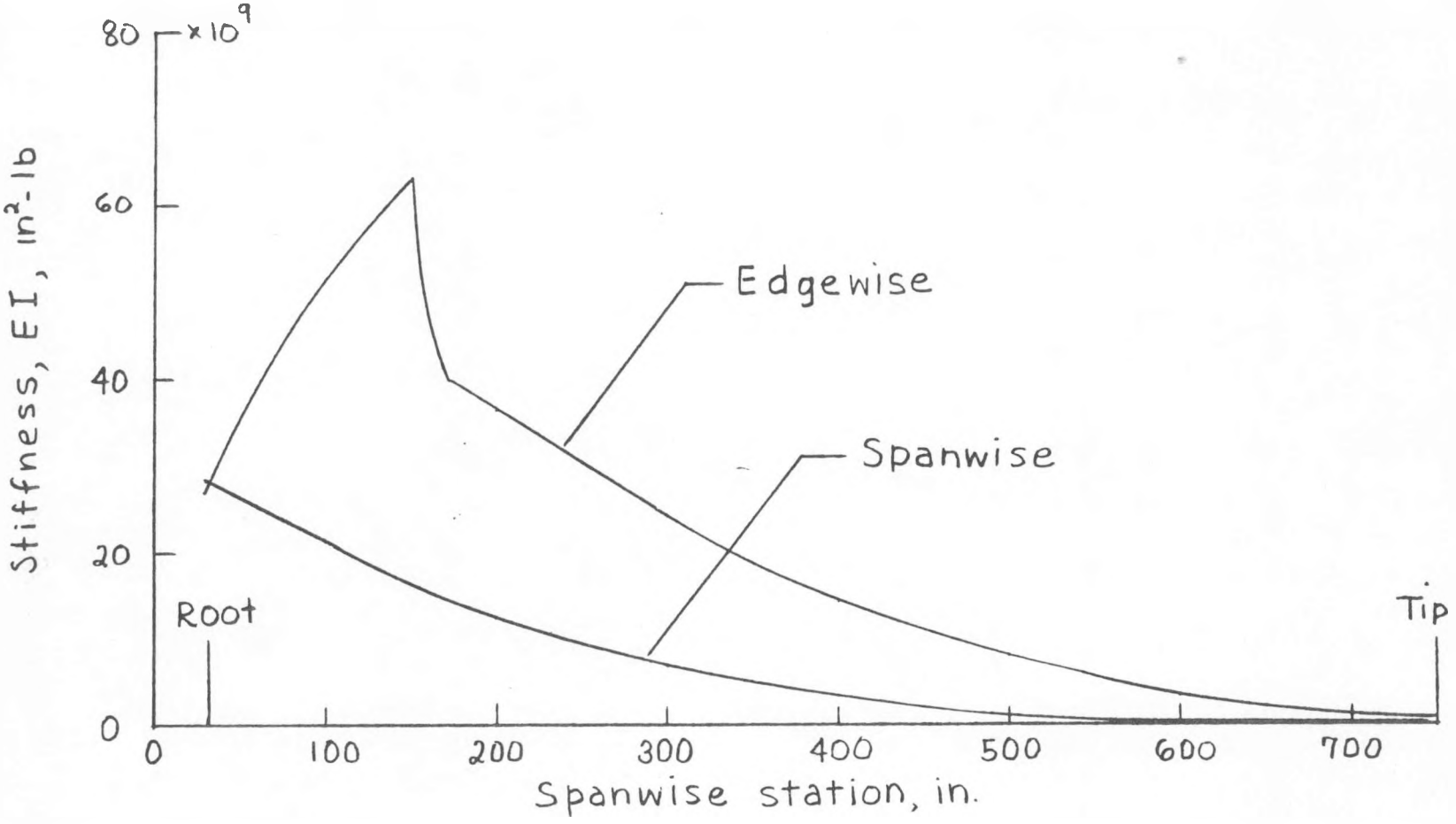

Figure 44.– Calculated spanwise stiffness distribution. Stress analysis configuration.

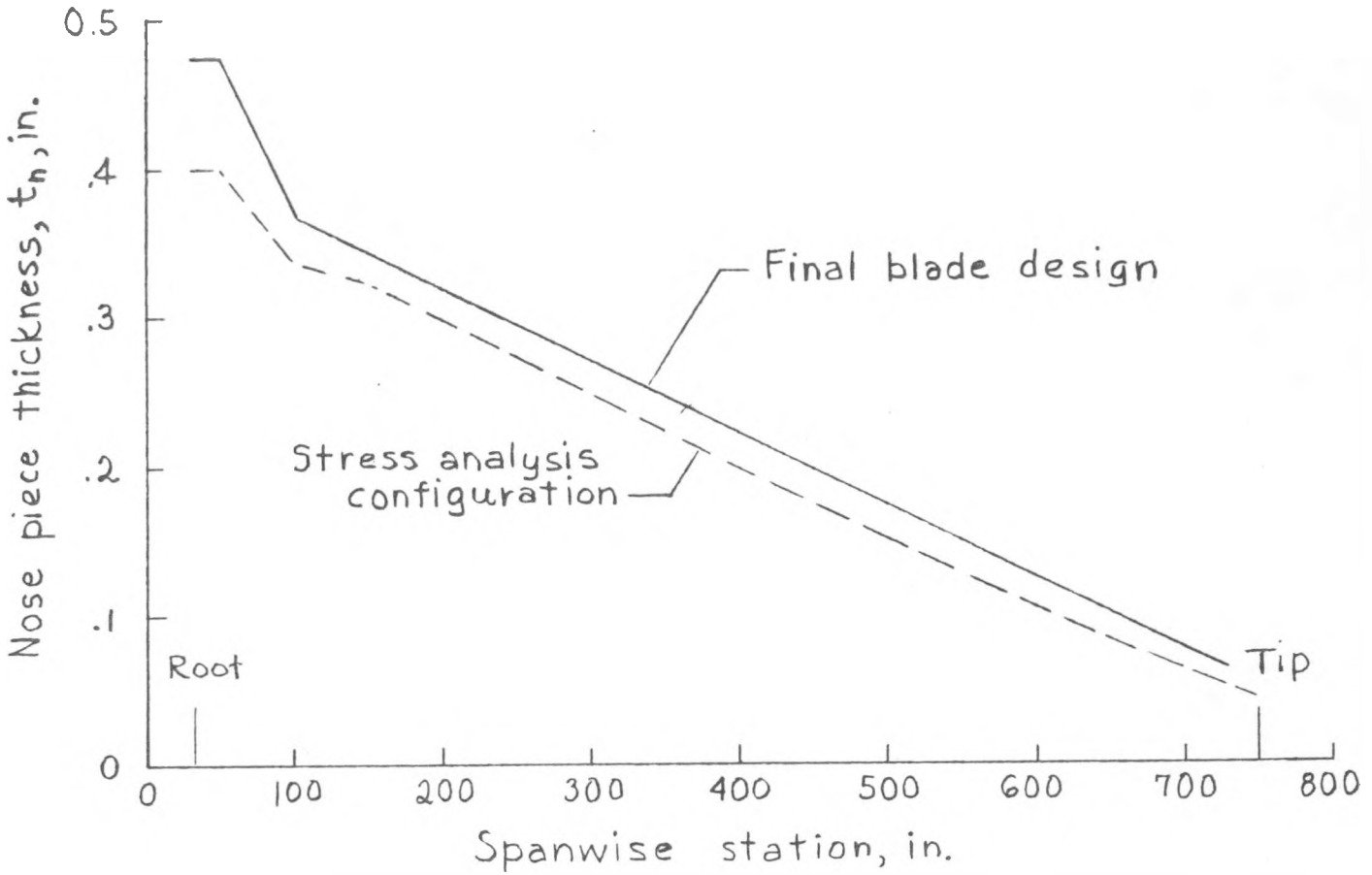

Figure 45.—Spanwise variation of thickness of laminated nose piece (fir veneers plus two birch plies).

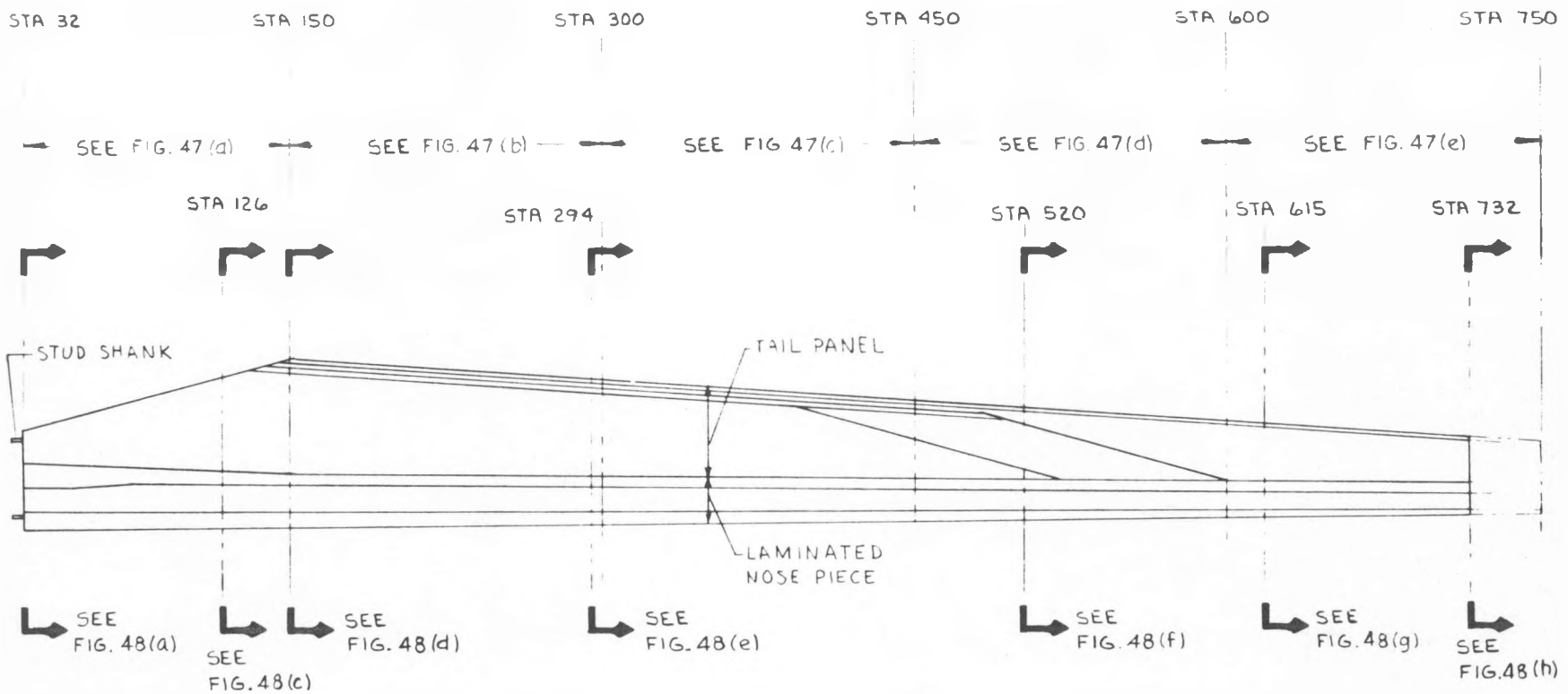

Figure 46. - Overall planform view of blade construction, looking into lower half of blade (upper half removed). Arrows indicate stations for which cross-sections are detailed.

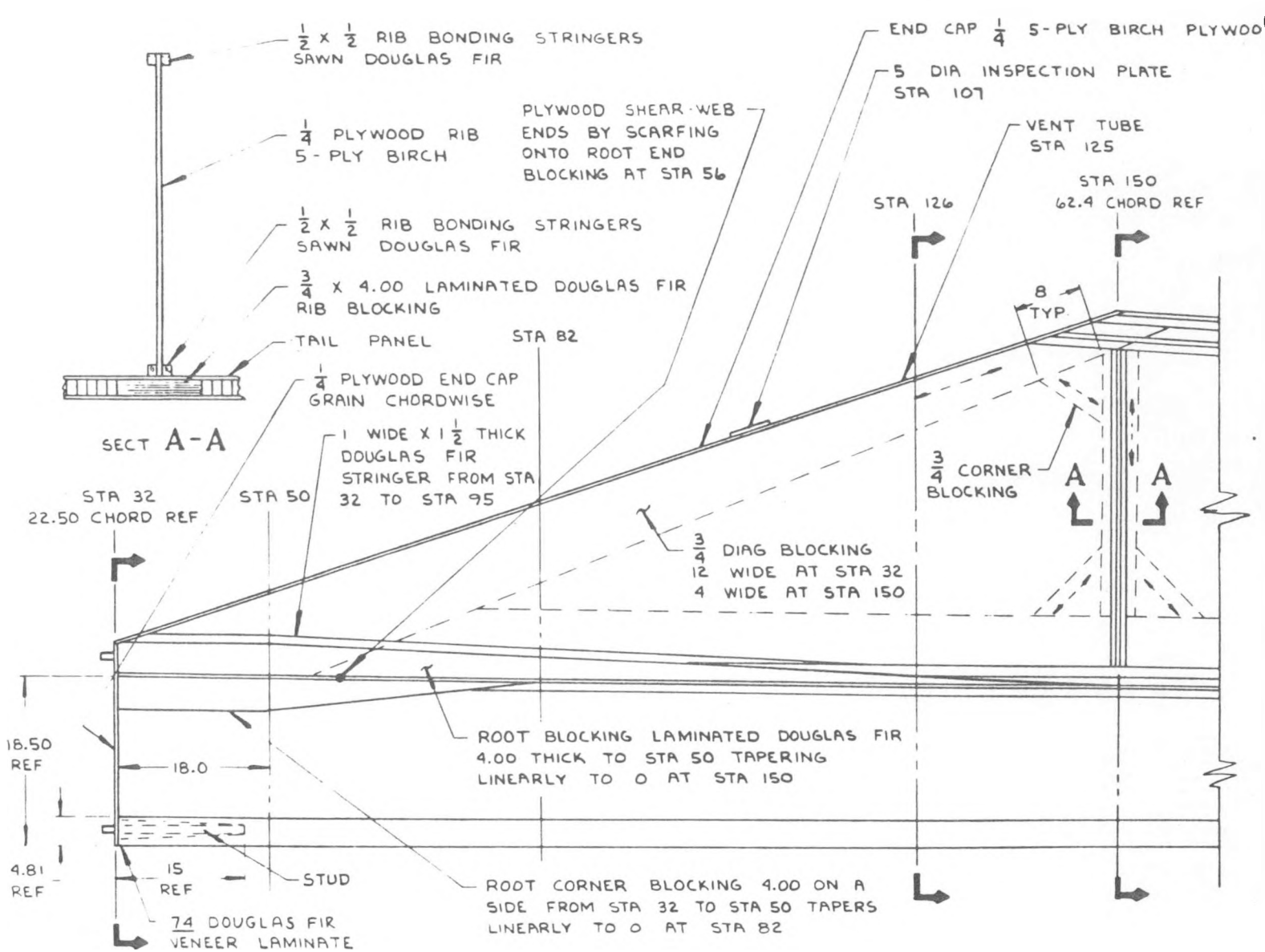

(a) Stations 32 to 150.

Figure 47. - Details of blade construction, planform view of lower half of blade. (Dimensions in inches)

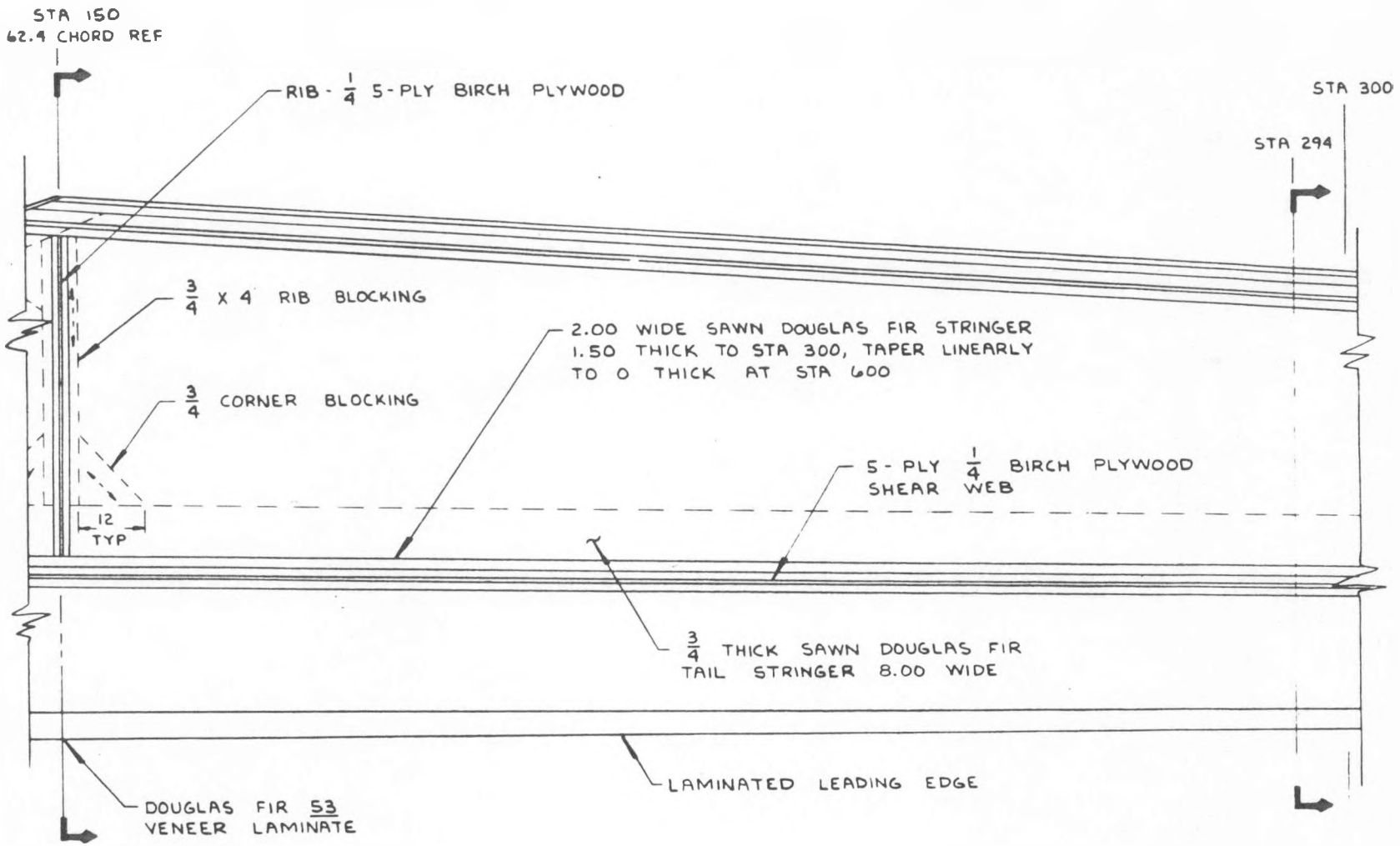

(b) Stations 150 to 300.

Figure 47. Continued.

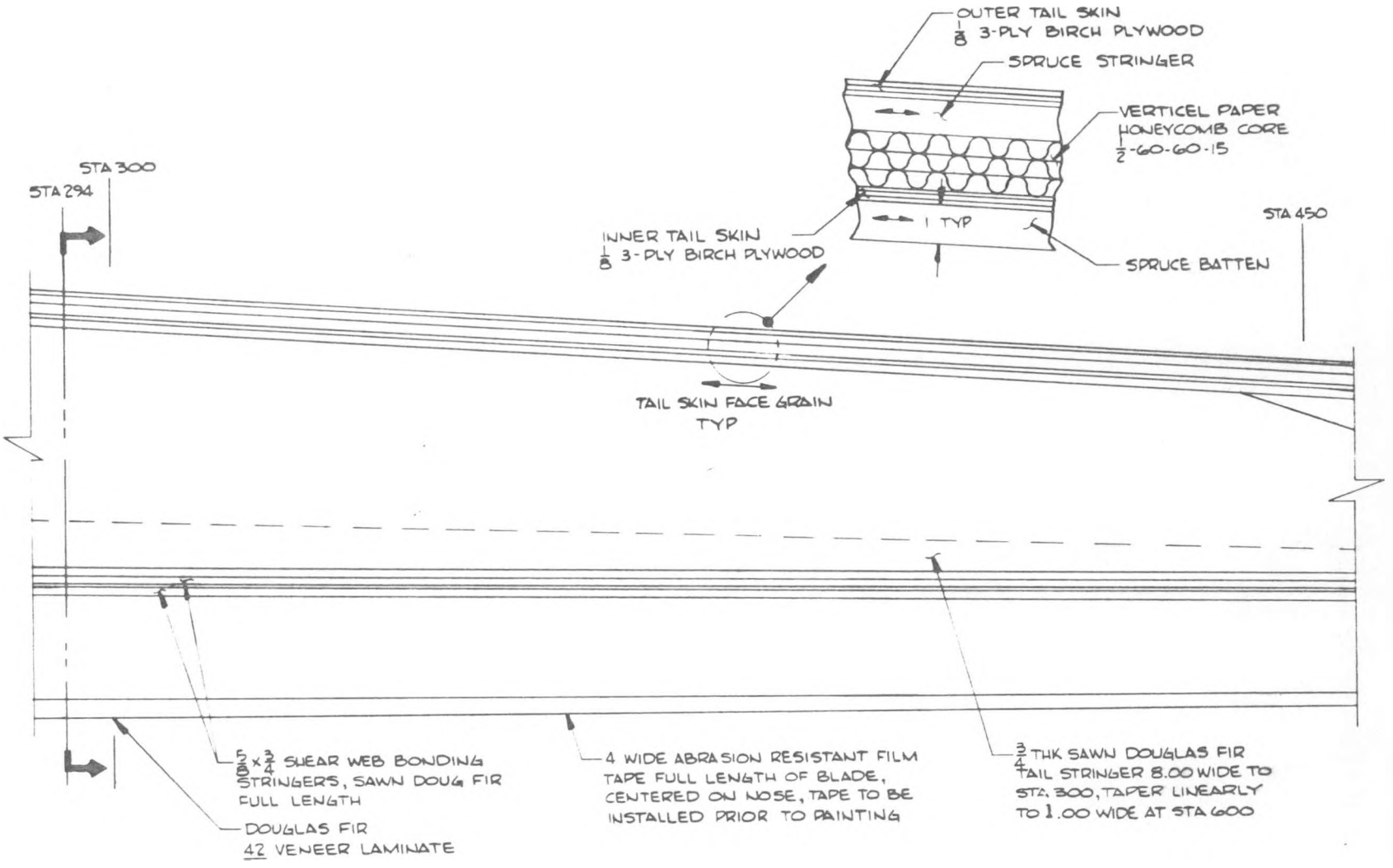

(c) Stations 300 to 450.

Figure 47. - Continued.

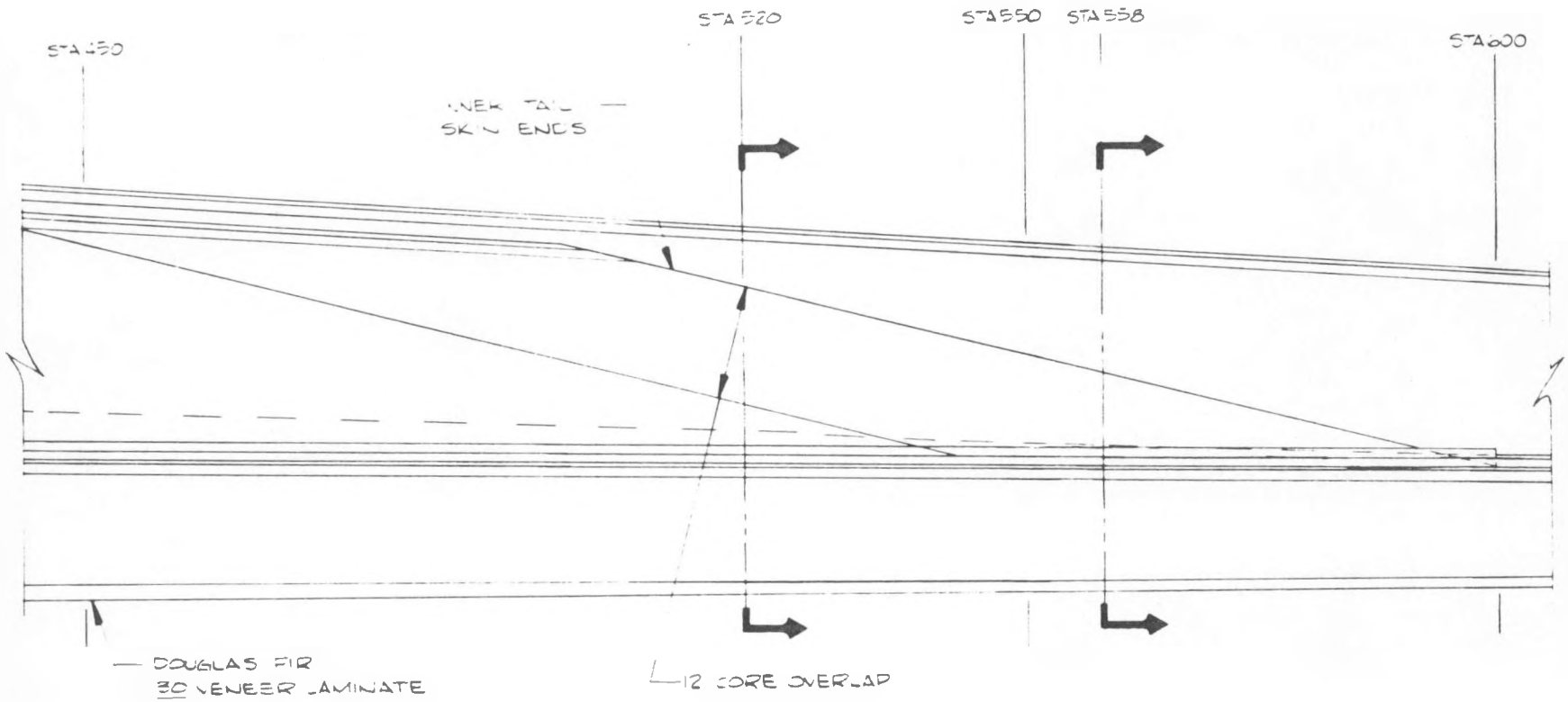

(d) Stations 450 to 600.

Figure 47. - Continued.

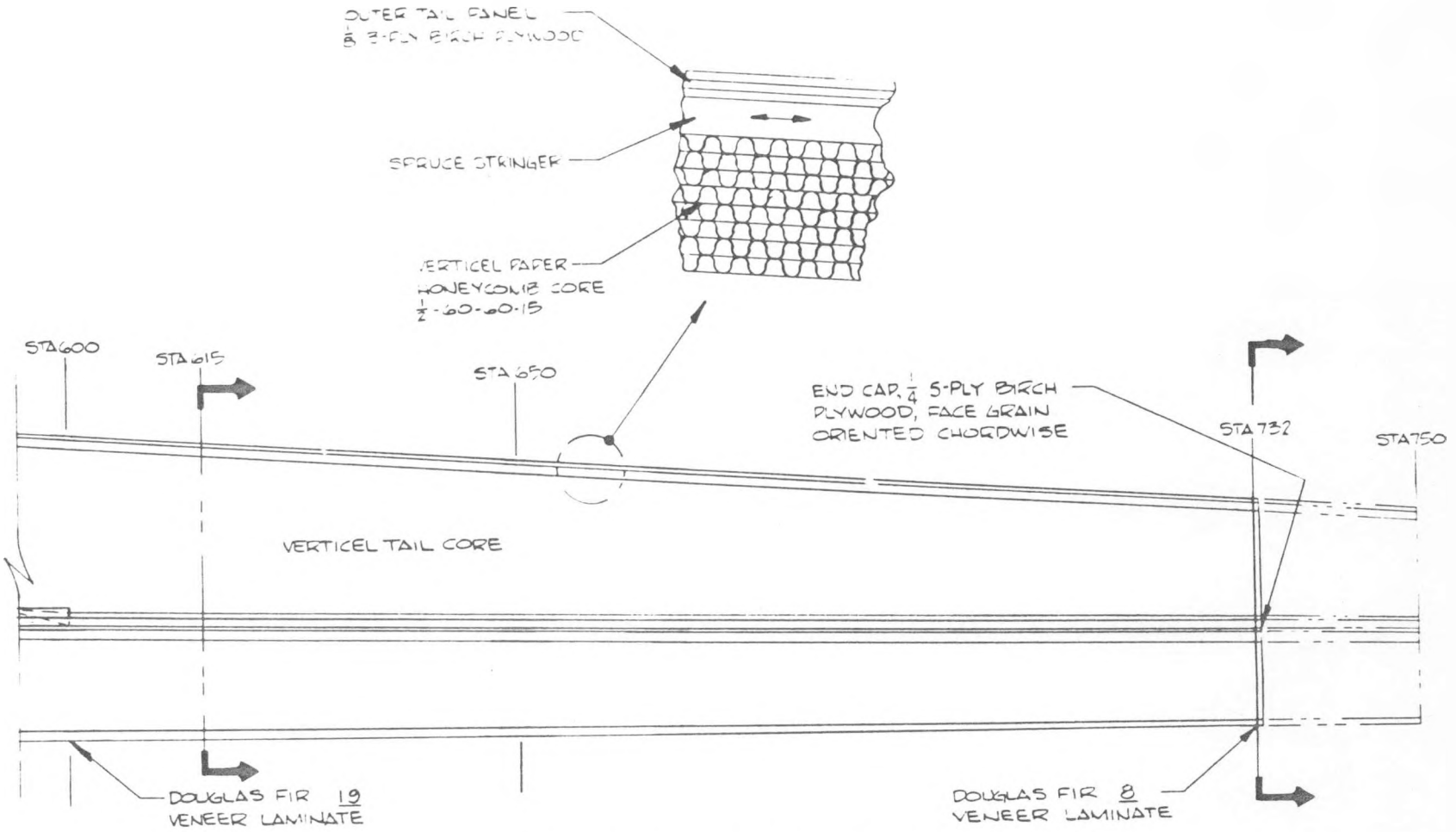

(e) Stations 600 to 732.

Figure 47. - Concluded.

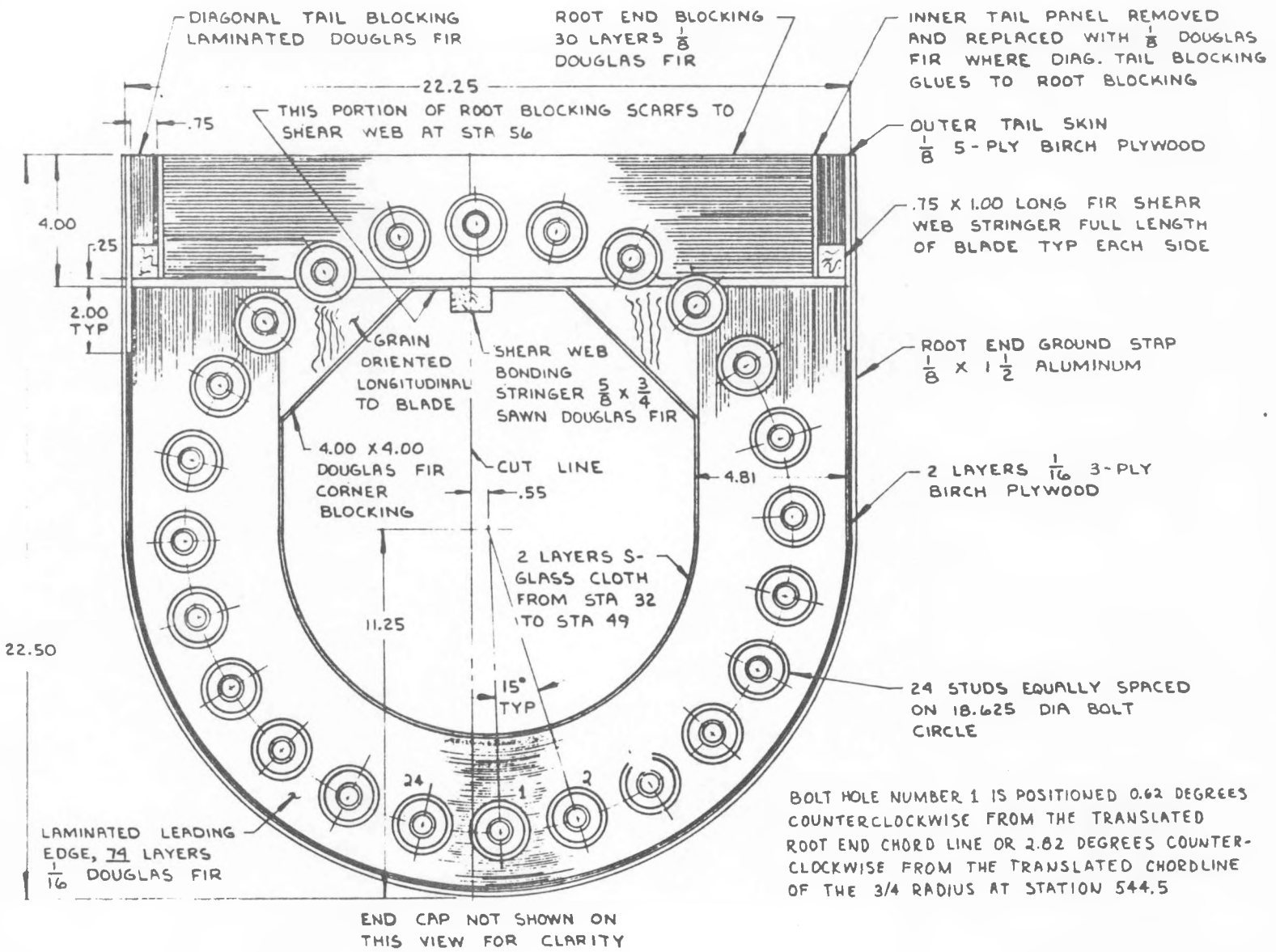

(a) Blade root end, station 32.

Figure 48. - Detailed views of blade cross sections.
(Dimensions in inches)

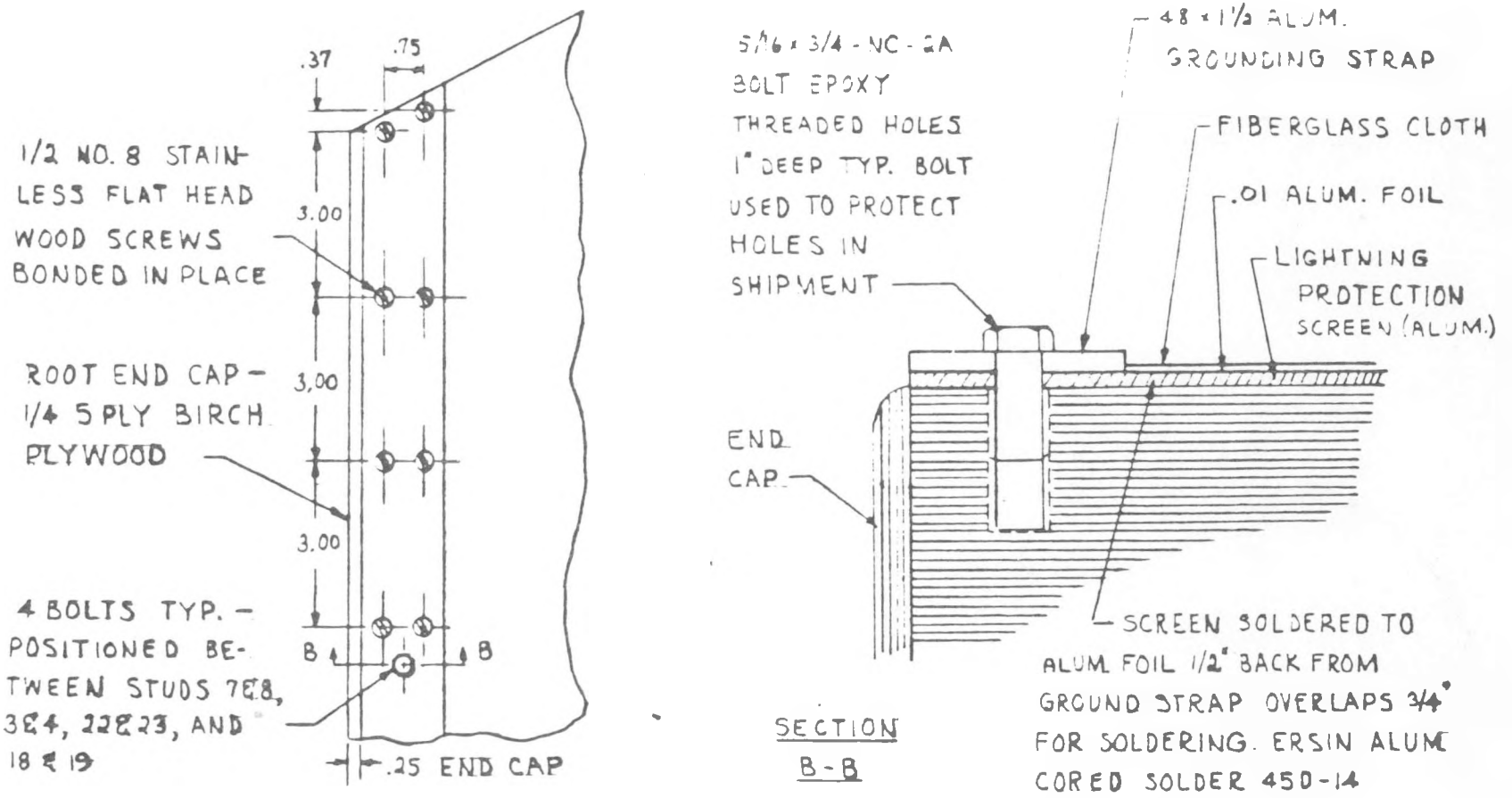

(b) Details of lightning protection grounding strap at blade root.

Figure 48. - Continued.

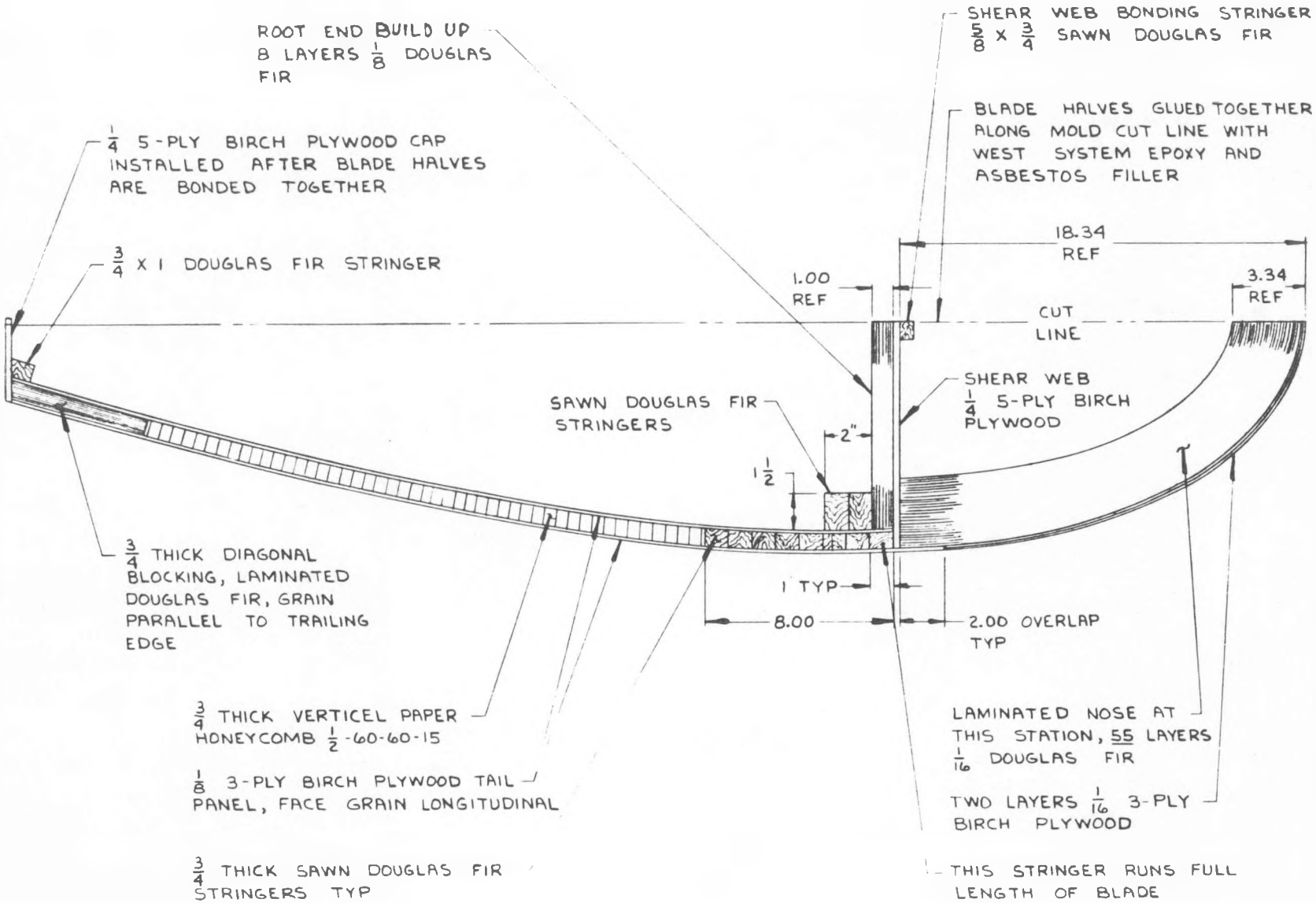

(c) Station 126.

Figure 48. - Continued.

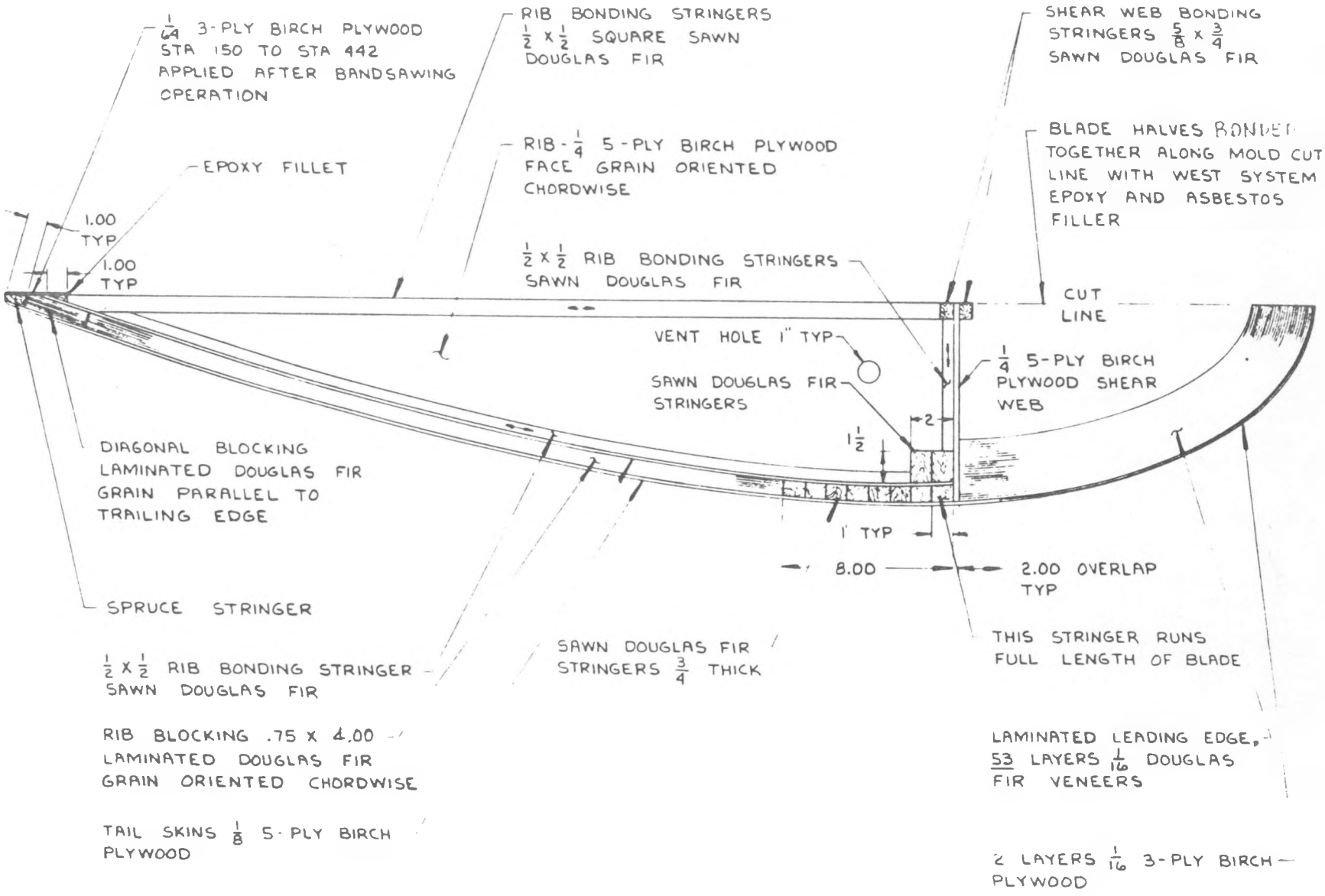

(d) Station 150.

Figure 48. - Continued.

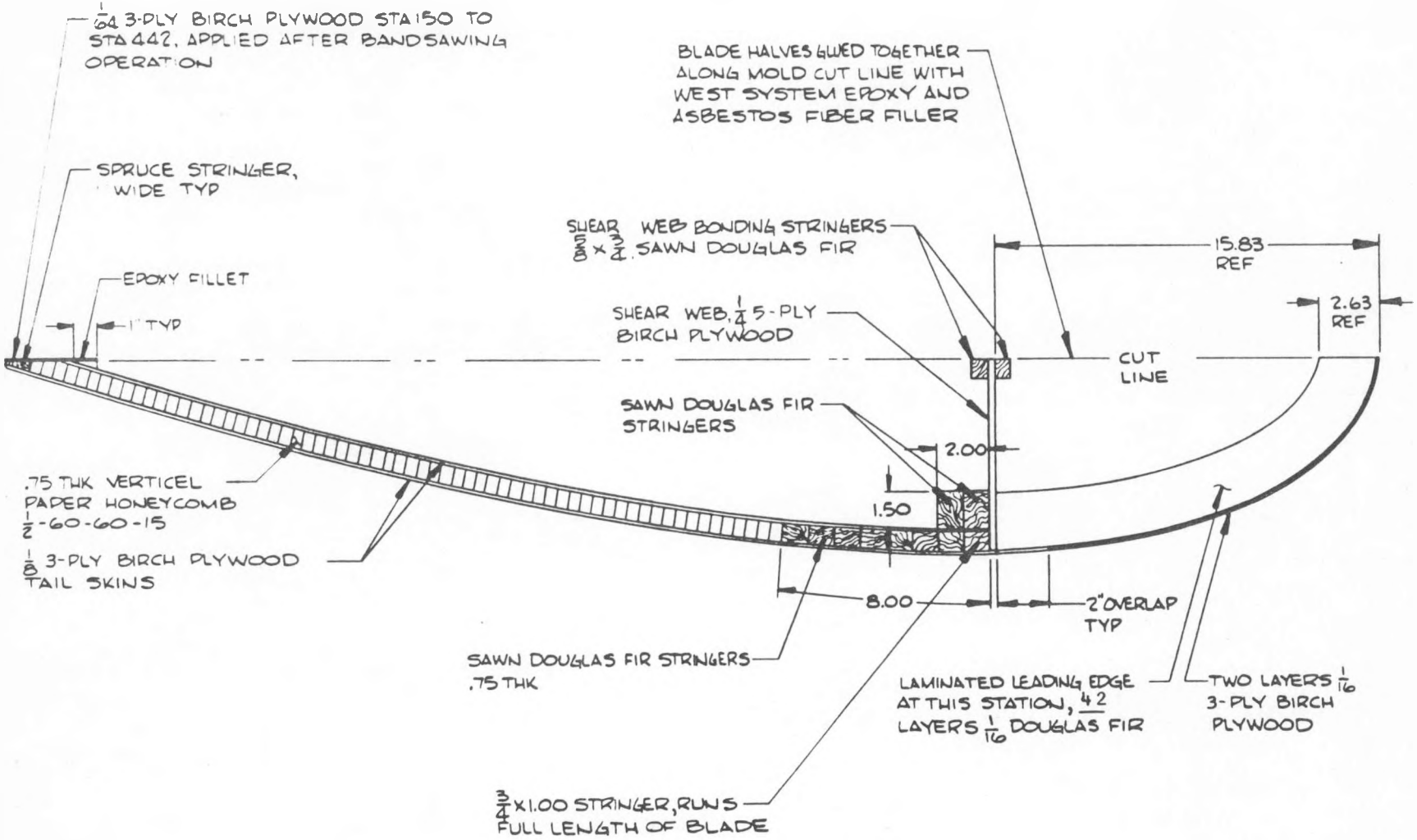

(c) Station 294.

Figure 48. - Continued.

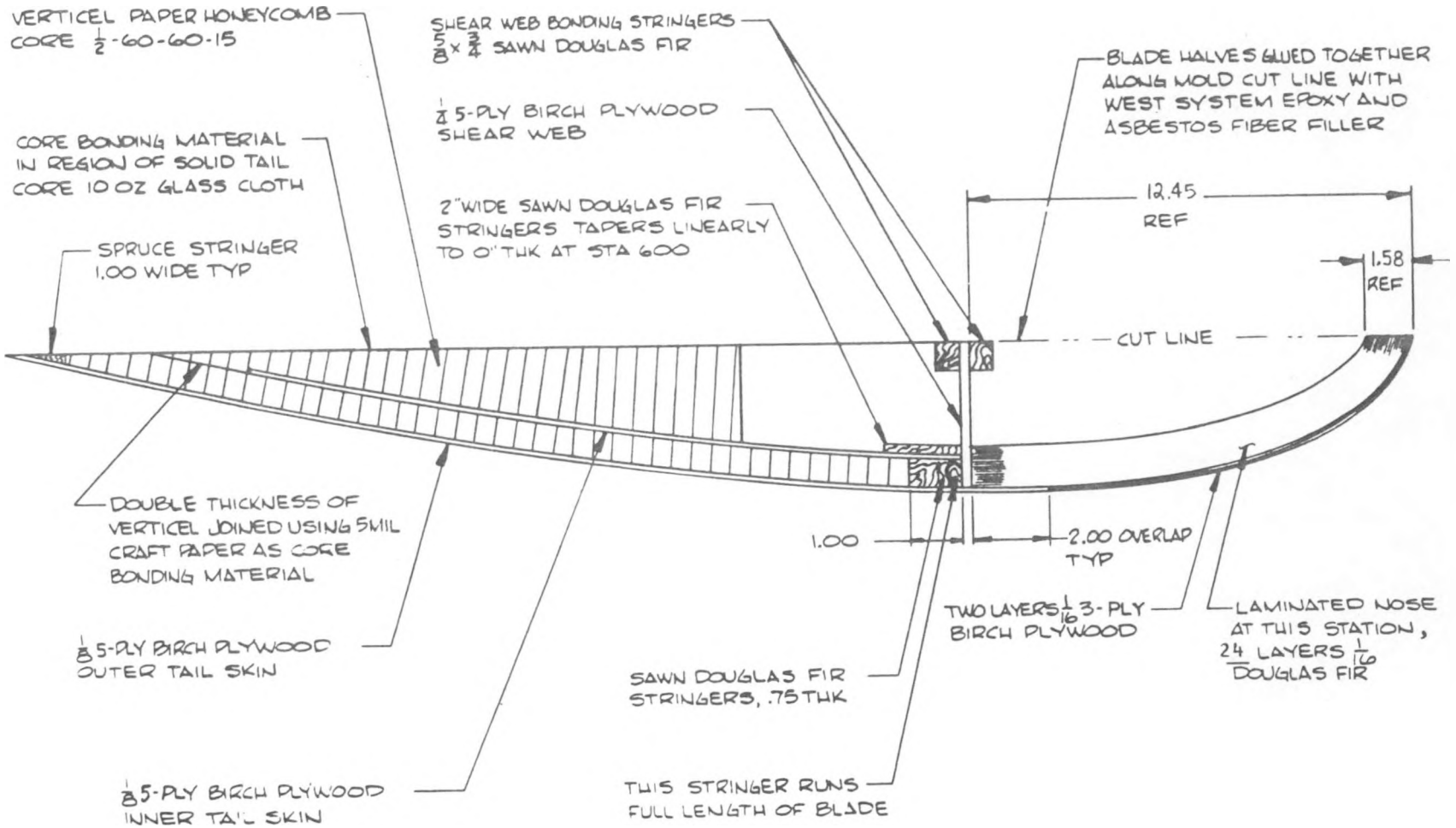

(i) Station 520.

Figure 48. - Continued.

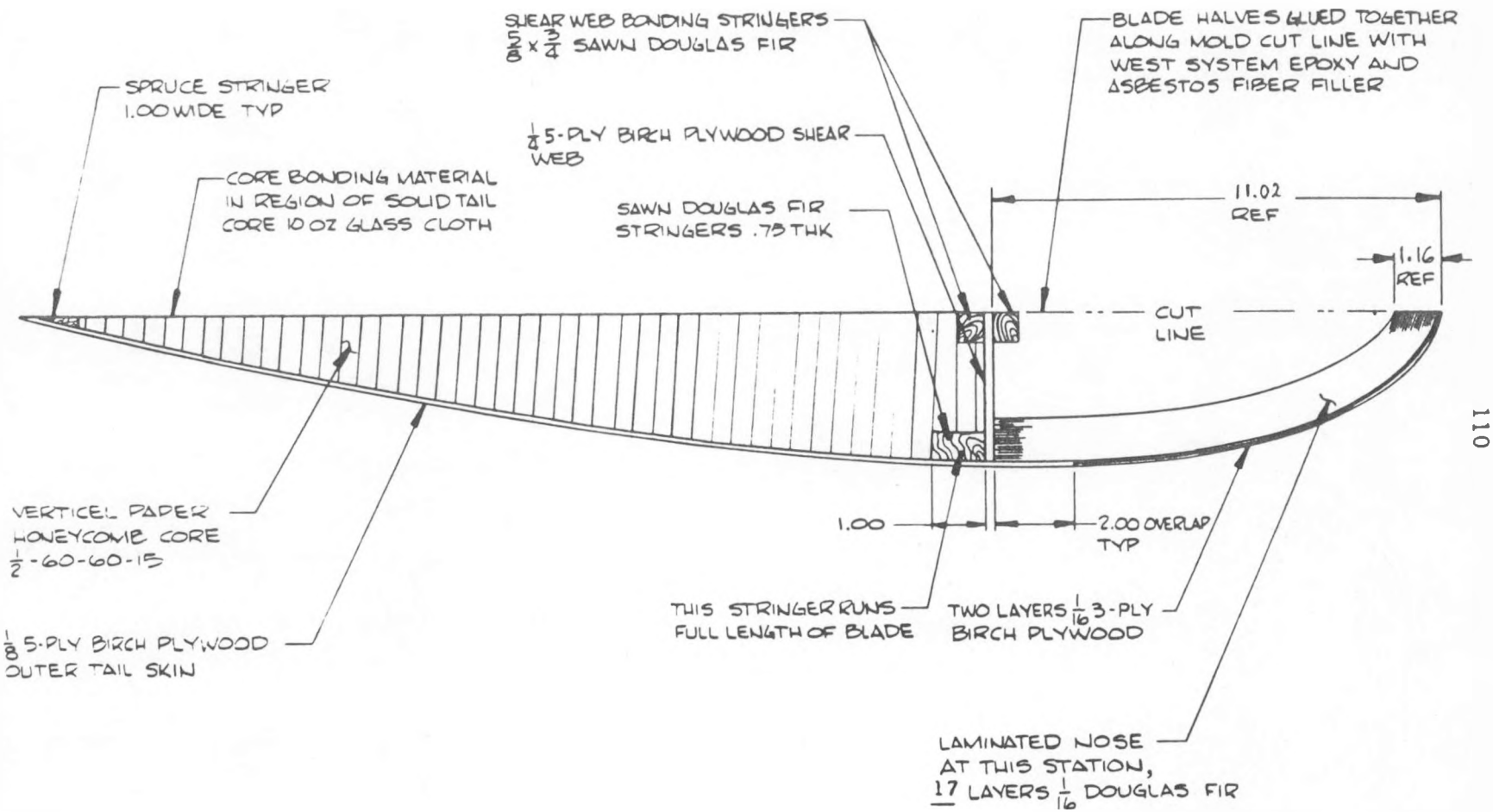

(g) Station 615.

Figure 48. - Continued.

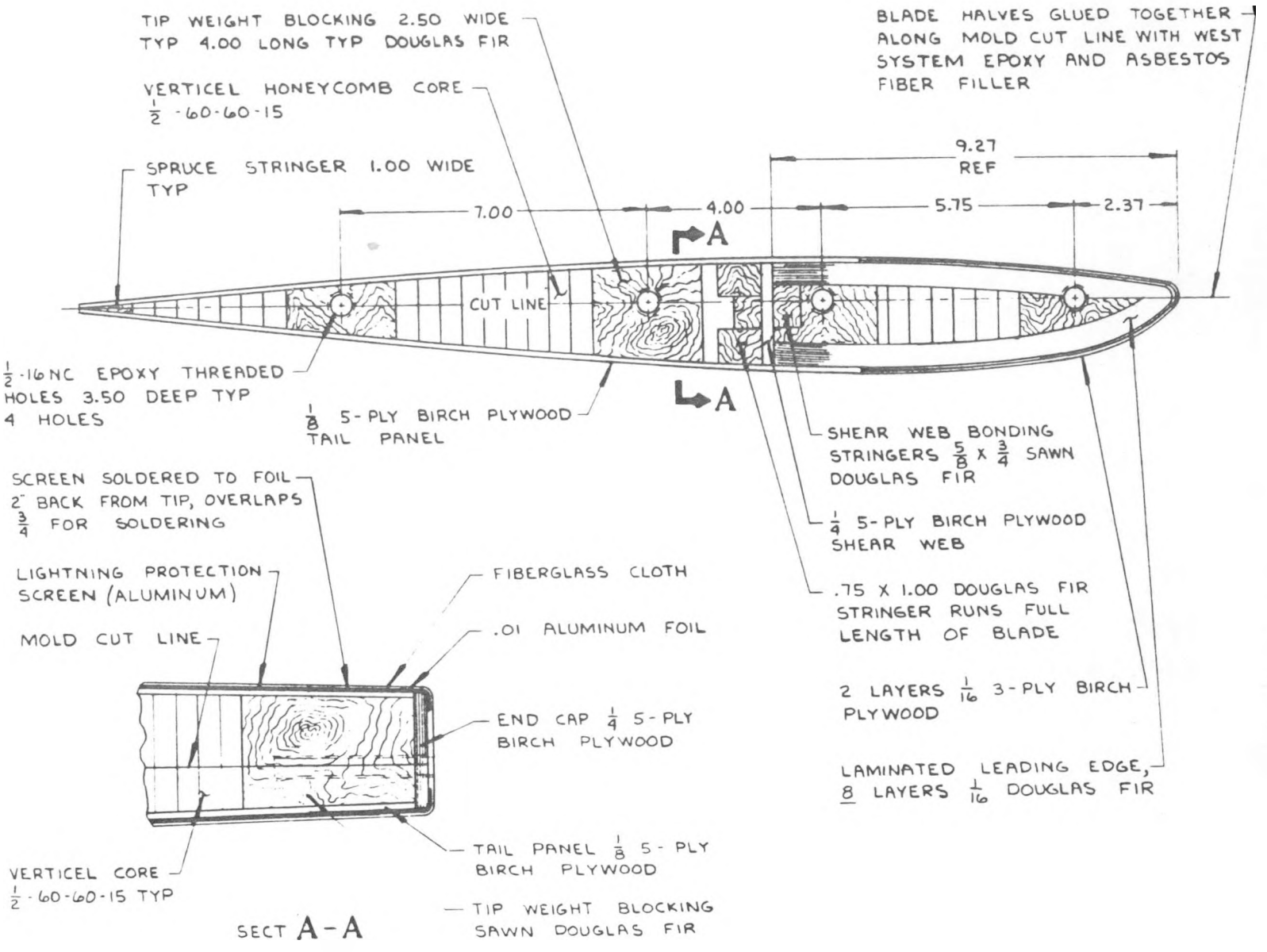

(h) Station 732.

Figure 48. - Concluded.

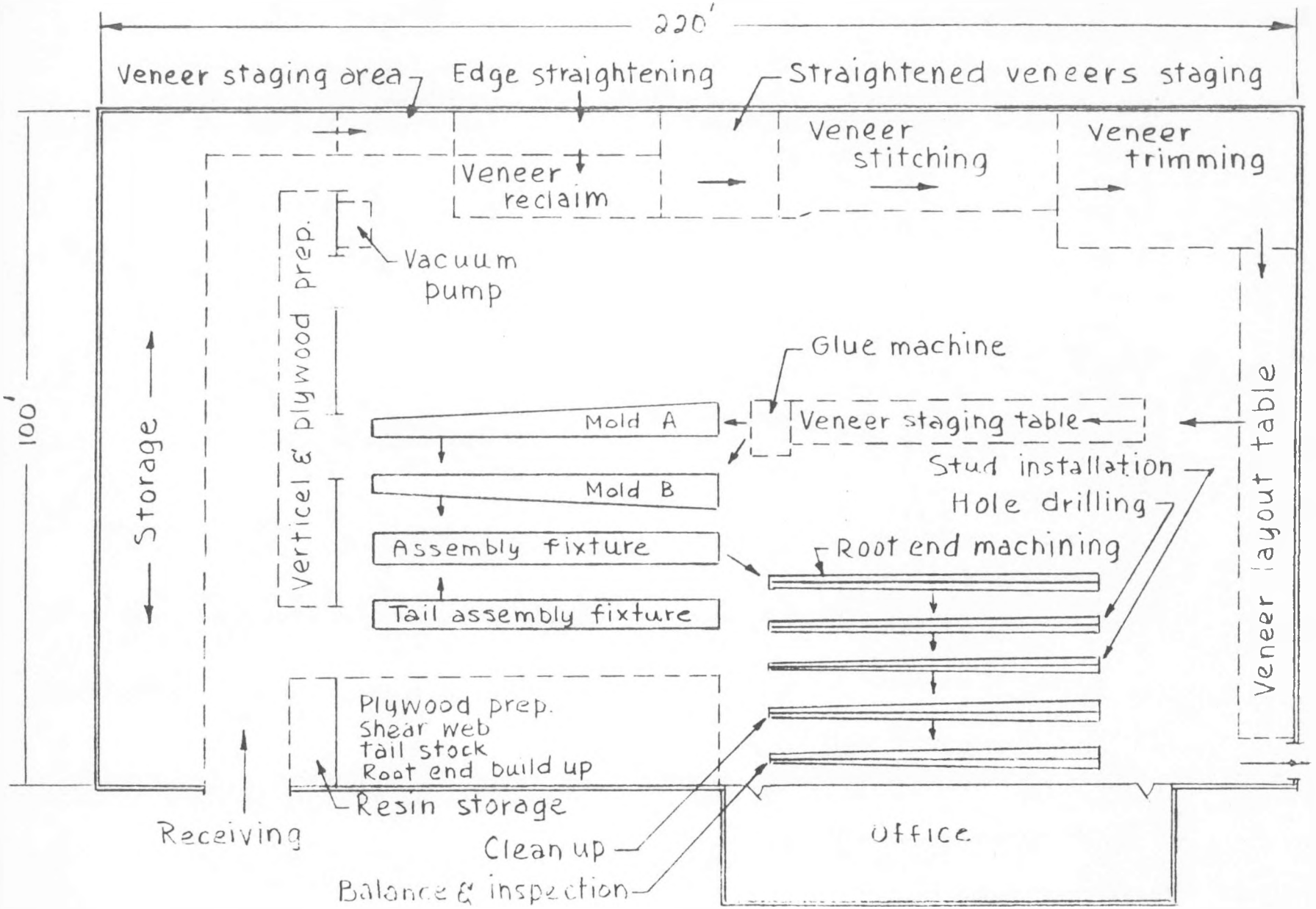

(a) Module for 120 blades/yr (1 shift) to 240 blades/yr (2 shifts).

Figure 49.-Proposed manufacturing plant for 62.5-ft laminated wood blades.

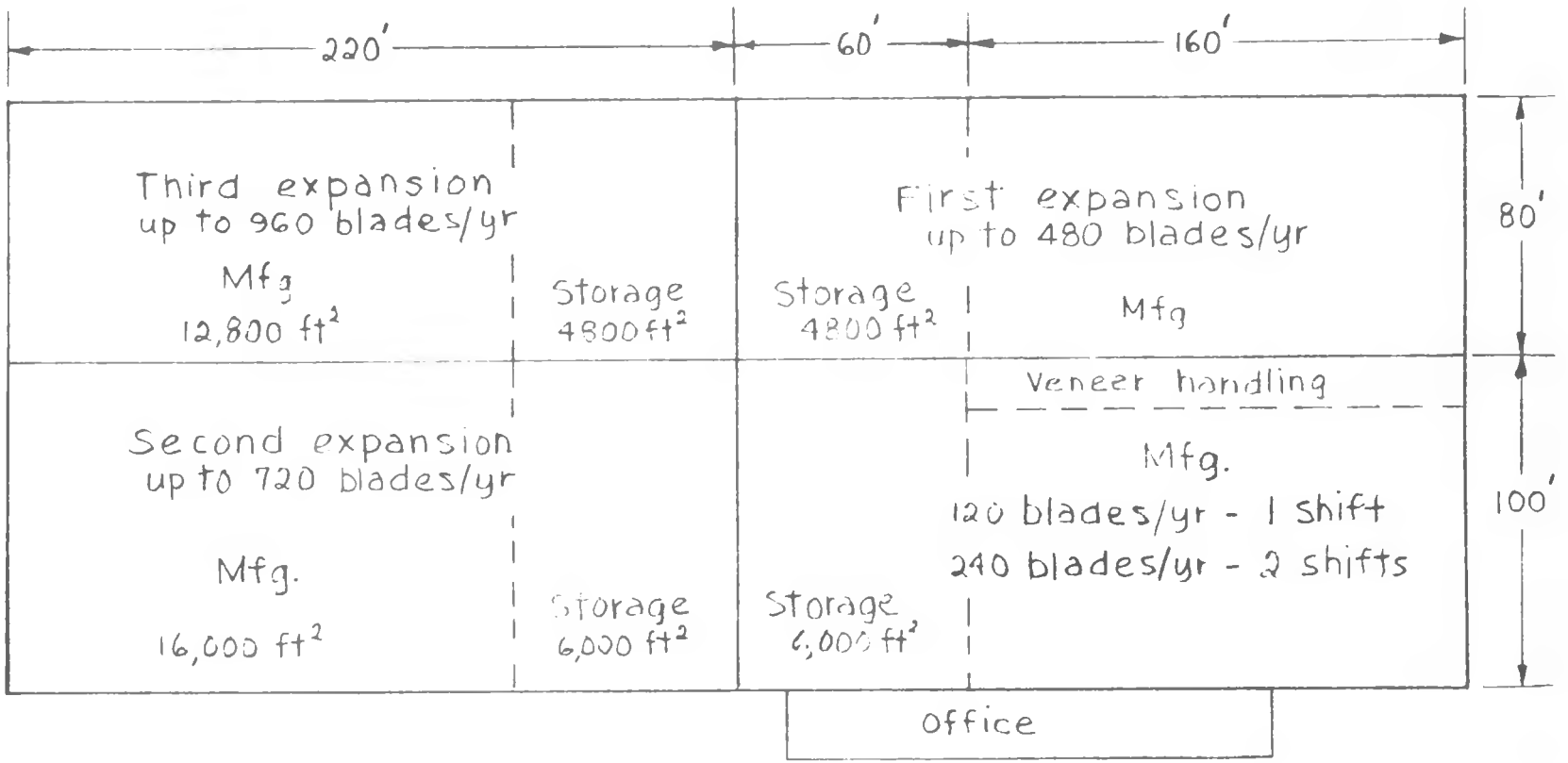

(b) Expansion plan for 960 blades per year (two shifts).

Figure 49.- Concluded.

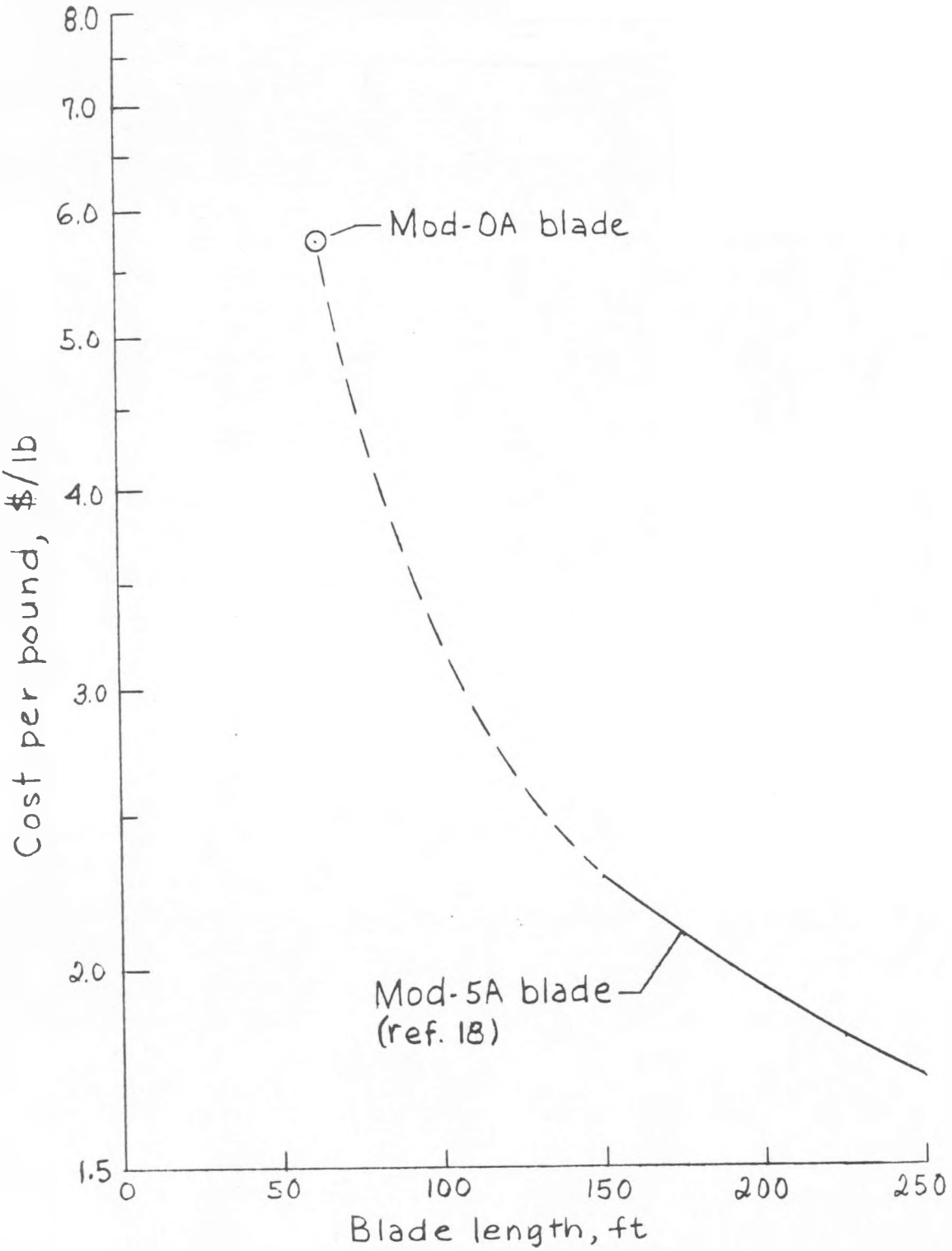

Figure 50.- Variation of estimated cost per pound of blade weight for wood composite blades in 1980 dollars for the 100th production blade.

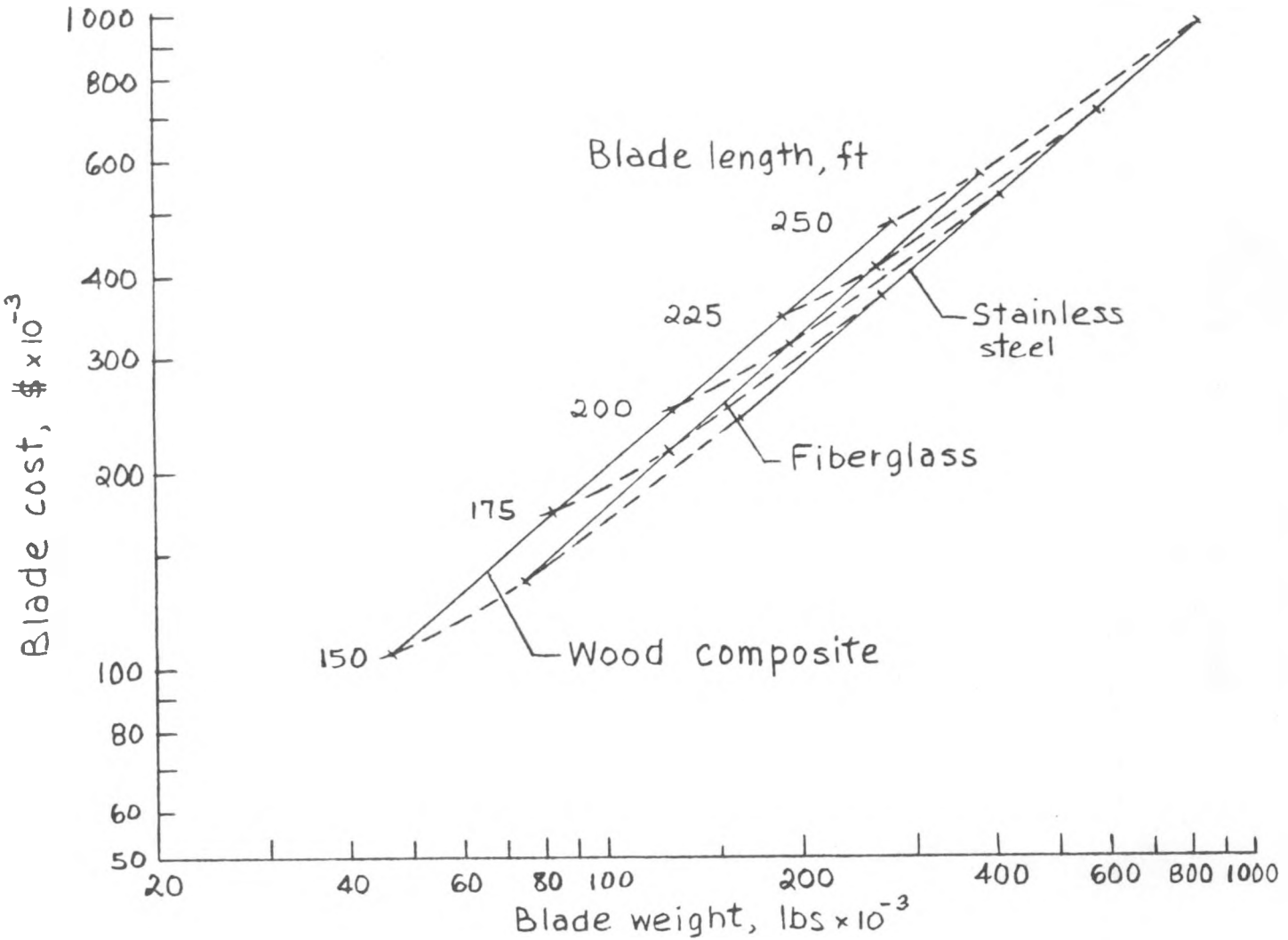

Figure 51.– Estimated blade cost and weight for blades for the Mod-5A wind turbine. Values in 1980 dollars for 100th production blade (from ref. 18).